COMPUTATIONAL ANALYSIS OF FLOW CHARACTERISTICS OF IRON ORE SLURRY IN PIPELINE AND BEND

A Dissertation

Submitted in fulfillment of the requirement for the award of degree of

Master of Engineering

In

Thermal Engineering

Submitted by

MANDEEP SINGH

(ROLL NO. 801683018)

UNDER THE GUIDANCE OF

Dr. Satish Kumar

Associate Professor

DEPARTMENT OF MECHANICAL ENGINEERING

THAPAR INSTITUTE OF ENGINEERING AND TECHNOLOGY, PATIALA

JUNE-2018

DECLARATION

I hereby declare that the work which is being presented in the dissertation work entitled, **"COMPUTATIONAL ANALYSIS OF FLOW CHARACTERISTICS OF IRON ORE SLURRY IN PIPELINE AND BEND"**, in partial fulfillment of the requirements for the award of degree of Master of Engineering in Mechanical Engineering with specialization in **THERMAL ENGINEERING** submitted in Mechanical Engineering Department of Thapar Institute of Engineering and Technology, Patiala, is an authentic record of my own work carried out under supervision of **Dr. Satish Kumar (Associate Prof. MED)** refers other researcher's works which are duly listed in the reference section.

The matter presented in this section has not been submitted for the award of any other degree of this or any other university.

Mandeep Singh

Date: 15/06/2018
Place: Patiala, Punjab

Mandeep Singh
(801683018)

This is to certify that the above statement made by the candidate is correct and true to the best of my knowledge.

Dr Satish Kumar
Associate Professor, MED
Thapar Institute of Engineering and Technology, Patiala

ACKNOWLEDGEMENT

I am highly grateful to the authorities of Thapar Institute of Engineering and Technology, Patiala for providing this opportunity to carry out the thesis work.

I would like express a deep sense of gratitude and thank profusely to my thesis guide **Dr. Satish Kumar, Associate Professor, MED, T.I.E.T, Patiala** for his sincere and invaluable guidance, suggestion and attitude which inspired me to submit thesis report in the present form.

I am also thankful to other faculty members of Mechanical Department, T.I.E.T, Patiala for their intellectual support. My special thanks are due to my family members and friends who constantly encouraged me to complete this study.

MANDEEP SINGH

ABSTRACT

Particulate transport in the form of slurry using pipeline system is continuously gaining popularity as it is economic, ensures real time inventory management, environment friendly and reliable at user's end. To design the pipelines and its associated facilities designers need accurate information regarding pressure drop, critical velocity, flow regimes, hold up etc. Multi-phase flows are complex and the correlations presently available in open literatures for the above mentioned parameters have a prediction error 25-35%. This much of error in design and slurry operation has serious cost implication and is totally unacceptable.

In the present study, an attempt has been made to simulate the mineral (iron ore) slurry flow through horizontal straight pipe and 90^0 pipe bend for prediction of head loss characteristics. To simulate the slurry flow commercial CFD software FLUENT 15 has been used. An Eulerian model based on kinetic theory of granular flow is used to represent multiphase phenomenon. To describe the turbulence present in the flow RNG k-ε turbulent model coupled with standard wall treatment with mixture properties had been employed. The Simulation is performed on pipeline having 50 mm diameter for both straight pipe and elbow. The solid concentration was varied from 20-60% (by weight) with flow velocity range of 2-5 m/s having mean particle size of iron to be 59 μm. The effect of particle size was also studied by varying the particle size range from less than 53, 53-75 and 75-106 μm. Before performing simulation on iron-ore slurry, the simulated results are validated with the experimental data taken from the open literature. The simulated data predicted the relative pressure drop showed fair agreement with the experimental results. The pressure drop increases non-linearly with solid concentration, velocity and particle size for straight pipe and elbow. Increase in solid concentration and velocity results in deposition of solid particles at the lower periphery of straight pipe. The higher solid concentration zone for elbow was at extrados of pipe due to the effect of centrifugal force on solid particles. The variation in radius-to-diameter ratio of elbow resulted in change in floe characteristics. The pressure drop was minimum at r/D 2.5. The disturbance in velocity profiles and concentration profiles was maximum for lower r/D ratio due to sudden change in direction of flow.

Table of Contents

List of Figures

List Tables

NOMENCLATURE

Symbol	Description
α_c	Solid Concentration of carrier phase
α_p	Solid Concentration of particulate phase
$\vec{v}_p$	Velocity of solid particulate
$\vec{v}_c$	Velocity of carrier phase
C_{vm}	Virtual mass force coefficient
C_l	Coefficient of lift
K_{pc}	Inter-phase drag coefficient
C_l	lift coefficient
P_p	Solid pressure
∇P	Static pressure gradient
∇P_p	Solid pressure gradient
$g_{o,pp}$	Distribution function
$\overline{\overline{\tau_{tc}}}$	Reynolds stress tensor
$\overline{\overline{\tau_p}}$	Viscous stress tensors for solid particulate
$\bar{\bar{\tau}}_c$	Stress tensor for carrier fluid
$\vec{v}_p^{tr}$	Transpose velocity vector for solid particulate
$\vec{U}_c^{tr}$,$\vec{\vartheta}_c^{tr}$	Transpose velocity vector for continuum
$\bar{\bar{I}}$	Identity tensor
μ_c	Shear viscosity
$\vec{U}_c$	Phase weighted velocity
λ_p	Bulk viscosity of the particulate solid
μ_{col}	Collisional viscosity
μ_p	Shear viscosity of solid, Pa s
μ_c	Molecular viscosity of fluid, m^2/s
$\mu_{p,col}$	Collision viscosity
$\mu_{p,fr}$	Frictional viscosity
$\mu_{p,kin}$	Kinetic viscosity

e_{pp}	Coefficient of restitutions
φ	Internal friction angle
θ_p	Granular temperature
C_D	Drag coefficient
Re	Reynolds number
$V_{r,p}$	Terminal velocity correlation for bulk solid phase
K_p	kinetic energy
$D_{t,pc}$	Binary turbulent diffusion coefficient
C_w	Concentration (by weight)
d_p	Particle diameter, μm
g	Acceleration due to gravity, m^2/s
ρ	Density

Subscipts

p	Solid particulate
c	Carrier phase
max	Maximum
col	Collision
kin	Kinectic
fr	Frictional

Abbrevations

CFD	Computational fluid dynamics

Chapter 1

INTRODUCTION

Hydraulically transport of Bulk Solids in a particle form is a well-known technique accepted by many chemical and mining industries. In general, industries use fluids as a carrying medium to transport material. The complete knowledge of principles governing the fluid transportation leads to more efficient and secure system. Slurry transportation is an environment friendly and is economical viable as compared to rail and roadways (**Wilson et al. 2005**).Premature studies for slurry transportation were based on low to moderate concentration (up to 25% by weight). Higher concentrations are encouraged and are now in trend. Study of the flow with high solid concentration multi sized particulate is very complicated (**Kaushal et al. 2013**).Slurry system designers should have precise knowledge regarding hold up, critical velocity, pressure drop, flow regimes etc. to enable them to design the pipeline and its associated facilities. Moreover, two-phase or multiphase flows are frequently observed in number of industries as petroleum, chemical, oil and mining industry. Multiphase flow can be defined as coterminous flow of number of phases, with two-phase flow to be simplest case. A two-phase flow is simultaneous flow of two distinct phases as gas-solid, gas-liquid, or liquid solid with coexistence in arbitrary field. Generally, in two-phase flow (i.e. liquid-solid or gas-solid), the liquid phase is consistently connected and the solid phase exists as discrete particles. Two-phase flow study is crucial from practical viewpoint applications (e.g. pneumatic and hydraulic particulate flow in pipes) and natural (e.g. biomedical/biological flow, sediment transport in water bodies). Flow in which granular materials are transported in the chemical, mining, petrochemical and food industry.

Physics of multi-phase flow is more cumbersome than single-phase flow as due to the presence of dispersive phase. Moreover, further fluctuated or continuous contact motion within particulates and turbulence between them increases the degree of complexity. Particularly for these types of cases, solid phase does not follow the flow while interacts and modifies the flow characteristics which results in uncertainty. Turbulence modulation for multi-phase flow is also important taking into view the industrial applications.

Particulate transport in the form of slurry using pipeline system is continuously gaining popularity as it is economic, ensures real time inventory management, environment friendly, reliable at user's end. The slurry raises less dust and is extremely safe. Further, it also broadens the economic ways to reach out to the rich mineral deposit in extremely dangerous areas. Advantages associated with slurry pipeline transportation system are listed below:

- Simplicity of operation and installation.
- Less requirement of man-force to construct, operate and maintain slurry handling system.
- Eliminates logistic bottlenecks and insurance of real time inventory
- Possibility of 100% automation.

Although having number of advantages it has some disadvantages also as:

- Initial investment is high as compared to other means of transportation
- Area of application is solely dedicated to transportation of solid particulate while rail and roadways have wide area of application.
- Transportation in the form of slurry requires carrying fluid as water which is depleting and not easily available at some places.

1.1 SLURRY FLOW

Slurry is a mixture of fined grinded solid particles and liquids (carrier fluid). The study of slurry flow in pipeline is much different as compared to single phase flow in pipeline. Single phase can be allowed to flow at low flow velocities but for multi-phase flow it is required to overcome deposition critical velocity. The physical properties of slurry is dependent on variety of parameters as particle size distribution, solid concentration, size of pipe, level of turbulence, temperature and viscosity of carrier medium.

The pressure gradient or head loss is one of another area in which careful treatment is required as compared for single phase flow. The form dp/dx, pressure gradient or frictional losses accompanied with the flow of slurry in pipeline is unambiguous. The mixture pressure gradient based on carrier medium density can be given as:

$$\text{Head loss} = \frac{1}{\rho_c g}\left(-\frac{dp}{dx}\right) \tag{1}$$

The characteristics of slurry are strongly dependent on the settling properties of the solid being conveyed. The measure of settling slurry is done with the application of settling velocity. Settling velocity is the velocity at which single solid particle settles in large volume of carrier liquid. Terminal velocity depends on the liquid and solid properties and particle size **Abulnaga (2002)**.

1.1.1 Basic elements of slurry transportation system

Solid in the form of fine particulates can be either of two ways by hydraulically or pneumatically. Basic difference between two being the nature of fluid used to provide motion to the solid particles. Slurry transportation system depends upon the type of solid to be transported through pipeline. However, general schematic layout of basic slurry transportation is shown in **Figure 1.1**. Three basic sub-system of slurry transportation system namely:

1. Slurry preparation system
2. Main pipeline and pumps
3. Terminal utilization facility

Initial process of the slurry transportation system is being the slurry preparation facility. Firstly, the solid to be transported are crushed to relatively smaller size using crusher so to make solid technically and economically feasible to provide the required power for creating suspension and hence their transportation. Further, the solid particulates are mixed with the carrier fluid and concentration of solid in fluid is maintained according to optimum transport concentration of transportation system. Finally, the prepared slurry concentration is stored in agitated/non-agitated tank if required.

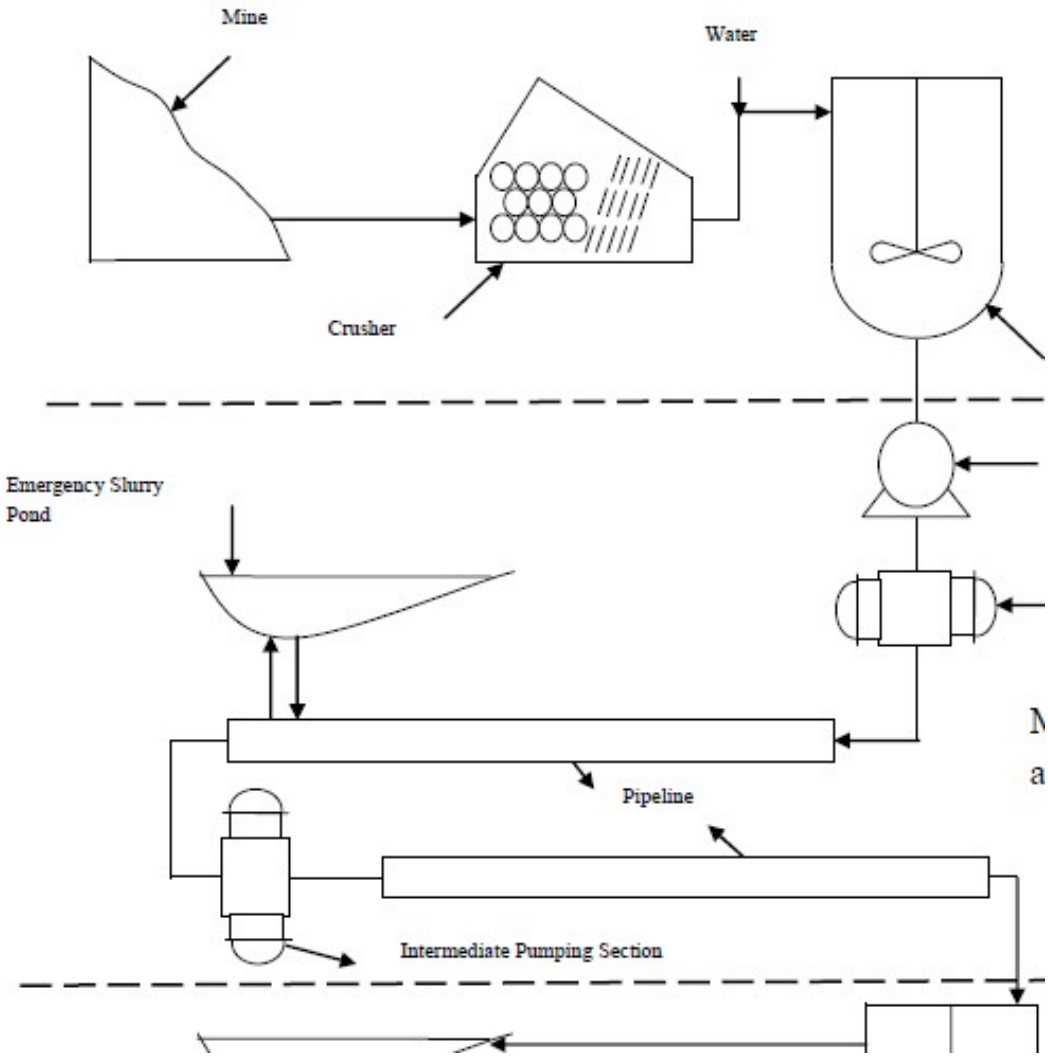

Figure 1.1 Schematic layout of a long distance slurry pipeline **Abulnaga (2002).**

Pumping power required to transport the slurry concentration is met either using one or more pump house. There can be one central pump house or a combination of central and intermediate pump houses to overcome the pressure losses during the transportation depending upon the length of transportation. At the terminal end there is separation facility where ore is separated from carrier fluid. The slurry at terminal end is dewatered, filtered, and dried to meet the requirement of end utilization of solids.

1.2 CLASSIFICATION OF FLOW REGIMES

Depending on the specific gravity of solid particles the flow can be classified into following four categories **Brennen (2005)**

- Homogenous suspension for particles smaller than 40 μm.
- Suspensions maintained by turbulence for particle sizes from 40 μm to 0.15 mm.
- Suspension with saltation for particle sizes between 0.15 mm and 1.5 mm.
- Saltation for particles greater than 1.5 mm.

The interdependency between deposition velocity, terminal velocity and solid particle size the above mentioned classification was modified into four flow regimes as shown in **Figure 1.2.**

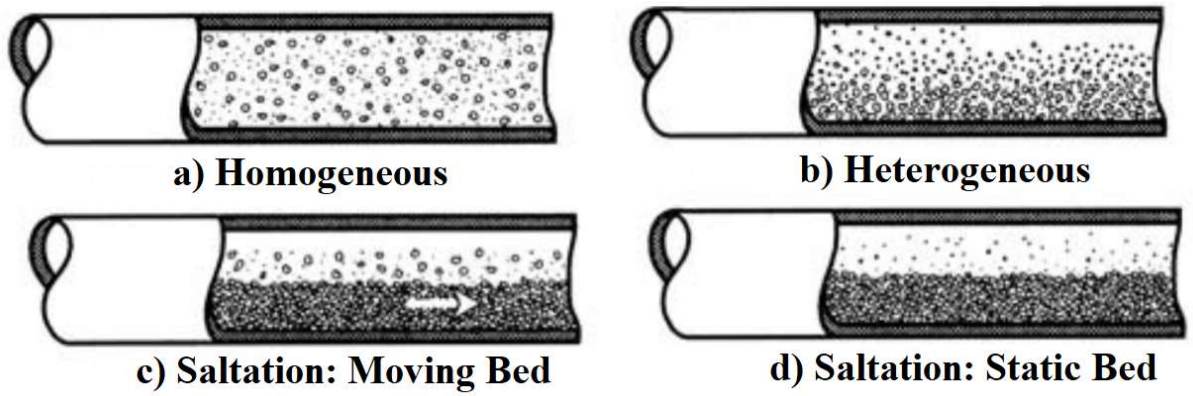

Figure 1.2 Flow regimes for slurry flow in a horizontal pipeline.

Flow velocity, phase material and pipe orientation are the main parameters affecting the two phase flow regimes in pipeline. Generally, particle size and solid concentration are used for classification of mixture nature and flow regimes in solid-liquid flow.

1.2.1 Classification based on particle size

The slurry flow is generally classified into broadly two categories: homogeneous and heterogeneous. Due to unavailability of proper distinction between homogeneous and heterogeneous flow the slurry containing solid particle size greater than 50 μm displays heterogeneous properties.

The behaviour of heterogeneous slurry flow is more complicated than that of homogeneous slurries. Due to submerged weight and effects of gravity on coarser particles, sedimentation occurs resulting in non-uniformity in concentration and velocity along the cross-section.

1.2.2 Classification based on solid concentration

The solid concentration of slurry is used as criterion to distinguish between dilute and dense solid-liquid heterogeneous flow. The mixture is considered to be dilute if the motion of the flow is governed by hydrodynamic forces or carrier medium interactions. Flow is considered to be dense if both particle-particle interactions and hydrodynamic forces govern the flow characteristics. No universal criterion is available in literature to distinguish between dilute and dense phase on basis of solid concentration. The creation varies with material to material and study to study.

1.3 CRITICAL VELOCITY AND HOLD UP

Critical velocity is the velocity at which solid form a bed at the lower periphery of pipe from fully suspended solid-liquid flow. It gives a measure of transition of flow from heterogeneous to saltation flow. For the optimizing the slurry through the study of critical flow is crucial and vital step. It represents the lowest velocity at which the system can perform the slurry transportation function with minimum pressure loss. The slurry in pipeline moves in the form of layers moving with different velocities. Holdups are due to slip velocity of layer large particles. Thus hold ups gives rise to a situation when the in-situ solid concentration is larger than the solid concentration delivered. This variation in concentration is known as Hold up. Hold up is key problem for the failure of many empirical relations for prediction of head loss.

1.4 HEAD LOSS/PRESSURE DROP

Head loss characteristics in pipe flow are studied for the designing slurry pipeline and pumping system. Numbers of researchers have performed experiments to obtain empirical correlations for the prediction of head loss by estimating the friction factor. The correlation developed depends on the rheological nature of slurry and experimental data of pressure using pilot test loops. Most of the relations developed are for the specific size ranges with very low to moderate solid concentrations. Hence, it is beneficial to study the flow characteristics with the computational scheme resulting lowering the capital cost and time for study.

1.5 SOLID CONCENTRATION AND VELOCITY PROFILES

Loss of pipe material due to abrasion and erosion is known as wear which is a very important consideration in the design and operation of slurry piping systems. This affects the initial capital cost and component lifetime. It is reasonable to assume that the wear depends on the number of particle collisions on the surface, depending on the flow rate and solid concentration. Therefore, in order to understand the wear phenomenon, you need to know the in-situ velocity profile and the solid concentration profile in detail. Solid concentration gives us with a detailed view of the solid volume fraction distribution along the plane while velocity profiles are used for prediction of velocity distribution of solids.

1.6 IRON-ORE

Ore is the natural form of mineral found in the earth's crust, extracted and treated for extraction of purest form of metal. This extraction process includes breaking of large ore lumps into smaller pieces, transportation, cleaning for removal of gangue and waste extracted with ore during mining i.e. tailings and treatment from oxides to pure metal. Iron ore largely found in the earth crust in the form of oxides of iron. Iron is primary raw material for manufacturing of steel. Australia, Brazil, India, China, and South Africa have the largest resources of iron in the world. Iron naturally is found in for of oxides of iron namely as siderite ($FeCO_3$), magnetite (Fe_3O_4), limonite ($FeO(OH).n(H_2O)$), goethite ($FeO(OH)$), and hematite (Fe_2O_3). Hematite and magnetite form of iron ore can be directly fed into the blast furnace. India is producing at an average of 10% of world consumption of iron ore per annum. India has 9,602 million tones of hematite and 3,408 million tones ofmagnetiterecoverable amount of iron ore reserves. Chattisgarh, Odisha, Madhya Pradesh, Jharkhand, Karnataka, Andhra Pradesh are the states having major reserves of iron ore.

1.7 APPLICATIONS

Processing of iron ore is done for the production of pig iron (metallic iron), which is further used for the manufacturing of steel. Iron plays significant role in the developed and developing economies of the world. Cast iron, wrought iron and layered iron auxiliary sheeting are used as a conspicuous material in the building development. Commercial applications of iron are listed as:

- Catalyst for production of ammonia and production of hydrocarbons from carbon monoxide.
- Iron is used for manufacturing of components for automobiles, production, tool and construction industries.
- Stainless steel an alloy of iron which has highest proportion of iron is used for manufacturing of cutlery, hardware, cookware, surgical equipments, boilers, storage tanks etc.
- Metallic iron is used for production of electro and permanent magnets.
- Iron chloride is used for the sewage treatment plants, colorant for textiles and paints industries and animal feeding additives.
- Iron sulphate is used as supplement for curing anaemia.
- Mixture Ignited iron oxide and aluminium powder is used for welding and purification process of ore.

These are some listed major commercial applications of iron. The utilization of iron is not limited to above mentioned fields but is above all counts and has wide application in our day-to-day life.

1.8 MODE OF TRANSPORTATION OF IRON-ORE

The growth of industrial revolution has increased the demand for raw material. Iron is one of the major raw materials for industries. With the increase in demand the means of transport need to be more reliable and requires improvement. The major means of transport are rail and roadways but increase in demand has resulted in increased environmental pollution and bottlenecks. The alternative of these problems is transportation of solid particulate in the form of slurry. Transportation of solid in the form of slurry is gaining popularity due to its wide range of application and advantages over conventional source of transportation. Therefore, major ways of transportation of iron ore are rail, road, ports and the slurry pipelines.

1.9 HYDRAULIC TRANSPORTATION OF IRON-ORE

Solid material in the form of solid particles of size in microns can be transported pneumatically and hydraulically. Solid of low specific gravity can be transported by both pneumatic and hydraulic ways but for high specific material hydraulic ways are preferred due

to high density of carrier fluid in hydraulic transportation. Hydraulic transport of iron ore in India using slurry pipeline is given in Table 1

Table 1.1 Iron ore slurry pipeline systems in India

Location	Pipe Length (km)	Industry	Capacity (Mt/year)
Kudremukh -Mangalore	68	KIOCL	8
Kirandul-Vishakhapatnam	267	ESSAR steel	8
Barbil-kalinganagar	230	BRPL	4
Joda-paradip	253	ESSAR steel	8

The Kirandul-Vishakhapatnam slurry pipeline has drastically brought down ESSAR Steel's ore transportation cost from Rs. 550 per tonne to merelyRs. 80 per tonne, besides eliminating logistic bottlenecks and ensuring real time inventory management. The 267-km pipeline is the longest slurry pipeline in India and the second largest in the world.

1.10 MATHEMATICAL MODELING IN HYDRAULICTRANSPORTATION OF IRON-ORE

Fluid motion is governed by the different governing equations. The unknown are usually the velocity, the pressure and density and temperature. The analytical solution of this equation is impossible hence scientists resort to laboratory experiments in such situations. The answers delivered are, however, usually qualitatively different since dynamical and geometric similitude are difficult to enforce simultaneously between the lab experiment and the prototype. Furthermore, the design and construction of these experiments can be difficult (and costly), particularly for stratified rotating flows. Therefore, when analytical methods are unproductive we can use numerical methods to obtain approximate solutions. Although they can never have the same generality as analytical solutions, they can be just as good in any particular instance.

1.11 MOTIVATION OF PRESENT WORK

Conveying solid through pipelines on large scale has now come to be accepted as a viable alternative to the conventional modes of transportation. Large number of slurry pipelines was already built around the world and lot more are still to come up. To design the pipeline, designers need accurate information regarding pressure drop, critical velocity, flow regimes etc. The need and benefits of accurately predicting velocity profiles, pressure drop, and concentration profile of slurry pipeline during the design phase is enormous as it gives better selection of slurry pump, optimization of power consumption. It has been the endeavour of researchers around the world to develop accurate models. The major empirical equations regarding pressure drop, hold up, critical velocity and flow regime identification when tested with experimental data of different systems collected from open literatures, it was found that prediction error ranges above 25% on average.

The motivation of the present work is to find the applicability of Computational Fluid Dynamics (CFD) in slurry flow modelling. The limitations of empirical equations based correlations are that they do not provide deeper insight of complex phenomena of slurry flow. In recent years with advancement in CFD techniques, CFD becomes a powerful tool for predicting fluid flow, heat/mass transfer, chemical reactions and related phenomenon by solving mathematical equation that govern these processes using a numerical algorithm on a computer. Considering the limitations in the published studies, the present work has been concentrated on a systematic development of CFD based model to predict the solid concentration profile, velocity profile and pressure drop in slurry pipeline

Chapter 2

LITERATURE REVIEW

A number of researchers have investigated various factors of slurry flow through pipeline experimentally and numerically. Many researchers worked on the effect of different parameters such as flow velocity, efflux concentration, pipe radius, bend angles, radius ratio on flow characteristics and physics of flow in-turn affecting the designing parameters when loaded with different types of slurry as coal slurry, coal-ash slurry, tailing slurry, ore slurry etc. transported by the means of pipeline and a review of published literature is presented in this chapter

Mukhtar et al. (1995) investigated the flow characteristics of heterogeneous slurry flow in pipeline. The study was carried to study effect of concentration and velocity on relative pressure drop of iron ore (sp. Gravity 4.2) and zinc tailing (sp. Gravity 2.6) slurry suspension. Experiments were carried on a horizontal 90^0 pipe bend of radius ratio of 4 and radius of curvature of 21 cm for velocity varying from1 m/s to 3 m/s for concentration varying from 10-40% (by weight) and 30-45% (by weight) for iron ore slurry and zinc tailing slurry respectively. The rheological experimentation of slurry revealed that iron ore slurry exhibited Newtonian behavior up to 30% concentration while, zinc tailing slurry exhibited the Newtonian up to 40% concentration. The relative pressure drop is higher at lower velocities and tends to become constant at higher velocities for both zinc and iron ore slurry.

Verma et al. (2006) investigated the pressure drop characteristics of fly ash slurry at high concentration along a 90^0 horizontal bend. They calculate the relative pressure drop and bend loss coefficient for slurry concentration ranging from 50 to 65% (by weight), particle size ranging from 300 μm to 3 μm having 84.4% of particles less than 75 μm. The pilot test loop plant used for experimentation was having a pipe diameter of 53 mm with a length of 30 m with radius ratio of 5.6. They found that relative pressure drop first increased with increase in slurry velocity and reached to a constant value at higher velocities but the bend loss coefficient showed a decreasing trend with increase in slurry velocity. They also concluded that disturbance along the flow downstream of the bend resulted in additional losses hence permanently contributing to pressure loss.

Mosa et al. (2007) experimentally investigated the variation in pH, temperature and particle size on flow and head loss characteristics for coal-water slurry flow. They employed a pilot test loop of 61 m pipe length having a nominal diameter of 63 mm to study the variation in particle size. The solid concentration of slurry was 10% (by weight) with pH of 7. The rheological characteristics of slurry flow was studied by varying the pH ranging from 1 to 12. The pseudo plastic nature of slurry was having a decreasing trend with temperature and pH up to 6. The pressure increased with degradation of solid particle size from 250 μm.

Eesa et al. (2009) investigated the slurry flow characteristics of coarser particulate slurry in pipeline by using commercial computational fluid dynamics (CFD) code ANSYS CFX with the application of Eulerian-Eulerian model to study the flow of coarser particles inside the pipe. They employed positron emission technique for tracking solid particles and particle in motion. They studied the flow properties under the influence of efflux concentration, particle size and slurry velocity. The concentration of particles was varied ranging from 5 to 40% (by volume) having mean particle size of 2 to 9 mm with slurry velocity of 25 to 125 mms^{-1}. They discussed that with the exception of smaller particles, they exhibited asymmetric velocity profile tending to increase with increasing particle size. They also concluded that with increase in solid concentration head loss also increases.

El-Nahhas et al. (2009) performed the experimental investigation of coarse particle sand-water slurry flow to study the influence of particle size. The experimentation was done using a stainless steel pilot test loop of having 18 m pipe length with diameter of 26.8 mm. The sand particle used for preparation of slurry was having particle size (d_{50}) of 200, 700 and 1400 μm. The solid concentration was varied in range of 4-33% was used for present study. The effect of particle size on pressure drop depends on solid concentration and velocity of slurry flow. The specific energy consumption decreased with increase in solid concentration.

Liu et al. (2009) experimentally investigated the pressure drop characteristics for different pipe fitting as pipe bend, gradual contraction and sudden contraction for coal-water slurry flow. The r/D ratio for bend was varied in range of 1.5-6 for three pipe diameter of 25, 40 and 50mm. The angle of contraction for gradual contraction pipe section was taken as 3º, 5º, 10º, 20º and 90º. The solid concentration of two sample taken was varied from 57-62% (by

weight). The pressure drop first decreases to a minimum and then increased with contraction angle. The pressure drop for sudden contraction of 68/25 mm was more than 50/25 mm. The pressure drop was minimum at r/D 2 for 25 and 50mm pipe diameter and 1.5 for 40 mm pipe diameter.

Lahiri et al. (2010) developed a generalized solid liquid flow model with the application of CFD and further utilized the model for prediction of concentration profiles. They employed the Euler-Euler model along with standard k-$\boldsymbol{\varepsilon}$ turbulence model using mixture multiphase properties. However, Eulerian-Langrangian model simulates solid phase as discrete phase and hence to be more promising and realistic in particle tracking. But after a number of trials were conducting, they concluded that the count of dispersed particle that can be tracked with the application of currently available commercial CFD packages is limited. The mapping of model developed was done with the commercial CFD FLUENT 6.2 solver. The model was validated with the experimental data of Kaushal et al. (2005).

Lei et al. (2010) proposed the use of additive for restart purpose of slurry pipeline after a shutdown of more than 24- hour. The investigation was aimed to find appropriate stabilizing agent for fly-ash water slurry for prevention of sedimentation. Suitability of four different additives was examined with the aid of rheological and sedimentation stability experiments. Stabilizing additives employed for the study was carboxymethyl cellulose (CMC), rhamsan gums (S-194, S-130), and xanthan gum (Vanzan). The addition of stabilizing additives resulted in increase in viscosity but the concentration of 0.2%, 0.2%, 0.45% and 0.3% (by weight) had same viscosities as that of untreated fly ash slurry for additive S-194, S-130, CMC, and Vanzan respectively. Naphthalene sulfonate-formaldehyde condensate (NSF) was used as a dispersing additive for reduction of viscosity and concentration of NSF was kept as 0.3% (by weight)/slurry. The reheological characteristic was measured using coaxial rotating cylinder rheometer. They concluded that S-194 was having the maximum stability as compared to other additives.

Lu et al. (2010) investigated the influence of particle size on flow and head loss characteristics of flow of slurries in pipeline. Three distinctive flow patterns were observed namely fully suspended, partial stratified and fully stratified for varying particle size and

velocities. Size of solid particles constituting the slurry affects significantly the flow patterns. Medium to fine sized particles having lower weight tends to be lifted under the action of turbulent dispersive force of carrier fluid hence, resulting in uniform flow distribution which in lieu making the flow to be fully suspended. However, coarser particles are heavy hence making it difficult for making flow to be fully suspended flow even at higher velocities. Mechanical friction and viscous friction are the two ways by which the solid particulate to the total friction of slurry flow.

Hossain et al. (2011) studied the flow characteristics of solid-liquid in a straight horizontal pipeline consisting of four bends. Numerical simulations were carried using commercial CFD code FLUENT 6.2. The solution for the multiphase flow phenomena was carried out for different solids with variation of particle size diameters. Mixture model was employedfor solving the governing equations. They investigated that the particle deposition is a function of particle diameter and flow velocity. They also found that deposition occurs along circumference of the pipe. Solid concentration of high magnitude was observed at 60^{o} from the bottom of pipeline for bend downstream and at bottom of pipeline near the bend upstream.

Kaushal et al. (2012) investigated numerically flow characteristics of high concentration solid-liquid flowing through pipeline using computational fluid dynamics code FLUENT. The simulations were carried on 3 m long horizontal pipe of diameter 54.9 mm. Experimental study was carried with glass beads having mean particle diameter of 125 μm and flow velocity up to 5 m/s. The efflux concentration was varied ranging from 0 to 50% (by volume). The method used for discretization was hexagonal cooper method. They compared the results of two models namely Eulerian and mixture models for simulation of solid-liquid slurry flow for the prediction of pressure drop and velocity distribution at varying concentrations. The results were validated by comparing the model reults with the experimental data of Kaushal and Tomita (2007). They concluded that the mixture model failed in the prediction of results accurately for pressure drop because of existence of higher error percentage at higher concentrations.

Kumar et al. (2012) investigated the numerical simulation of slurry flow in pipeline with the aid of Eulerian model. Solid particulate of having mean diameter of 440 μm was transported

using carrier fluid with solid concentration varying up to 30% for pipe diameter of 54.9 mm. The discretization of computational domain was done using unstructured, non-uniform mesh and control volume finite difference method for governing equations. RNG k-$\boldsymbol{\varepsilon}$ turbulence model with ASM was used for precisely prediction of flow characteristics. The simulated results of the pressure drop of water flow in pipe were in a good agreement of with the experimental data.

Mazumder et al. (2012) investigated the influence of elbow ratio on head loss characteristics with the application of CFD. Numerical simulations were performed on the air-water flow through a 90^0 elbow. The diameter of elbow pipe was taken as 12.7 and 6.35 mm. The radius ratio of the elbow was varied from 1.5 to 3 with velocity of air varying from 15.24 to 45.72 m/s and for water was 0.1 to 10 m/s. The method used for discretization of solid geometry was hexahedral method. The numerical results showed a close agreement with the experimental and empirical results calculated using Chisholam and Azzi-Friedel model.

Seitshiro et al. (2012) experimentally investigated the flow characteristics of multi-sized sand-water and Bakelite slurry flow through straight pipe of diameter 26.2 mm. The experimental results were compared with two mathematical models as Wasp method and Condolios-Chapus method. The particle size was taken ranging from 1.21-2.18 mm and solid concentration was taken maximum up to 25%. They found that the Wasp method can be applied for slurry flow of lower concentrations. The hydraulic gradient was having a decreasing trend with increase in mixture ratio.

Messa et al. (2013) numerically studied the solid-water slurry flow through upward-facing step in a channel. The solid particle used for preparation of slurry was having a specific gravity of 2.465 and solid concentration was varied from 5-20% (by volume). They validated the Eulerian multi-phase based model with other numerical and experimental data for simulation of slurry flow. They also studied the effect of the above parameters upon the degree of coupling between the phases and the extension of the disturbance region in the pressure and solid volume fraction fields downstream the step.

Kim et al. (2013) numerically investigated the sand-water slurry flow through pipeline with the application of commercial FLUENT code. They employed Eulerian granular multiphase

(EGM) approach with k-$\boldsymbol{\varepsilon}$ model for the simulation of turbulence in the flow. They investigated the effect of pipe diameter and solid concentration on the flow characteristics. The meshing of the flow domain was done in non-uniform hexahedral system. The median particle size and density of slurry used for preparation of slurry was 0.54 mm and 2650 kg/m^3. They found that with decrease in Reynolds number the effect of efflux concentration on pressure gradient and solid increases. For smaller Reynolds number pressure drop increased with increase in volumetric concentration delivered.

Nabil et al. (2013) numerically studied solid-liquid i.e. water-sand slurry flow in a pipeline. They study was carried using a CFD code generated using FLUENT to simulate the slurry flow with the application of Eulerian-Eulerian scheme and k-ε turbulence model. They used square pipeline of dimension 26.8×26.8 mm. The geometry was discretized using tetrahedral type mesh. They used varied the particle size diameter (0.2, 0.7 and 1.4 mm) of slurry with efflux concentration ranging from 5-30% (by volume) at different velocities ranges 0.5–5 m/s. The discretization of governing equations was done with the application of first order upwind approach for solving the momentum equation, turbulent kinetic energy, turbulent dissipation rate and volume fraction. Numerically simulated results showed a close agreement with the experimental data for coarse and medium sized particulate slurry flowing at low concentration (5-10%) and failed for the flow of coarser slurry at high concentration.

Ravelet et al. (2013) experimental investigate the head loss characteristics for coarse particle sized slurry flow through horizontal pipe. The pilot test loop used for the study was having a pipe diameter of 100 mm and length 30 m. The slurry sample was prepared using alumina of particle size 10.5, 8.25 and 5.5 mm and stones having particle size ranging from 8-18 mm. The pressure gradient was more for the vertical pipeline as compared to for horizontal ones. The pressure drop increased with particle size while critical velocity remained unaffected. The pressure drop and critical flow velocity increased with specific mass of solid particles.

Hashemi et al. (2014) investigated the solid velocity and concentration profiles for concentrated sand-water slurry in horizontal pipeline. The solid concentration was taken as 20-35% (by volume) having particle size (d_{50}) of 100 μm. The flow velocity was taken as 2-5 m/s flowing through a 52 mm diameter pipe. The concentration of solid was grater near the

pipe wall and increases with velocity. The fluctuations in concentration were largely due to particle-fluid interactions as compared to fluid-fluid or particle-particle interactions. They compared the concentration fluctuations with results collected for fluidized bed flows on basis of Stokes number.

Panda et al. (2014) numerically investigated head loss characteristics for the coal-ash slurry flow through straight pipe and 90^0pipe bend. The modeling of pipeline was done using Gambit version 2.2. The ratio of bottom ash to fly ash was maintained as 6:4, 8:2 and concentration of additive in bottom ash slurry was maintained at 4 and 6%. The solid concentration of slurry was varied from 20-50% and flow velocity was varied from 1.5-3 m/s. The head loss was having an increasing trend with concentration and flow velocity. The mixing of additives was having more effect on head loss as compared to addition of bottom ash in fly ash slurry flow.

Wu et al. (2015) investigated the head loss characteristics of solid-liquid flow in pipe line using computational fluid dynamics code generated with the application of COMSOL Multiphysics. They used coal mixture of coal gangue, cement, fly ash as a solid material. The mixture solid concentration varied from 78-79.5% concentration (by weight) at different flow rate (60, 70, 80 and 90 m^3/h). They employed a experimental test loop system of diameter 120 mm and 35 m long to investigate the flow behavior of slurry in pipeline. They observed that the slurry behaved as a Bingham Fluid at high solid concentration. CFD simulations were carried out to compare the outcomes of simulated results with loop test. They observed that the total and partial pressure drop increased with increase in slurry flow rate resulting in increase of Darcy friction factor (f_d) and frictional resistance loss. For a given volumetric flow rate, pressure drop decreased with increase in internal diameter of pipe. The simulated results had a good agreement with the experimental results of test loop.

Gopaliya et al. (2015) studied the effect of solid particulate size on solid-liquid i.e. sand-water slurry flow properties in horizontal pipe using Computational code generated with the application of GAMBIT and FLUENT 6.3. The efflux concentration was varied ranging from 15-45% with four grain sizes (0.18 mm, 0.29 mm, 0.55 mm, and 2.4 mm) and velocity ranging from 1.8-3.1 m/s. The geometry under consideration consisted pipe of diameter53.2mm and length of 2.7m horizontal pipe created using GAMBIT for simulation of slurry flow. There

were 357120 hexahedral volume mesh cell generated. They have adopted a pipe wall roughness of 0.2 mm and convergence criterion 10^{-3}. Pressure drop was calculated for the one meter length of pipeline at the end. The pressure drop increases with increasing value for efflux concentration and velocity for all grain sizes. The particle at the central core was having higher velocity as compared to particles at other pipe cross section.

Ofeiet al. (2016) investigated the effect of grain size and efflux concentration on solid concentration and velocity distribution along with frictional pressure gradient in solid-liquid slurry flows through horizontal pipe using two-phase Eulerian CFD model. They also checked the robustness of various turbulence models using experimental data of solid concentration profiles and found *k-ε* model to be most suitable as compared to other models. They highlighted that study of variations in different slurry flow parameters across pipe cross-section is very crucial; especially for better understanding of pipeline wear and particle attrition or agglomeration.

Rawat et al. (2016) numerically investigated flow characteristics of fine coal ash slurry at higher concentration by using CFD code FLUENT. They used SST k-ω turbulence model to calculate the pressure drop of coal ash slurry inside pipeline because SST k-ω gave least deviation with the experimental data used for validation. Rheological study reveals that slurry behavior was non-Newtonian at higher concentrations. They found that pressure drop to be a function of flow velocity. The head loss in pipeline increases with increase in velocity.

Tebowei et al. (2017) numerically investigated the flow characteristics of sand slurry flow through V-inclined bend. They employed two fluid Eulerian-Eulerian model with granular temperature to tackle the solid phase properties. The k-$\boldsymbol{\varepsilon}$ turbulence model was used for the turbulence study of the flow. The results were found for slurry flow at 10D, 2.5D and 15D away from pipe dip for both upstream and downstream flow. They found that correlations used for predicting minimum sand transport is not valid for V-inclined bends. They concluded that for efficient pipeline design the critical mass transport equation should be incorporated for study of slurry flow and to enable unhindered slurry flow through bend sections.

Mishra et al. (2017) numerically investigated the flow characteristics of coal-water and copper ore-water slurry flow through pipeline. They employed a simplified 3-D ASM model

along with RNG k-ε turbulence model for study of coal and copper-ore slurry flow. The particle size for coal was varied from 70.5-275.7μm and copper ore was varied from 40.1-278.5 μm. The specific gravity of coal and copper ore was 1.98 and 2.84 respectively with volume fraction of slurry varying from 0.08 to 0.19. The pressure drop was maximum for copper-ore slurry flow of coarse sized particle i.e. 275.7 μm but for coal slurry flow it was for 70.5 μm. The pressure was having a increasing trend with volume fraction loading.

Nayak et al. (2017) numerically investigated the thermo-fluidic characteristics of fly ash slurry through 180^0 return pipe bend. The concentration of slurry was varied from 10-50% with flow velocity ranging from 1-5 m/s. The particle size of fly ash was taken as 13 μm. The head loss through the pipeline had an increasing trend with flow velocity and particle volume concentration. They also found that decrease in radius ratio from 5.6 to 2.98 the pressure drop changed from 14% to 83% for change in concentration from 10-50%. The concentration profile depicted the formation of secondary flows at the inner side of pipe bend which starts at an angle of 45^0 and increased upto 180^0.

2.1 GAP IN RESEARCH

Based on literature review, following gaps on erosion wear characteristics of the solid–liquid suspensions are observed.

- The literature about numerical simulation studies for complex mineral slurry flow is quite limited.
- Lot of multiphase models has been employed to predict the flow behaviour inside pipeline for the flow of different slurries. But there is no adequate model which can describe the flow behavior of minerals inside pipeline.
- It is very difficult to visualize the pressure drop in pipeline by using conventional methods. Moreover, simulation results provide information of fluid flow characteristics inside the pipeline which helps to analyze the flow phenomenon at different locations on pipeline for complex mineral slurry flow.

Chapter 3

MODELING OF SLURRY FLOW

Computational Fluid Dynamics make use of numerical algorithms and methods to simulate the real life behavior of fluids. It gives us the independence of optimizing the design parameters without using the costly prototype testing facility. CFD is powerful tool to visualize the internal flow characteristics and physics which otherwise would be very difficult in practical conditions. Governing equations used to model flow behavior, but the applicability does not gives the freedom to apply them to many complex flow patterns directly due to many unknown variables. In CFD, the domain geometry is divided into integrated small elements to create manageable discrete sections. Governing equations are applied to each of these small elements individually, but the effect of neighboring elements is also considered and hence the flow governing equations are solved simultaneously on all elements to obtain a full solution for the whole fluid flow. The limitations of CFD are its accuracy or validity dependence on variety of factors: the quality and appropriateness of the mesh, degree with which the chosen equations match the type of flow modeled, the interpretation of results, and accuracy of boundary conditions fed by the user or convergence criteria.

Computational fluid dynamics is a technique to replace the integrals or derivatives in governing equations with discretized algebraic equations, which are used to obtain numbers of flow field parameters at discrete points in space or/and time. Computational fluid dynamics is one of the branches of Engineering, finding numerical solutions of governing equations (**Anderson 1955**). CFD solutions are obtained by repetitively manipulated thousands times.

3.1 DISCRETIZATION TECHNIQUES

Discretization is a technique of transferring closed form integral and differential equations into discrete counterparts. It is regarded as an infinite continuous value of the entire domain, and the approximation is a quasi-expression that values only for discrete points. Discretization is the process of breaking differential equations into solvable linear and non-linear. **Figure 3.1**shows various discretization techniques used for the solution of partial differential equations. The application of the method depends upon the complexity and nature of equations.

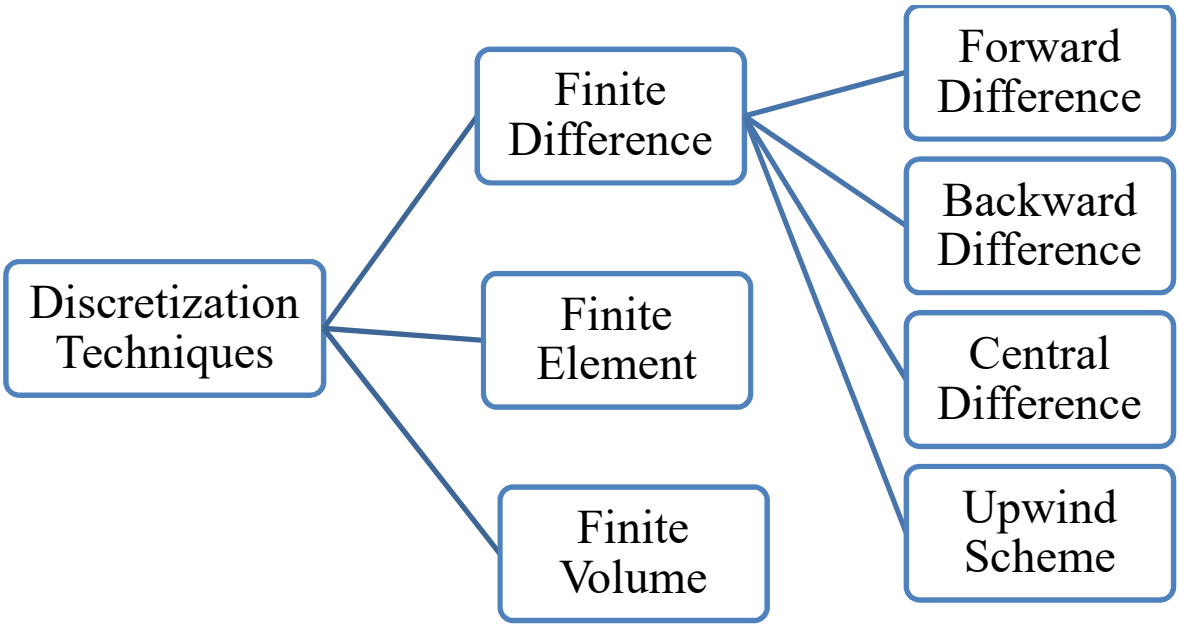

Figure 3.1 Discretization Techniques

Discretization method is chosen appropriately according to the application. For example finite volume is generally used for fluid flow problems while finite element is used for structural and mechanics study. For present study FLUENT is used which uses the finite volume technique for the discretization of flow domain.

3.2 CFD METHODOLOGY

The CFD methodology can be broadly divided into three major steps as discussed below

- Pre-Processing
- Solver
- Post-processing

Pre-processing-This is the first step of CFD simulation process geometry generation. One needs to identify the fluid domain of interest. The domain of interest is then further divided into smaller segments known as mesh generation step. This formation of the flow problem for CFD analysis includes:

- Modeling and design the geometry.
- Generation of computational mesh.

- Explain the fluid material properties, initial and boundary conditions for the model.

Solver- Once the problem physics has been identified; fluid material properties, flow physics model, and boundary conditions are set to solve using a computer. Using this it is possible to solve the governing equations related to flow physics problem.

- Selection of flow equations and numerical schemes.
- Predetermined convergence criteria, then iterations.
- Compiling and exporting results for post-processing

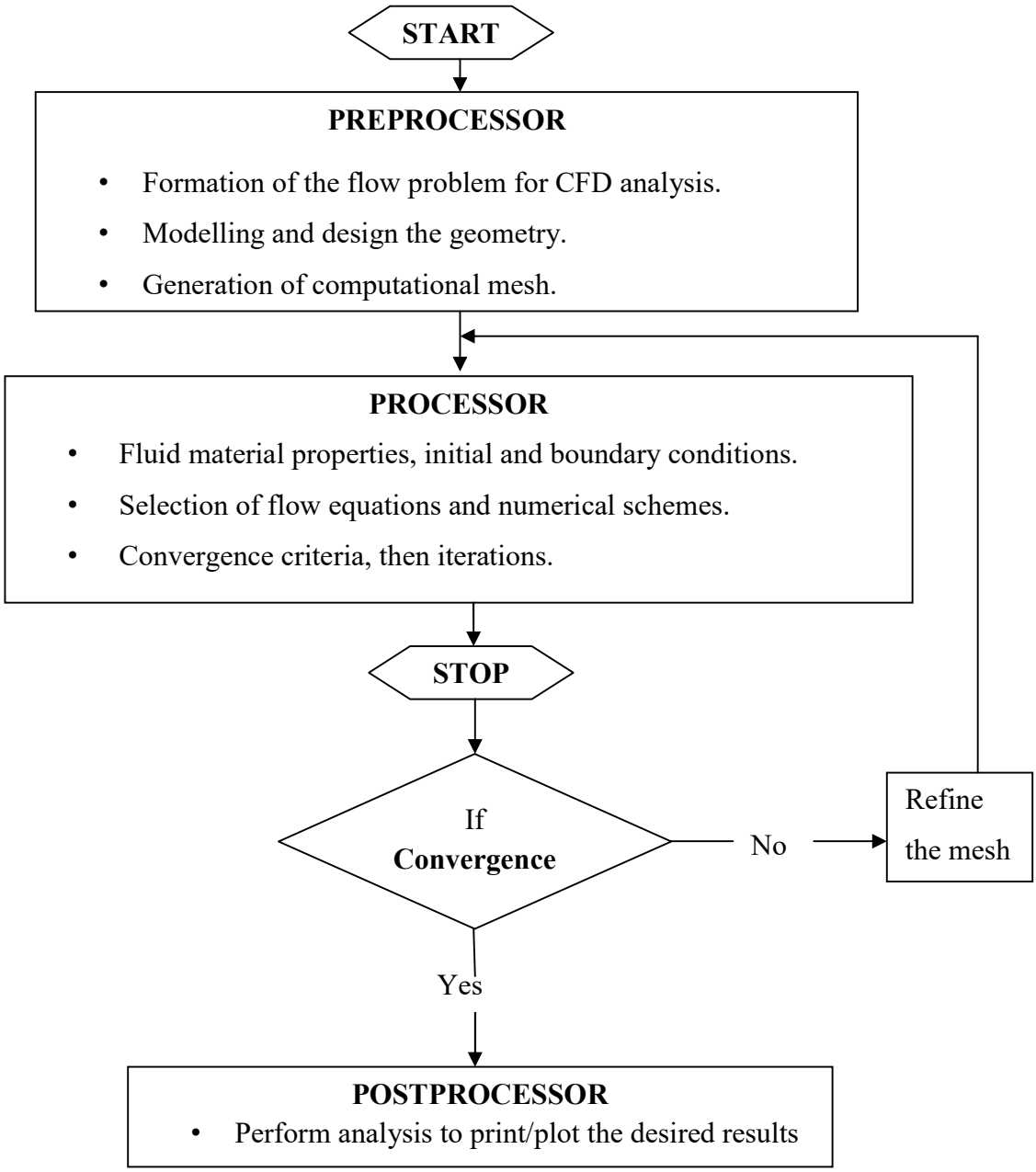

Figure 3.2 CFD Methodology Flowchart

Post-processing- The next step after getting the results is to analyze the results with different methods like contour plots, vector plot, streamlines, data curve etc. for appropriate graphical representations and report.

- CFD distribution images, contours and animations then Analysis and Reporting.

The aim and objective are achieved by:-

- The sample collection of iron-ore.
- The physical, chemical and morphological properties of sample collected.
- The flow characteristics of iron-ore slurry.
- The numerical investigation of pressure drop characteristics of two phase flow at different velocities, concentration and particles size.
- Results, discussion, conclusion and future scope.

3.3 ADVANTAGES AND DISADVANTAGES OF CFD

The CFD has wide range of application due to flexibility to cater wide range of practical applications. Few of advantages of CFD are listed are as below:

Advantages

- CFD is relatively inexpensive as compared to experimental studies.
- The development of new models have increased accuracy and resulted in higher level of consistency.
- CFD have given access to study the variations in design variables.
- CFD has helped the designers for visualizing the flow characteristics of complex geometry and boundary conditions.
- CFD helped engineers for examination of region of interest, and its performance through set of thermal and flow parameters.

Disadvantages

- The numerical errors are generated which depends on the type of hardware, software used and complexity of the problem.

- The input and boundary conditions need to be chosen with great care for accuracy in results.
- The models have a robust system of applicability of physical problems for which they are designed.

3.4 APPLICATIONS OF CFD

CFD had wide range of applications and its advent is increasing with further advancements in computing and hardware facilities. Some of prominent applications are listed as:

- Heat transfer and fluid flow studies.
- Aerodynamics and modeling industries.
- Automobile industry for the study of aerodynamics of car body.
- Structural, cooling flows and ventilation in buildings.
- Designing industries (piping, energy, turomachinery industries and many more).

3.5 MULTIPHASE MODELING

Advancements in the computational fluid mechanics have helped by providing the insights of the multiphase flow. The multiphase modeling has two different approaches. (**Fluent 2011**)

- Euler-Lagrange approach
- Euler-Euler approach

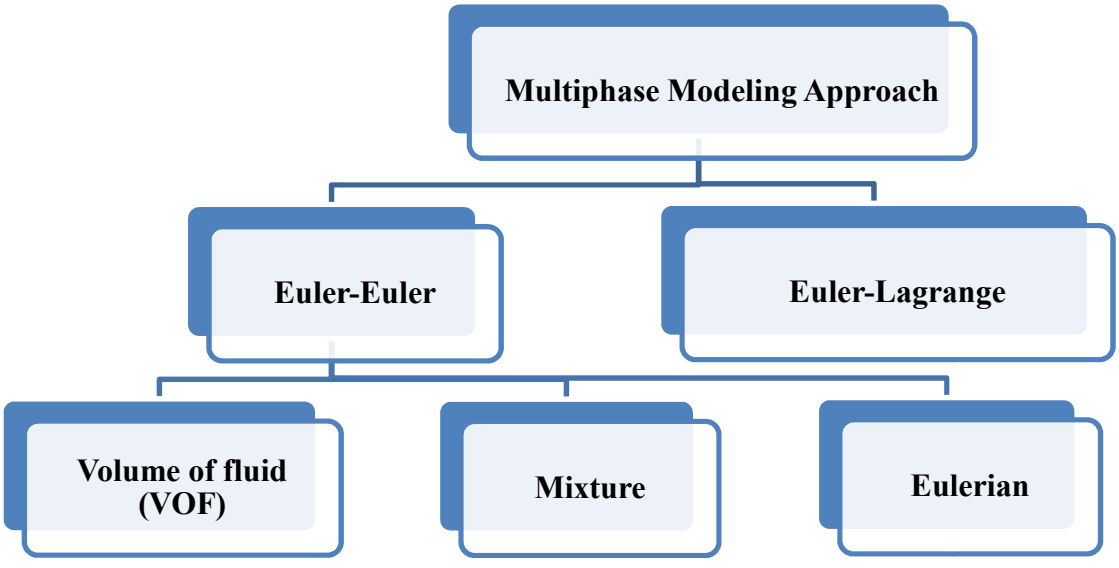

Figure 3.3 Multiphase modeling approaches

3.5.1 Euler-Lagrange Approach

The **Figure 3.4** shows vast continuums of blue colour in which small particles are dispersed as secondary phase. The motion of the continuum phase affects the motion of dispersed phase and continuum phase in the flow. The Euler-Lagrangian model treats the fluid phase as continuum by solving the momentum conservation equations. The dispersed phase or solid phase for solid-liquid flow is solved by tacking large number of particles through calculated flow fields. The exchange of momentum, mass and energy is done between the liquid and dispersed phase. This exchange results in fluid-particle and fluid-fluid interactions which are studied by this approach.

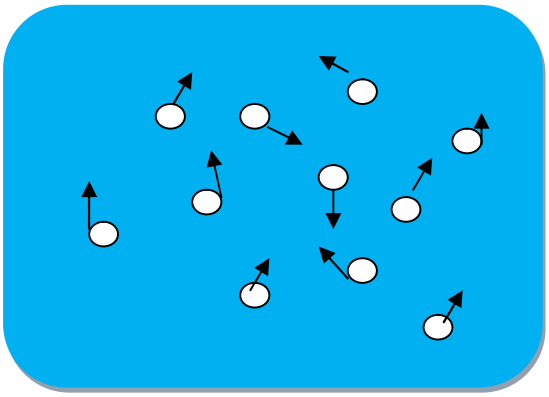

Figure 3.4 Euler-Lagrangian approach

The Euler-Lagrange approach neglects the particle-particle interactions for the simplification of the fluid flow problem. The lower volume fraction loading s required for this model. The particle path throughout the flow is computed individually. The technique of particle tracking for multiphase flow made the approach appropriate for spray dryers, coal and liquid fuel combustion in which the solid loading is low. But, the model is inappropriate for the multiphase flow in which the volume fraction of solid phase cannot be neglected as in modeling of liquid-liquid, fluidized bed flows.

3.5.2 Euler-Euler approach

Euler-Euler is based on the approach that both the dispersed or solid phase and liquid phase are solved using the governing equations i.e. Eulerian approach. The Lagrangian approach is not applied to for dispersed as it was in Euler-Lagrange approach. **Figure 3.5** represents the

continuum phase or liquid phase in blue colour while white spheres dispersed phase. From figure it is shown that the dispersed phase and fluid phase are modelled using governing equations solved within the control volume defined. The flow velocities and volume fractions both the phases are obtained in the control volume using the Eulerian approach for both solid and liquid phases. The exchange of momentum and energy is solved using the governing equations with the application of Reynolds average Navier-stokes equation. The Euler-Euler model is applied to the solid liquid of dense volume fraction of solid phase. Three Euler-Euler models are available in commercial FLUENT software as:

- Volume of fluid (VOF) model
- Mixture model
- Eulerian model

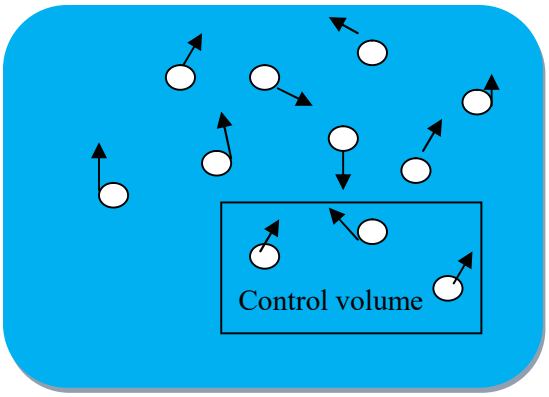

Figure 3.5 Euler-Euler approach

Volume of fluid (VOF) model

The VOF model is applied to the flow in which the solid phase is well separated from the continuum phase as shown in **Figure 3.6**. Therefore, the VOF model is particularly applied for stratified and separated flows. The VOF model solves the conservation equations for both phases using combined solid-liquid mixture properties. The mixture properties affected by the weight of phases is volume fraction which is obtained using the volume fraction o each phase. The weighted properties of slurry are density, viscosity, specific heat etc. The applications of VOF model include stratified flows, free surface flows, filling, sloshing, and the motion of large bubbles in a liquid.

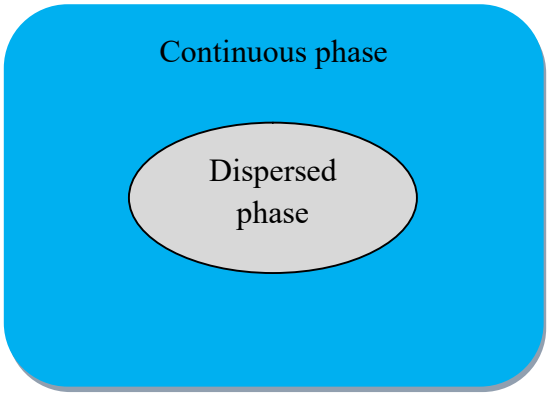

Figure 3.6 VOF model

Mixture model

Mixture model is defined as model applied to the solid-liquid containing two or more phases. The mixture flow is used where the velocity of different phase is different. This model can also be applied to homogeneous solid-liquid flow with strong coupling. The solution of the flow domain is obtained by solving the mixture momentum equation and relative velocities for dispersed phase. The mixture model finds its application to the flow problems as particle-laden flows with low loading, bubbly flows, sedimentation and cyclone separators.

Eulerian Model

Eulerian model have 'n' number of governing equations for each phase, making it to be most complex model. Coupling is achieved through pressure and interphase exchange coefficient. The manner of managing the coupling for granular (solid-liquid) flow is different from non-granular flow (liquid-liquid) flow. The granular flow the properties of the flow are obtained by the kinetic theory. The momentum exchange in-between can be controlled in ANSYS using the user-defined function for customization of momentum exchange. The Eulerian models can be successfully applied to the bubble columns, risers, particle suspension and fluidized bed flows.

3.6 CRETERIA FOR MULITPHASE MODEL SELECTION

Selection of appropriate multiphase scheme depends upon the flow under consideration. The selection of regime is done using which the flow the multiphase model selection is made. The general types of flow and the multiphase model used for their study according to **Fluent 2011**is shown in **Figure 3.7**. From Figure it can be concluded that the selection of multiphase flow approach depends entirely on the nature of flow. For flow study of solid-liquid flow with volume fraction of dispersed medium less than or equal to 10% Discrete phase model (DPM) is employed. Mixture and Eulerian multiphase models are found appropriate for flows having phases mix or separate or flow having the dispersed-phase volume fraction greater than 10%. The extent of accuracy also depends upon model selected. The level of accuracy of Eulerian is more as compared to that of mixture model is more expensive and time consuming.

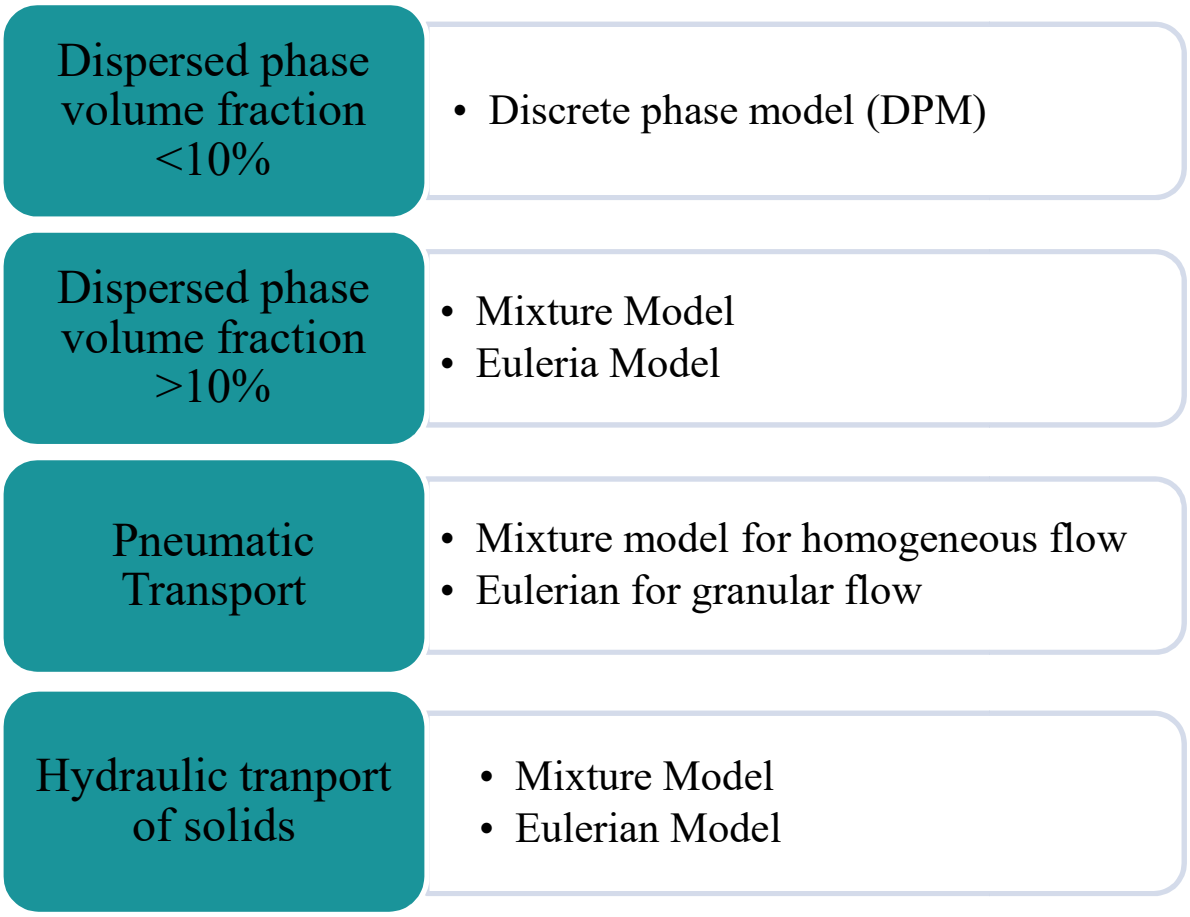

Figure 3.7 Multiphase flow with mulitphase model.

Generally, the regime of flow is determined for selection of multiphase system, appropriate model can be select on the basis of given guidelines:

- For bubbly, droplet and particulate loaded flow having dispersed phase volume fraction greater than 10% mixture or Eulerian model can be employed.
- The study of slug flows and stratified/free surface flow can be done using the VOF model.
- The mixture model for homogenous pneumatic flow and Eulerian for granular based pneumatic flow.
- The study slurry flow and fluidized bed can be made with the application of Eulerian model.

Therefore, the Eulerian model was employed for present study with granular form.

3.7 TURBULENCE MODELING

Turbulence modeling is used to model and simulate disturbances caused due to turbulence in flows. For modeling the turbulence the averaged form of Navier-stokes is used knwon as RANS (Reynolds averaged Navier-stokes equation). The averaging can be time averaging or space averaging or both. The averaging of N-S equation is done to filter out the small fluctuations resulting ease in modeling of turbulence. The first turbulence model is known as Prandtl mixing length theory or one equation turbulence model.

3.7.1 Classification of turbulent modeling

The turbulent flows study can be accomplished using several approaches. There are turbulence models starting from one equation to seven equation turbulence models. The modeling of the turbulence can be done by RANS with suitable model or by computing them directly. The mainly used turbulence models are shown in **Figure 3.8.**

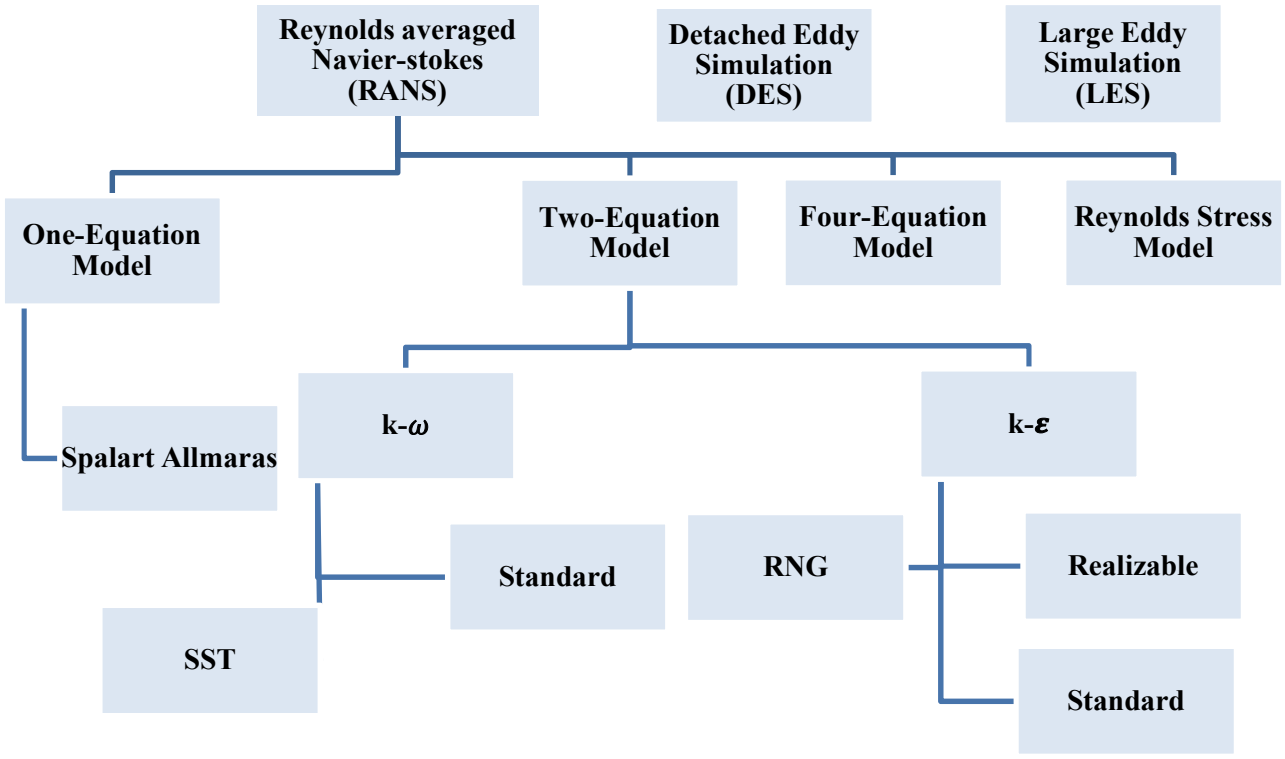

Figure 3.8 Turbulence Models

3.8 COMPUTATIONAL MODEL FORMULATION

Present study is focused on detailed CFD modeling of the flow of Iron ore slurry through pipeline to numerically study the effect of variations in solid concentration, particle size, velocity of flow, radius to diameter ratio for pipe bend on slurry flow characteristics. Mathematical technique adopted is validated with the experimental data of relative pressure drop of iron ore slurry flow.

The application of particular Multiphase model (the discrete, mixture model, Eulerian model) for characterization of the momentum transfer depends upon the volume fraction and the fulfilling the requirements for selection of appropriate model. Generally, the slurry flow is not a dilute system therefore the discrete phase models cannot be applied to these problems. Hence, both the mixture model and Eulerian model are applicable in slurry flow systems. Granular version was preferred than non-granular version of model because slurry flow comprises of medium-particle, medium-medium and particle-particle interaction in the form of collisions and friction which are not taken into account by non-granular version. **Lun et al. (1984)** and **Miller et al. (1992)** proposed a model replacing the gas phase of gas-solid flow with water and taking into account maximum settled concentration. In present study the flow is modeled using granular Euler model.

3.8.1 Eulerian Model

Eulerian approach treats different phases mathematically as interpenetrating continua. It uses the concept of phase volume fraction that volume of one phase cannot be occupied by another phase. α_p and α_c be the volume fraction of particulate "p" in the form of fine powder and carrier fluid "c" in the solid-liquid suspension. These volume fractions are supposed to be in continuum with the space and time and sum is equal to one. Conservation laws are applied individually on each phase separately but are of similar structure. Pressure and interfacial exchange coefficient serves the function for achieving coupling.

Single fluid particle in the suspension bears the forces namely:

1) Force as a result of static pressure gradient, ∇P.
2) Force as a result of solid pressure gradient, ∇P_p.
3) Body force, ρg

4) Drag force as a result of difference between the velocities of two phases i.e. $K_{pc}(\vec{v}_p - \vec{v}_c)$, where K_{pc}represents the coefficient of inter-phase drag and $\vec{v}_p \; and \; \vec{v}_c$ represent velocity of particulate and liquid phase respectively.
5) Force as a result of virtual mass, $C_{vm}.\alpha_p.\rho_c.(\vec{v}_c.\nabla\vec{v}_c - \vec{v}_p.\nabla\vec{v}_p)$, in which $C_{vm} = 0.5$.
6) Viscous force, $\nabla.\overline{\overline{\tau_c}}$, where $\overline{\overline{\tau_c}}$ represents stress tensor for carrier phase.
7) Lift force,$C_l.\alpha_p.\rho_c.(\vec{v}_c - \vec{v}_p)$ X (∇ X$\vec{v}_c$), C_l usually taken as 0.5.

3.8.2 Continuity equation

$$\nabla . (\alpha_a \rho_a \vec{v}_a) = 0 \tag{1}$$

where, *a* can be either *c* or *p.*

3.8.3 Momentum equations

For carrier fluid phase

$$\nabla . (\alpha_c \rho_c \vec{v}_c \vec{v}_c) = -\alpha_c \nabla P + \nabla.(\overline{\overline{\tau_c}} + \overline{\overline{\tau_{t,c}}}) + \alpha_c \rho_c g + K_{pc}(\vec{v}_p - \vec{v}_c) + C_{vm}.\alpha_p.\rho_c.(\vec{v}_c.\nabla\vec{v}_c - \vec{v}_p.\nabla\vec{v}_p) + C_l.\alpha_p.\rho_c.(\vec{v}_c - \vec{v}_p) \text{ X } (\nabla \text{X } \vec{v}_c) \tag{2}$$

For solid particulate phase

$$\nabla . (\alpha_p \rho_p \vec{v}_p \vec{v}_p) = -\alpha_p \nabla P - \nabla P_p + \nabla.(\overline{\overline{\tau_p}}) + \alpha_p \rho_p g + K_{cp}(\vec{v}_c - \vec{v}_p) + C_{vm}.\alpha_p.\rho_c.(\vec{v}_c.\nabla\vec{v}_c - \vec{v}_p.\nabla\vec{v}_p) + C_l.\alpha_p.\rho_c.(\vec{v}_p - \vec{v}_c) \text{X } (\nabla \text{X} \vec{v}_c) \tag{3}$$

Drift velocity is used to models the values of terms comprising of drag forces [$K_{pc}(\vec{v}_p - \vec{v}_c)$ and $K_{cp}(\vec{v}_c - \vec{v}_p)$] for both liquid and solid phase. Turbulent fluctuations in volume fraction are result of this velocity.

P_p is the solid pressure as given by:

$$P_p = \alpha_p \rho_p \theta_p + 2\rho_p(1 + e_{pp})\alpha_p^2 . g_{o,pp} . \theta_p \tag{4}$$

Where, $g_{o,pp}$ is Distribution function signifies the probability of collision of particulates and is given by:

$$g_{o,pp} = \left[1 - \left(\frac{\alpha_p}{\alpha_{p,max}}\right)^{\frac{1}{3}}\right]^{-1} \tag{5}$$

For equation (2) and (3), $\overline{\overline{\tau_{t,c}}}$ is the Reynolds stress tensor, further$\overline{\overline{\tau_c}}$ and $\overline{\overline{\tau_p}}$ is the viscous stress tensor for carrier fluid and particulate solid, are given as:

$$\overline{\overline{\tau_{t,c}}} = -\frac{2}{3}(\rho_c k_c + \rho_c \mu_{t,c} \nabla \vec{U}_c)\bar{\bar{I}} + \rho_c \mu_{t,c}(\nabla \vec{U}_c + \nabla \vec{U}_c^{tr}) \quad (6)$$

$$\overline{\overline{\tau_p}} = \alpha_p \mu_p (\nabla \vec{v}_p + \nabla \vec{v}_p^{tr}) + \alpha_p (\lambda_p - \frac{2}{3}\mu_p) \nabla \vec{v}_p \bar{\bar{I}} \quad (7)$$

$$\overline{\overline{\tau_c}} = \alpha_c \mu_c (\nabla \vec{v}_c + \nabla \vec{v}_c^{tr}) \quad (8)$$

For Solid particulate Bulk viscosity (λ_p) given by:

$$\lambda_p = \frac{4}{3}\alpha_p \rho_p d_p g_{o,pp}(1 + e_{pp})(\frac{\theta_p}{\pi})^{\frac{1}{2}} \quad (9)$$

3.8.4 Shear stress on Solids

Shear and bulk viscosities of suspension is incresed due to momentum exchange because of collision and translation between the solid particulate**Chen et al. (2009)**, $\mu_p$in equation (7) represents the shear viscosity of particulate solid is given by:

$$\mu_p = \mu_{p,col} + \mu_{p,fr} + \mu_{p,kin} \quad (10)$$

where $\mu_{p,col}$, $\mu_{p,fr}$and $\mu_{p,kin}$ are the collision, friction and kinectic viscosities which are given as

$$\mu_{p,col} = \frac{4}{5}\alpha_p \rho_p d_p g_{o,pp}(1 + e_{pp})(\frac{\theta_p}{\pi})^{\frac{1}{2}} \quad (11)$$

$$\mu_{p,fr} = \frac{P psin\varphi}{2\sqrt{I_{2D}}} \quad (12)$$

$$\mu_{p,kin} = \frac{10\rho_p d_p \sqrt{\theta_p \pi}}{96\alpha_p(1+e_{pp})g_{o,pp}} + [1 + \frac{4}{5}\alpha_p \rho_p d_p (1 + e_{pp}) g_{o,pp}]^2 \alpha_p \quad (13)$$

Gidaspow, Bezburuah, and Ding (1992) kinectic enerfgy theroy is used to calculate the granular temperatur

$$\varphi_{cp} = -3K_{cp}\theta_p \quad (14)$$

where K_{cp} is known as coefficient of inter-physical momentum exchange and is given as:

$$K_{cp} = K_{pc} = \frac{3}{4}\frac{\alpha_p \alpha_c \rho_c}{V_{r,p}^2 d_b} C_D(\frac{R_{ep}}{V_{r,b}})|\vec{v}_p - \vec{v}_c| \quad (15)$$

where C_D Is the coefficient of drag and given as:

$$C_D = [0.63 + 4.8\left(\frac{R_{ep}}{V_{r,b}}\right)^{\frac{-1}{2}}]^2 \quad (16)$$

where R_{ep} is given by following relation:

$$R_{ep} = \frac{\rho_c d_c |\vec{v}_p - \vec{v}_c|}{\mu_c} \quad (17)$$

$V_{r,b}$, in equation 15 represents the terminal velocity for particulate solid phase achieved when the accerleration of solid particulate becomes zero. Equation (18) and (19) are the equations used for calculating the values of $V_{r,b}$ for $\alpha_c \leq 0.85$ and $\alpha_c > 0.85$ is given by:

$$V_{r,b} = 0.5(\alpha_c{}^{4.14} - 0.06R_{ep} + \sqrt{[(0.06R_{ep})^2 + 0.12R_{ep}(1.6\alpha_c{}^{1.28} - \alpha_c{}^{4.14}) + \alpha_c{}^{8.28}}] \quad (18)$$

$$V_{r,b} = 0.5(\alpha_c{}^{4.14} - 0.06R_{ep} + \sqrt{[(0.06R_{ep})^2 + 0.12R_{ep}(2\alpha_c{}^{1.28} - \alpha_c{}^{4.14}) + \alpha_c{}^{8.28}}] \quad (19)$$

3.8.5 RNG k–$\boldsymbol{\varepsilon}$ TurbulenceModel

RNG k–$\boldsymbol{\varepsilon}$ model was proposed by (Yakhot and Orszag, 1986) using a statistical technique known as the renormalization group theory. It is similar to the standard k-$\boldsymbol{\varepsilon}$ model, but included the following important enhancements:

1. It further formulates dissipation equations with the application of an additional term to increase the accuracy of the high-speed flow.
2. The RNG model contains turbulent flow effect for swirling flow and accuracy of the swirling flow improves.

RNG theory provides analytical formulas for Prandtl turbulence number while standard k-$\boldsymbol{\varepsilon}$ model uses constant values. RNG turbulence model also provides an analytical differential formula for the effective viscosity considering the effects of Reynolds number. The transport equations for the turbulent kinetic energy and its dissipation rate used for RNG k-$\boldsymbol{\varepsilon}$ model are given as:

$$\frac{\partial}{\partial t}(\rho k) + \frac{\partial}{\partial t}(\rho k \bar{u}_i) = \frac{\partial}{\partial x_j}[(\mu + \frac{\mu_t}{\sigma_k})\frac{\partial k}{\partial x_j}] + P_k - \rho\varepsilon \quad (20)$$

$$\frac{\partial}{\partial t}(\rho\varepsilon) + \frac{\partial}{\partial t}(\rho\varepsilon \bar{u}_i) = \frac{\partial}{\partial x_j}[(\mu + \frac{\mu_t}{\sigma_k})\frac{\partial \varepsilon}{\partial x_j}] + C_{\varepsilon 1}\frac{\varepsilon}{k}P_k - C^*_{\varepsilon 2}\rho\frac{\varepsilon^2}{k} \quad (21)$$

The model constants and the auxiliary relations are c_μ=0.0845, $C_{\varepsilon 1}$= 1:42; $C_{\varepsilon 2}$ = 1:68, $\sigma_k = \sigma_\varepsilon$ =0:7178, $\boldsymbol{\beta}$ = 0.012

$$C^*_{\varepsilon 2} = C_{\varepsilon 2} + \frac{c_\mu \eta^3(1-\eta/\eta_0)}{1+\beta\eta^3} \qquad \text{with } \eta = \frac{Sk}{\varepsilon} \text{ and } \quad \eta_0 = 4.38 \quad (22)$$

The values of the model constants are explicitly obtained in the RNG k–$\boldsymbol{\varepsilon}$ model.

Chapter 4

PRESSURE DROP CHARCTERISTICS OF SLURRY FLOW IN PIPE

In previous chapter the theoretical background of multiphase modeling was discussed. The present chapter focuses on the prediction of heal loss characteristics in straight pipeline for the iron ore slurry flow. The chapter with the discussion on the properties of iron ore and iron ore slurry used for present investigation. Then input parameters for the simulation code are discussed. The results of simulation are verified with the experimental data. The head loss characteristics, volume fraction distribution, turbulent intensity and solid phase velocity profile for straight pipeline is discussed in this chapter

4.1 PROPERTIES OF IRON-ORE SUSPENSION

In present study, an investigation of the pressure drop for multiphase iron-ore water suspension flow through slurry horizontal straight pipe and 90^0 bend is conducted using CFD FLUENT code. The pressure drop characteristics are studied by varying different influencing parameters like fluid velocity, particle size and particle concentration

4.1.1 Particle size distribution

Hematite ore of iron collected from Naomundi Iron ore mines, Jharkhand, India. The known weight of oven dried sample was passed through series of British standard sieves (BS-410) to obtain the particle size distribution (PSD). The result of PSD is shown in **Figure 4.1**. From PSD following conclusion were reported all particles were finer than 250 μm 93.9% particles finer than 106 μm 83.5% particles are finer than 75 μm 31.8% are finer than 53 μm. For simulation purposes the weighted mean diameter was calculated and was found to 59 μm.

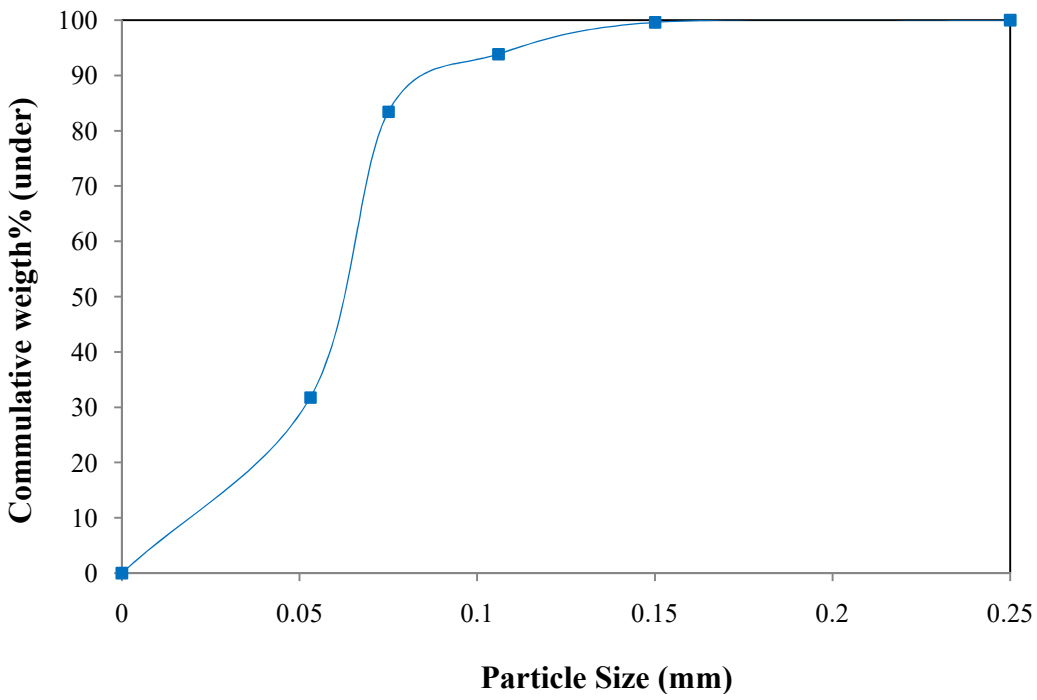

Figure 4.1 PSD of Iron-ore sample

4.1.2 Preparation of iron–ore slurry suspension

Fine sized solid particulate of iron ore were used for preparation of slurry suspension. For each rheological experiment 50 ml solution of iron ore slurry was prepared by carefully mixing of known amount of fine sized iron ore particles with tap water required for preparation of required solid concentration. Amount of solid particles to be mixed with the water were carefully weighed in a beaker. Required amount of water was added. The mixture was gently mixed for 15-20 mins for proper mixing of suspension. Then the solution was poured into the cylindrical arrangement for rheological and settling experiments.

4.1.3 Properties of slurry

Viscosity is essential property of the slurry which plays a vital role in flow behaviour of slurry flow through pipeline system. Viscosity of iron-ore suspension is measured for varying concentration ranging from 20-60 %. Concentration by weight was converted to volume fraction. The values of viscosity and volume fraction for varying concentration of solid (by weight) are given in **Table 4.1**. **Table 4.2** represents the slurry properties with varying particle size from less than 53 μm to particle of size between 75-106 μm.

Table 4.1 Variation of viscosity and volume fraction with concentration

Concentration (% by weight)	Viscosity (Pa.s)	Volume fraction	Nature
20	0.0023847	0.0547	Newtonian
30	0.0049816	0.09025	Newtonian
40	0.0228	0.13369	Non-Newtonian
50	0.046684	0.18797	Non-Newtonian
60	0.054616	0.257732	Non-Newtonian

Table 4.2 Variation of viscosity with particle size for 60% solid concentration (by weight)

Particle Size (μm)	Concentration (% by weight)	Viscosity (Pa.s)
Less than 53	60	0.064298
53-75	60	0.055475
75-106	60	0.38542

4.2 FLOW DOMAIN

Pipeline geometry was modelled by using ANSYS R15.0 software package. The length of the straight pipe was taken greater than 1 m which is sufficient enough to maintain fully developed flow. **Figure 4.2** shows schematic diagram of straight pipe. The diameter of pipe was kept constant i.e. 50 mm. Material of pipelines was considered as mild steel. Multiphase fluid flow contains water taken as liquid phase and iron ore was injected at inlet face of pipeline. The solid concentration of iron ore slurry was varied ranging from 20% to 60% (by weight) with particle diameter 26-90μm.The velocity of flowing fluid was varied from 2 to 5 m/s. The properties of iron-ore slurry are discussed in Table 4 and Table 5.Simulations were carried out at Windows based Intel Xenon E51607v2 3.0 machine having 2.59 GHz processing unit and 16 GB RAM and converged when residuals of governing equations drops below 10^{-4}.

Figure 4.2 Schematic diagram of straight pipe

4.3 DISCRETIZATION OF THE DOMAIN

In order to evaluate the flow behaviour accurately at every section of pipe, the pipe was discretized into smaller number of elements. The systematic meshed domain of straight pipe is shown in **Figure 4.3**.

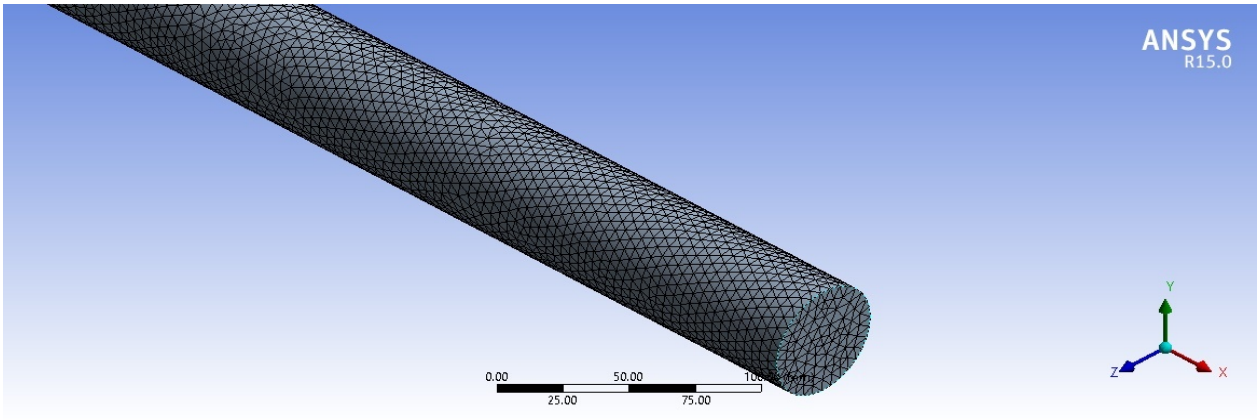

Figure 4.3 Meshed Domain of straight pipe

4.4 BOUNDARY CONDITIONS

The boundary conditions applied were velocity inlet, pressure outflow and no-slip boundary conditions. Volume fraction and velocity was applied at the inlet of the pipe for generating the fully developed flow. Outlet boundary condition was applied at horizontally long outlet section 1.5 m apart having similar grid structure. The wall surface having roughness constant of 0.5 mm was subjected to no-slip condition. First order scheme was employed for solving momentum, turbulent kinetic energy, pressure correction and turbulence dissipation rate. The SIMPLE algorithm (**Patankar,1980**) was used to couple the pressure and velocity. The convergence was achieved when variation of residuals of governing equations for consecutive iterations drops below 10^{-4}.**Table 4.3** gives the detailed information of the input parameters given for the simulation.

Table 4.3 Input parameter for simulation in FLUENT

Category	Description	Input
Model	Multiphase Model	a) Eulerian Model b) No. of phases - 2
	Viscous Model	a) k-ε turbulence, RNG b) standard wall function c) mixture phase
Interaction and Phase properties	Phase 1 (Primary)	Water
	Phase 2 (Secondary)	Iron ore, (Granular)
	Particle Diameter	59 μm 26, 64 and 90 μm
	Granular viscosity	Symlal-Oberian
	Granular Bulk Viscosity	Lun et al.
Operating Parameters	Operating Pressure	101325 pa
	Acceleration due to gravity	-9.81 m/s^2 in negative y direction
Boundary Conditions	Inlet	Constant velocity at inlet for both phases. Velocity inlet normal to boundary and constant volume fraction of secondary phase.
	Outlet	Pressure outlet with 0 gauge pressure
	Wall	No-slip at wall
Solution control	Pressure velocity coupling	PC-SIMPLE
	Momentum	First order upwind
	Volume fraction	First order upwind
	Turbulent Kinetic Energy	First order upwind
	Turbulent Dissipation Rate	First order upwind

4.5 GRID INDEPENDENT TEST

Tetrahedral-cooper type mesh was used for discretization of flow domain. Grid independency was performed to analyse the optimum mesh size. Meshing was done using ANSYS 15.0 Design Modeler (DM) with five different cell sizes. Total number of elements for 4, 5, 6, 7 and 8 mm cell size was found as 410146, 211533, 123014, 77204, and 52836 respectively. The grid independency was performed on 59 μm particle size for solid concentration of 60% for flow velocity of 5 ms^{-1}. The variation in head loss with number of elements is represented in Figure 3. Results showed that decrease in head loss becomes independent after 211533 elements. Therefore, the optimum mesh size was found to be 5 mm and was further used for numerical investigations.

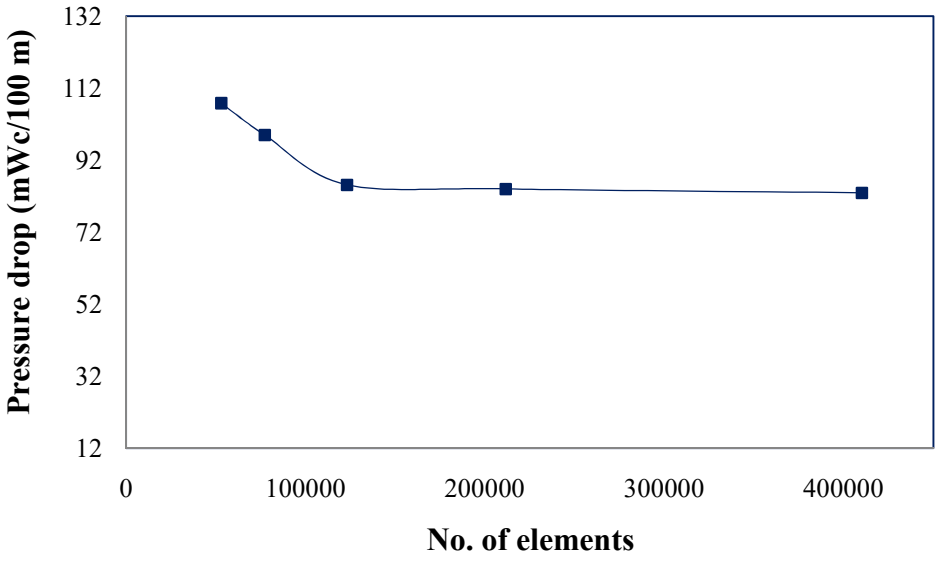

Figure 4.4 Pressure drop with increase in number of elements

4.6 COMPARISON OF DIFFERENT TURBULENT SCHEMES

Computational analysis was done on ANSYS Fluent 15.0 commercial version. The validation of numerical code was done by comparing the simulation results with the experimental results of **Mukhtar et al. (1995)**. Various numerical simulation models were compared prior to carry out the simulations. Literature study reveals that models used for the computational study of flow characteristics of multiphase flow are k-ω (SST and standard) and k-(Realizable, RNG and Standard). **Mukhtar et al. (1995)** had performed an experimental study on iron ore-water slurry flow in horizontal straight pipeline and elbow (90º). Numerical simulation was carried

for the iron ore-water slurry flow in straight pipeline and 90^0 bend at varying velocity range of 1.106 to 3.06 m/s with solid concentration of 40% (by weight). The specific gravity of the particle was taken as 4.2 with mean particle size of 49 μm. Figure 4 depicts the comparison of experimental data with numerical simulation of five different turbulent models. The standard deviation between experimental and simulated data of relative head loss for standard *k-ω*, SST *k-ω*, Standard *k-ε*, RNG *k-ε* and Realizable *k-ε* was found to be 16.87, 15.2547, 13.39, 10.66 and 12.02% respectively. Simulated results using RNG *k-ε* was found to be showing least deviation with the experimental result. Therefore, RNG *k-ε*model was used in further investigation.

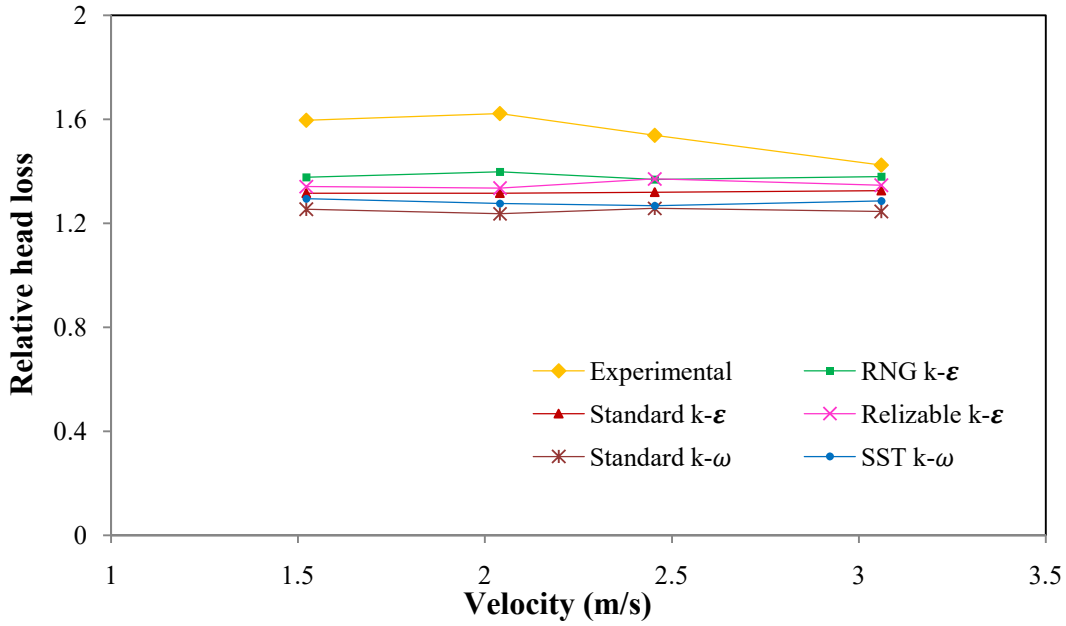

Figure 4.5 Comparison of different computational models with experimental results

4.7 PRESSURE DROP FOR STRAIGHT PIPE

4.7.1 Effect of concentration and velocity

The effect of concentration and flow velocity on the head loss characteristics is shown in **Figure 4.6**. It was found that head loss increases with increase in velocity as well as concentration of solid particles. The rate of increase in head loss was higher at low velocities as compared to high velocities. The increase in head loss with flow velocity was observed due

to increase in particle-particle, particle-liquid and liquid-liquid interactions. Increase in solid concentration resulted in overcrowding of slurry flow. The root cause of increase in head loss with increase in solid concentration was due to increase in viscosity and density of iron ore slurry. Therefore, the head loss was found to be having an increasing trend with solid concentration and velocity. At 20% solid concentration, the head loss was increased by 52.56, 41.28 and 34.11% with increase in flow velocity from 2-3, 3-4, and 4-5 m/s respectively. The increase in head loss was 51.59, 42.59 and 34.91% for 60% solid concentration with increase in flow velocity from 2-3, 3-4, and 4-5 m/s respectively.

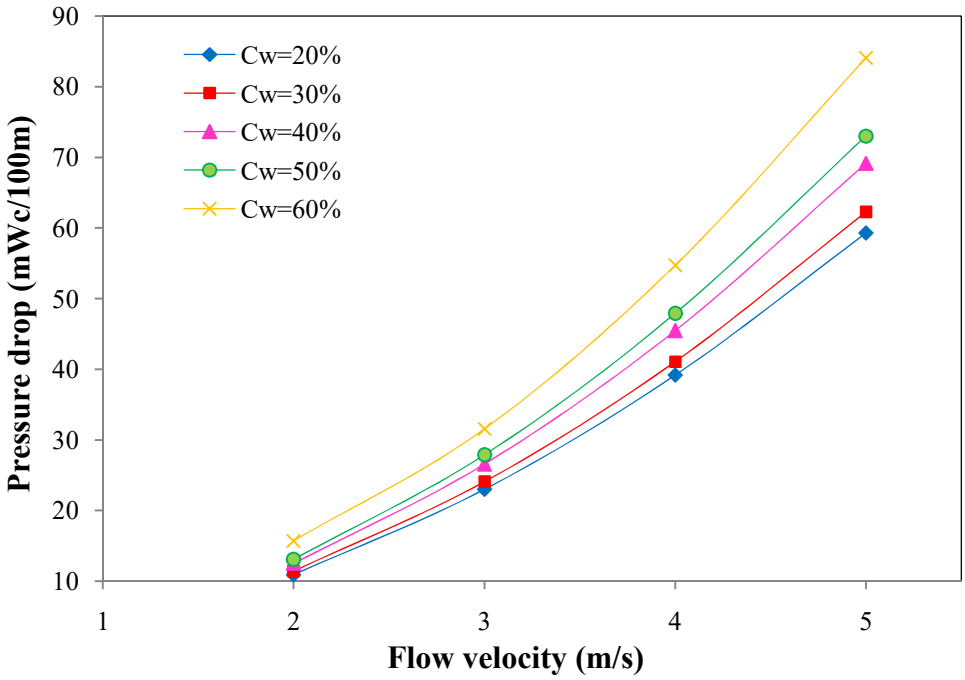

Figure 4.6 Pressure drop for varying velocity and concentration of iron ore slurry

Similar trend was observed for other solid concentration. For flow velocity of 5 m/s head loss was increased by 5, 11.03, 5.636 and 15.09% with increase in solid concentration from 20-30, 30-40, 40-50 and 50-60% respectively. Maximum head loss was observed at 60% solid concentration and 5 m/s flow velocity.

4.7.2 Effect of particle size

The study of head loss characteristics is a crucial step for optimization of slurry piping and pumping system. The study of head loss with varying particle size was studied as particle size distribution of solid particles plays a predominant role. The variation of particle size results in change of slurry properties due to which flow behavior changes. The mean size of solid particles was taken as 26, 64 and 90 µm. Head loss characteristics for straight pipe with the variation in mean particle size is shown in **Figure 4.7**. From results it was observed that head loss increased with solid particle size. Higher head loss was noticed for flow of coarser particle slurry (90 µm) as compared to finer particulate slurry. This occurs as iron being hard solid exhibits higher viscosity for coarse particulate slurry as compared to finer. The increase in viscosity of coarse particulate slurry is due to increase in surface irregularities with particle size. At flow velocity of 5 m/s the head loss was increased by 5.65 and 11.89% when particle size was increased from 26-64 and 64-90 µm respectively. As the particle size was increased from 64-90 µm the head loss was increased by approximately two times as compared to particle size range of 26-64 µm.

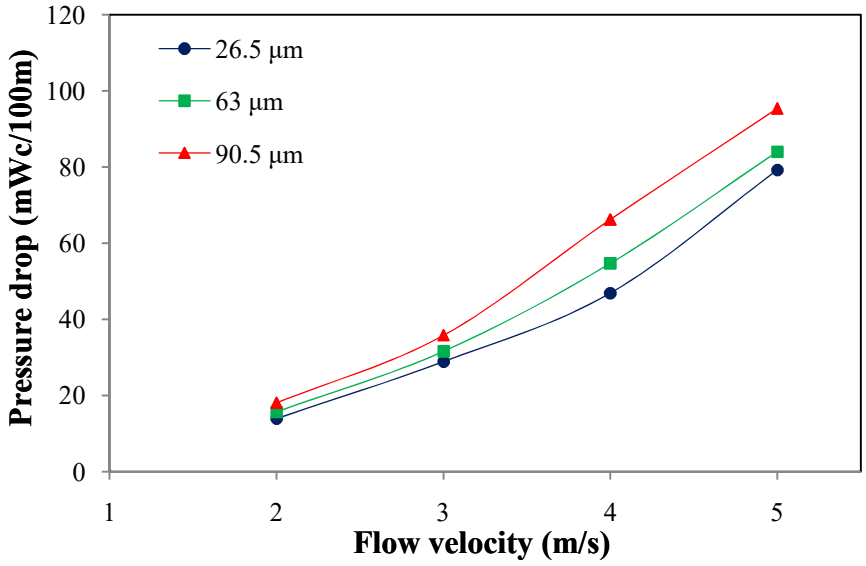

Figure 4.7 Effect of particle size on pressure drop of iron ore slurry at 60% solid concentration

4.8 VOLUME FRACTION DISTRIBUTION FOR STRAIGHT PIPE

4.8.1 Effect of particle size

The volume fraction distribution is highly affected by solid particle size**. Figure 4.8** depicted the variation in volume fraction distribution with particle size for 60% solid concentration at flow velocity of 5 m/s through straight pipeline. The higher settling zone was observed at the bottom of the pipe. The accumulation of solid particles at bottom of pipe was due to gravity. The higher concentration area was largest for coarser particle size (90 µm) and smallest for finer particle size (26 µm). With increased particle size the momentum required to keep the particles in motion due to increase in mass of particles. The settled concentration region widened with increase in particle size was due to variation in viscosity of slurry.

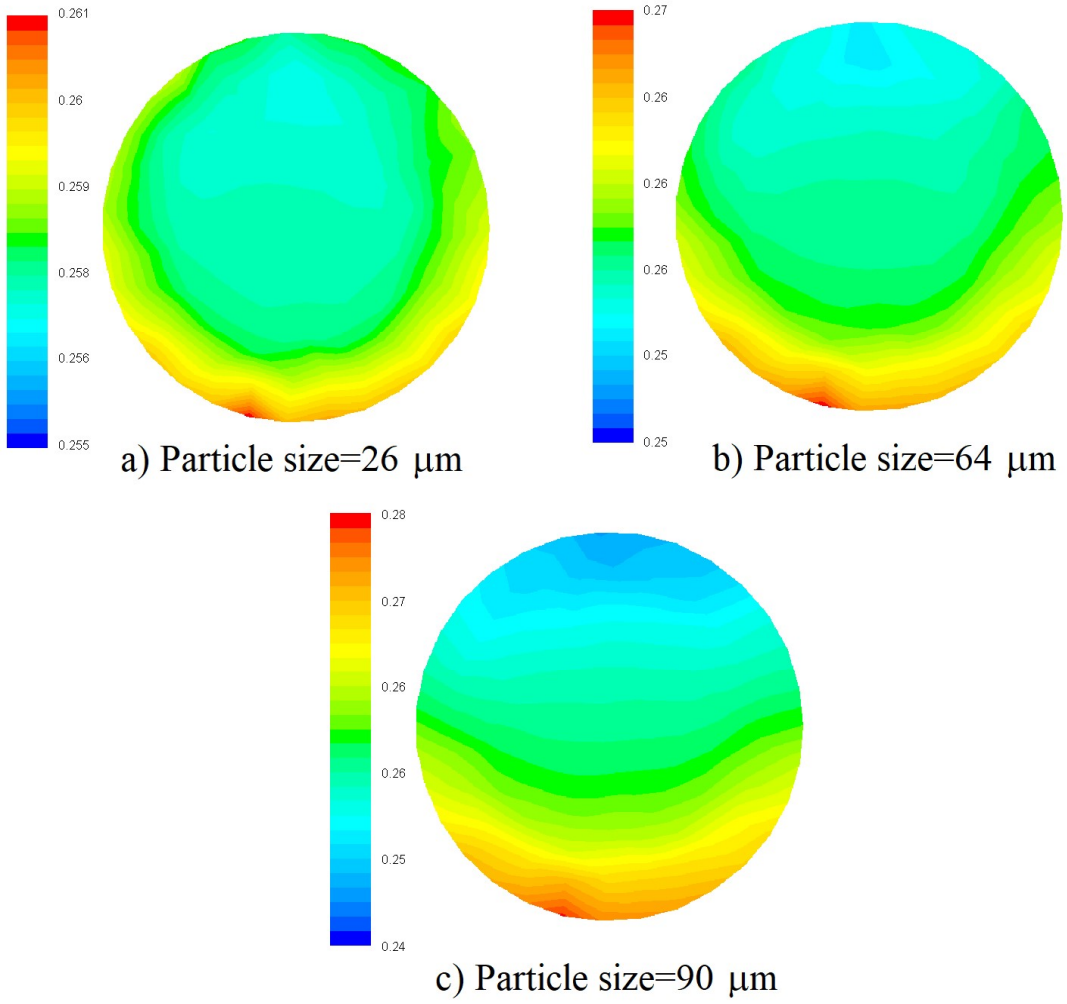

Figure 4.8 Effect of particle size on volume fraction distribution

4.8.2 Effect of concentration and velocity

The volume fraction distribution of solid particles is influenced by the solid concentration and flow velocity of the slurry. **Figure 4.9** represents the volume fraction contours at varying velocity range of 2-5 m/s for 60% solid concentration. From results the existence of higher volume fraction was the action of gravity on the solid particles. For 2 m/s flow velocity this region is larger as compared to for 5 m/s because with increase in velocity the solid carrying capacity of water increases. With increase in velocity the kinetic energy of fluid flow increases hence decrease the settling and similar trend was observed for lower solid concentrations. **Figure 4.10** shows the volume fraction distribution for 5 m/s flow velocity with varying concentration range of 20-60% for iron ore-water slurry. The increase in solid concentration resulted higher volume fraction of solid at bottom of pipe. This happened due to increase in density of slurry with solid concentration. From contours it was depicted that region of lower and higher solid concentration decreased with flow velocity while increased with solid concentration.

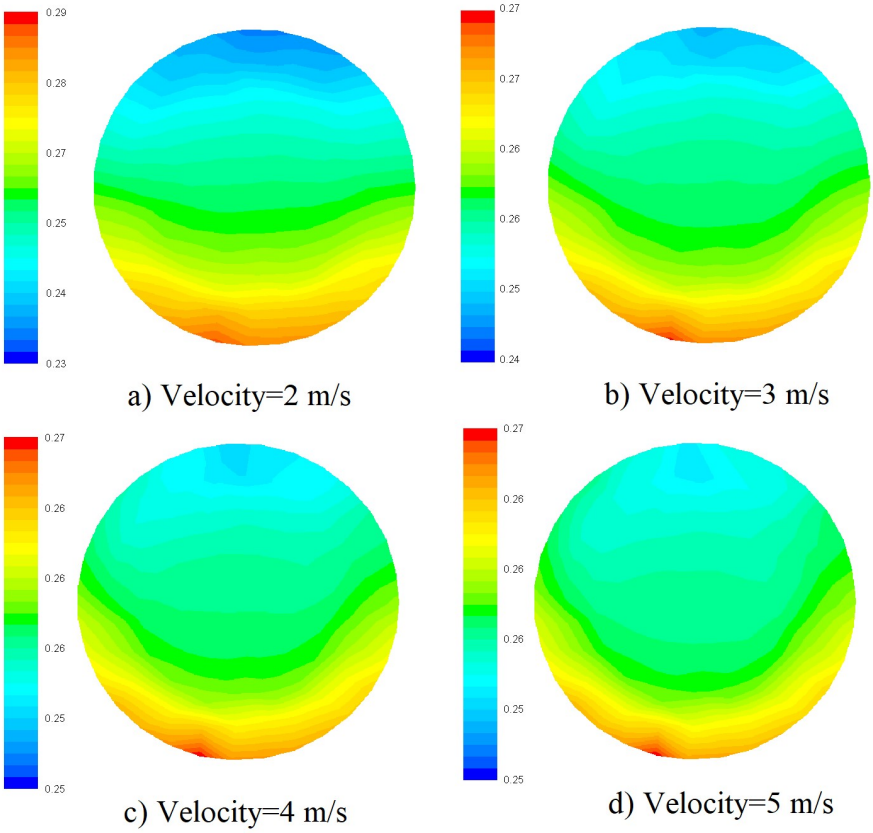

Figure 4.9 Volume fraction contours at varying velocity at 60% solid concentration

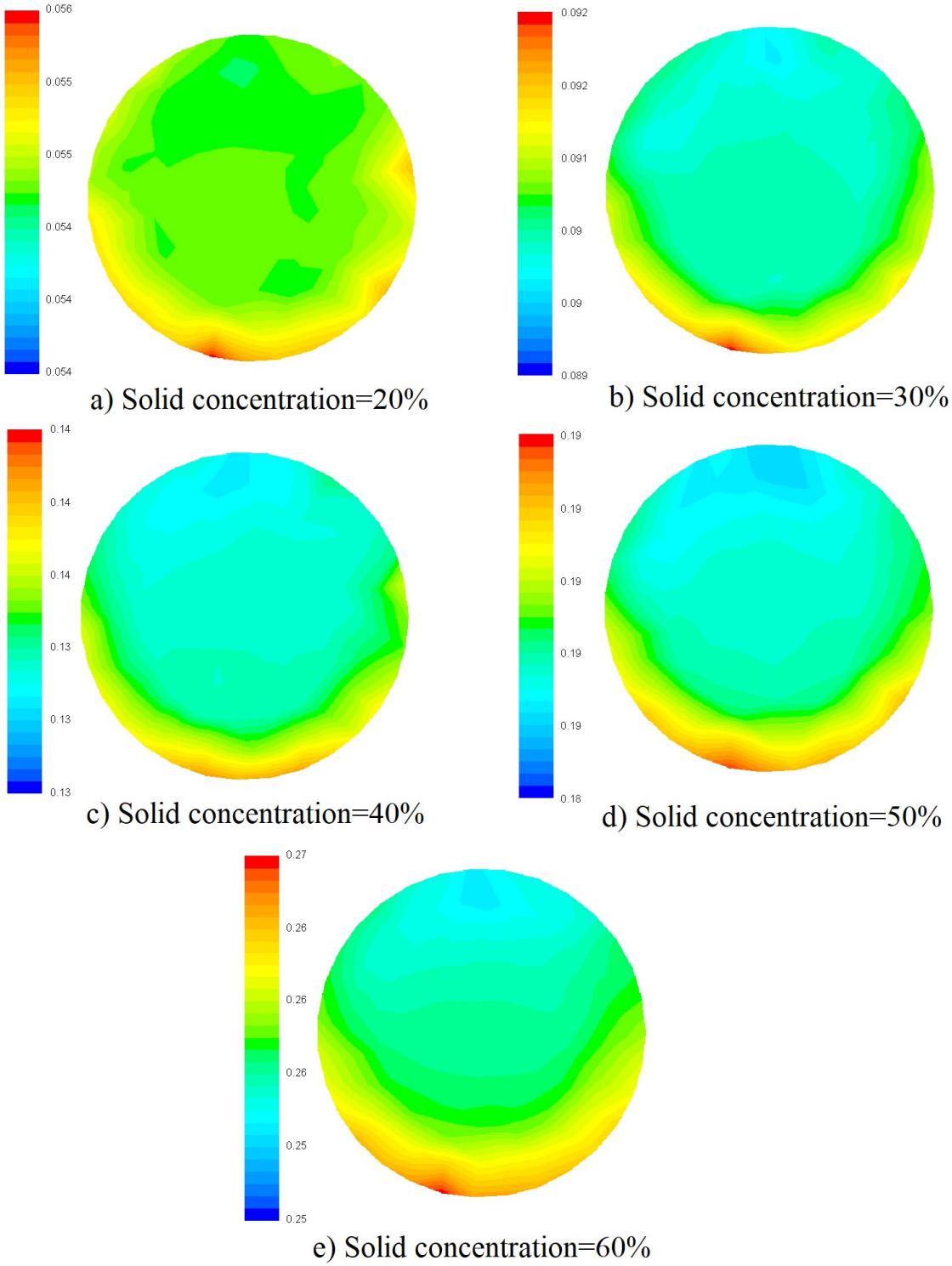

Figure 4.10 Volume fraction contours at varying solid concentration at 5 m/s flow velocity

4.9 TURBULENCE INTENSITIES FOR STRAIGHT PIPE

4.9.1 Effect of particle size

Turbulent intensity gives measure and location of losses due to turbulence. Turbulent intensity contours of slurry flow at horizontal pipe outlet with varying particle sizes are shown in **Figure 4.11.** The efflux concentration was taken as 60% with flow velocity 5 m/s. For straight pipe the increase in particle size resulted in small fluctuations in turbulence intensities. The increase in particle size from 26-90 µm resulted marginal increase in higher turbulence region. The higher turbulent intensity region was found at the outer periphery of pipe while lower at the central region of flow. The turbulence generated due to the interaction of solid particle with wall of pipe resulted in higher turbulent region at pipe periphery. The area increased with particle size due to increased interaction of particles with wall. This increase in turbulent intensities can be seen due to anomalies generated with the action of change in viscosity and density with increase in particle size.

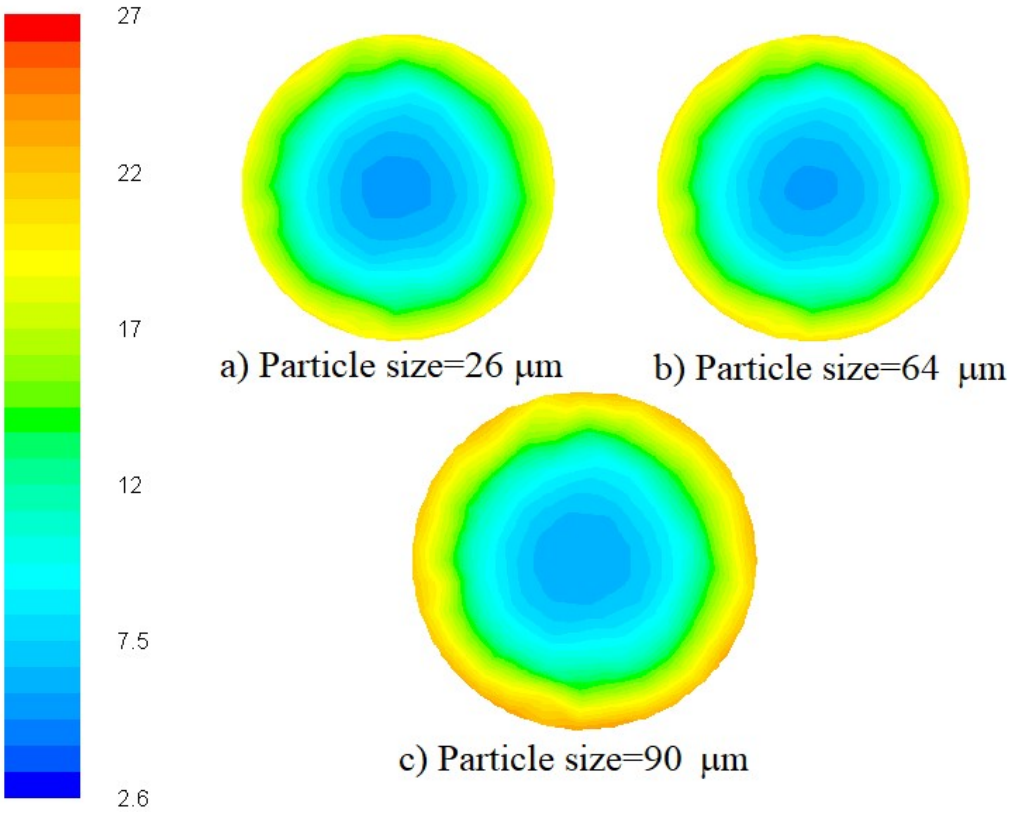

Figure 4.11 Turbulent intensity contours with varying particle size

4.9.2 Effect of concentration and velocity

The effect of velocity on turbulent intensity at pipe outlet for iron ore slurry flow of solid concentration 60% solid concentration is shown in **Figure 4.12**. The increase in flow velocity resulted for increase in turbulent intensity. This increase can be attributed due to the fact that increase in velocity caused increase in losses due to turbulence. The upper range of turbulent intensity increased 33.33, 28.57 and 19.23% with increase in flow velocity 2-3, 3-4 and 4-5 m/s respectively. **Figure 4.13** represents the effect of variation in solid concentration ranging from 20-60% for flow velocity of slurry taken as 5 m/s flowing through straight pipe. Results showed that the variation in turbulent intensity was very marginal with increment in solid concentration. Hence, with the combined effect of concentration and velocity, velocity plays a dominating role. The influence of variation in velocity on turbulent intensity contours was more than with solid concentration.

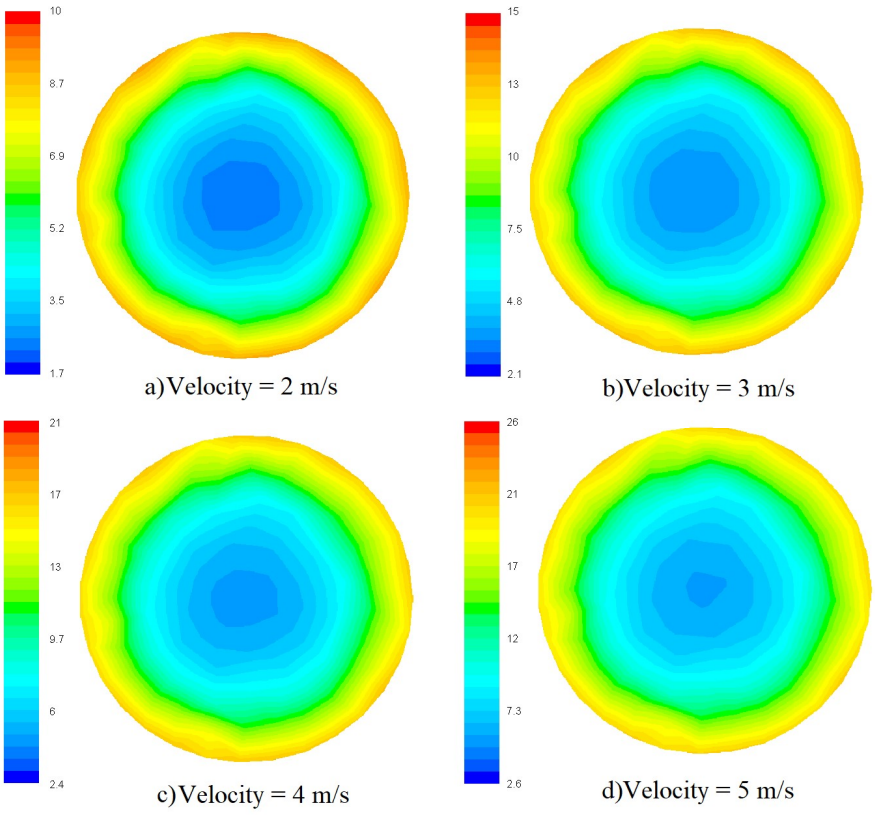

Figure 4.12 Turbulent intensity contours at varying velocity at 60% solid concentration

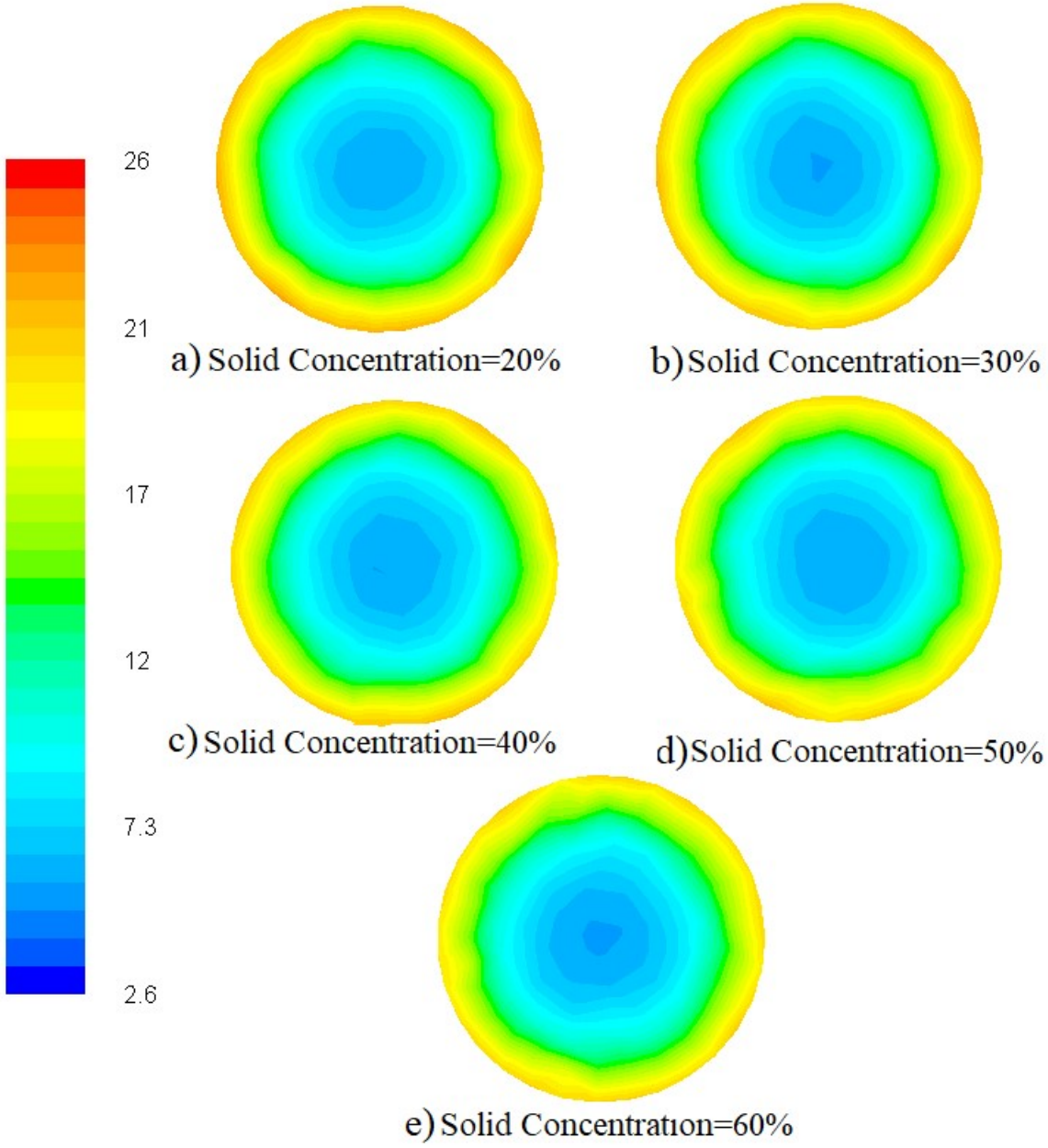

Figure 4.13 Turbulent intensity contours at varying solid concentration at 5 m/s flow velocity

4.10 SOLID PHASE VELOCITY PROFILE FOR STRAIGHT PIPE

4.10.1 Effect of particle size

The effect of particle size on velocity profile at the outlet of horizontal pipe for iron ore slurry flow of 60% efflux concentration for flow velocity of 5 m/s is shown in **Figure 4.14**. From **Figure 4.14** it was depicted that velocity profiles are having asymmetric profile and degree of asymmetry increases with particle size. The velocity was highest at the centre region of the pipe. As moving from pipe wall to centre of pipe the velocity of solid phase increased. The minimum value was near the wall of pipe due to frictional resistance offered to solid particles by pipe wall. The resistance to flow decreased as moving towards the centre of pipe.

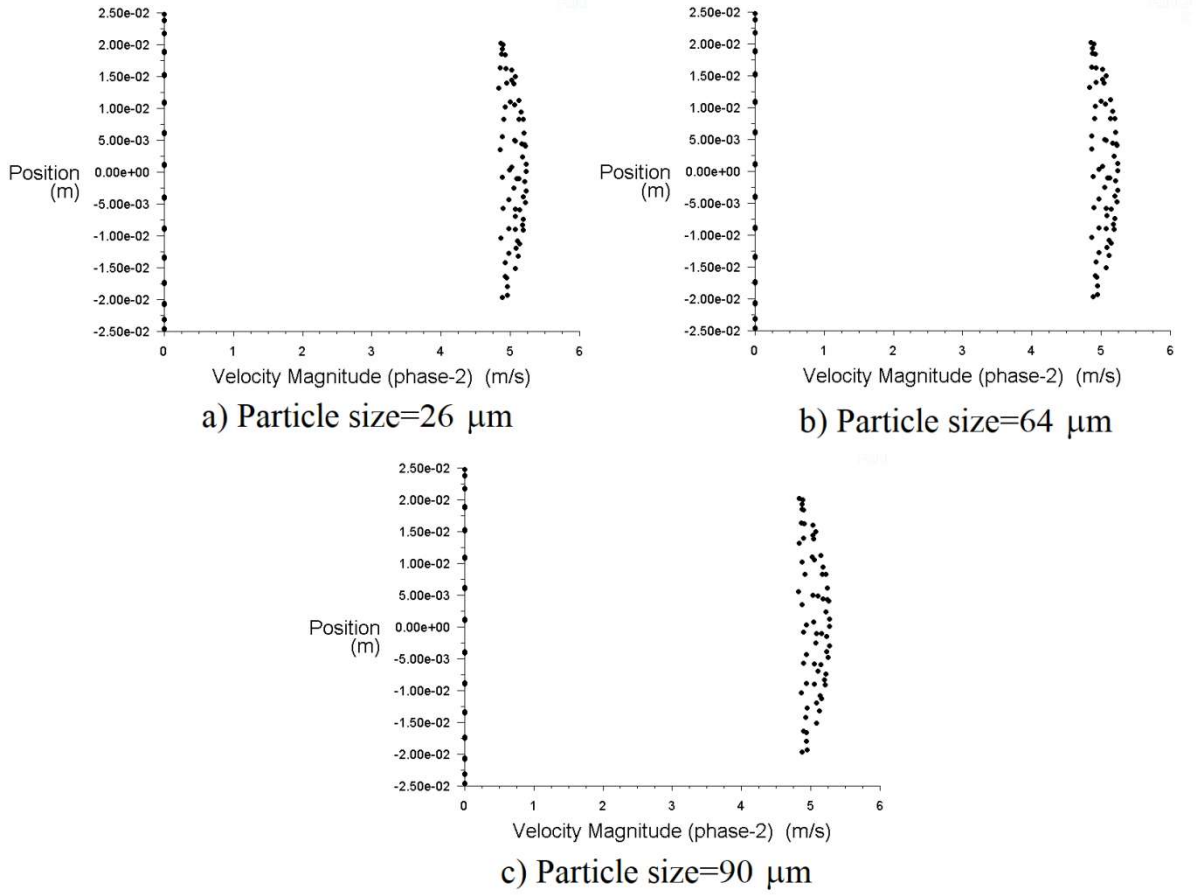

Figure 4.14 Velocity profiles with varying particle size

4.10.2 Effect of concentration and velocity

Effect of solid concentration varied range of 20-60% on solid phase velocity distribution is shown in **Figure 4.16** with flow velocity 5 m/s. The profiles are having marginal changes with variation in solid concentration. The change was due to variations in flow properties i.e. viscosity and density of slurry flow. Effect of solid concentration on velocity distribution is shown in **Figure 4.15**with velocity varied range of 2-5 m/s at solid concentration of 60%Velocity distribution curves were having similar profile with increase in velocity. The increase in velocity resulted the shifting of mean velocity curve to the given flow velocity.

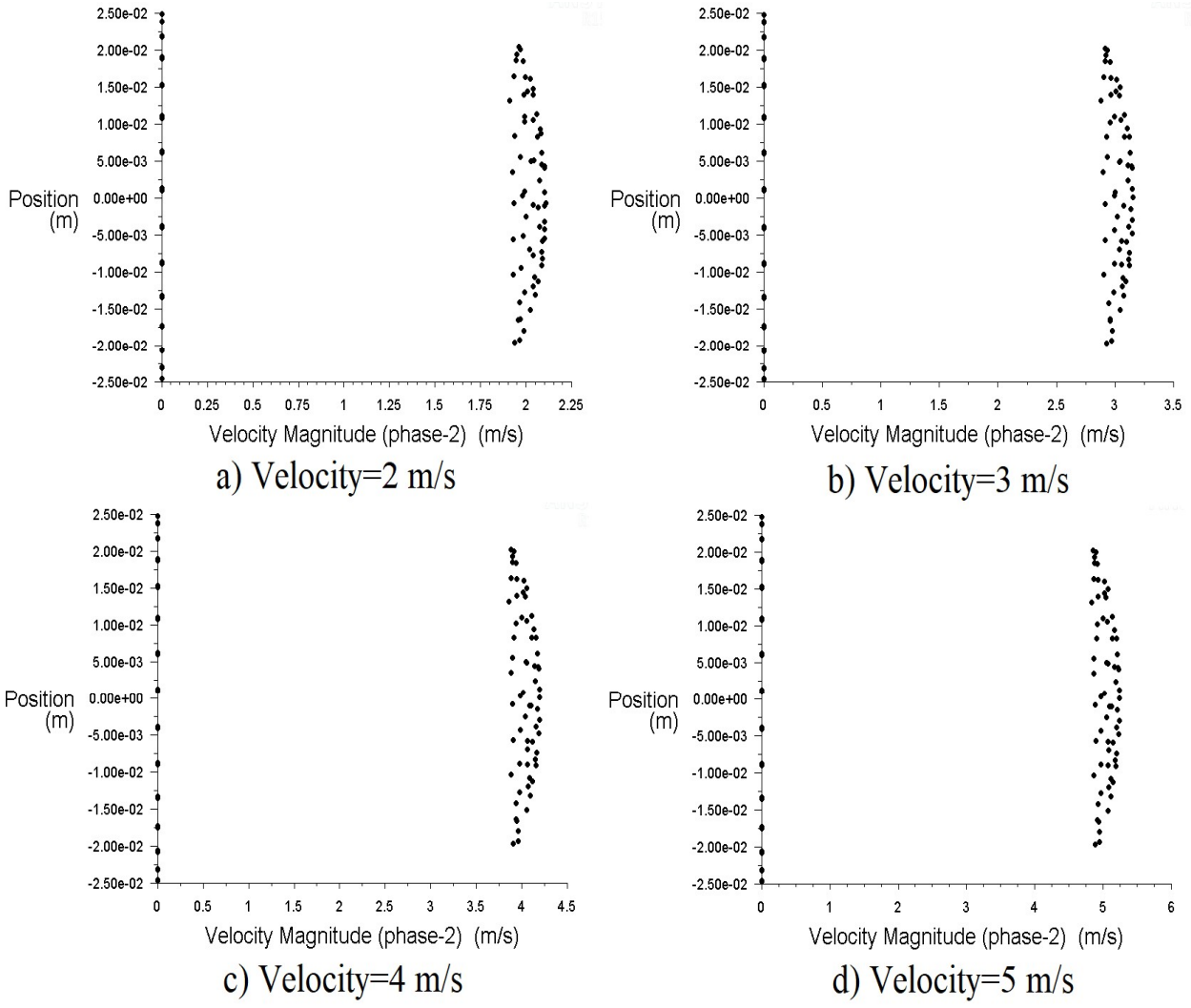

Figure 4.15 Velocity profile at varying velocity at 60% solid concentration

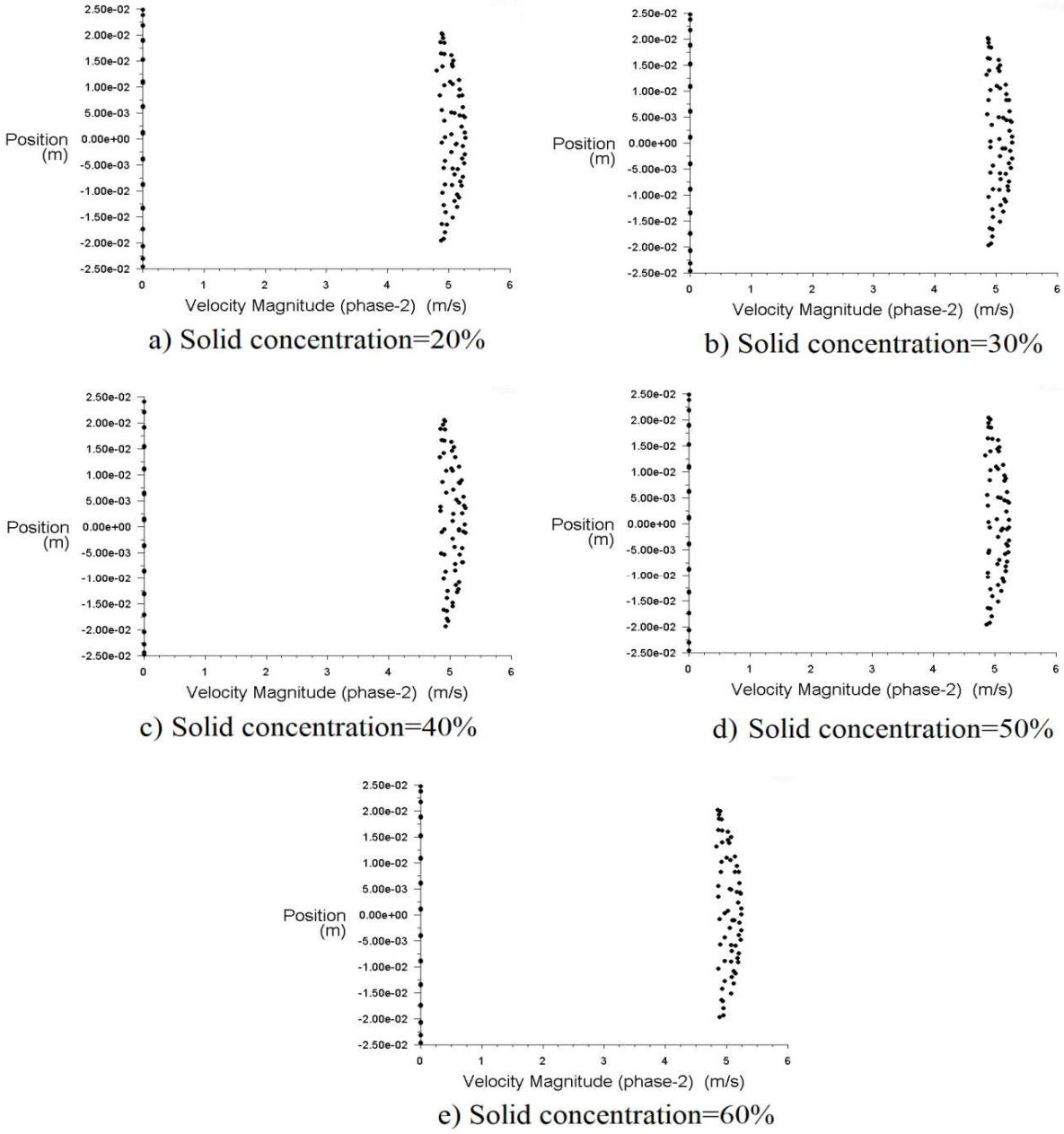

Figure 4.16 Velocity profile at varying solid concentration at 5 m/s flow velocity

Chapter 5

PRESSURE DROP CHARCTERISTICS OF SLURRY FLOW IN PIPE BEND

In previous chapters, the model was developed for the study of iron ore slurry flow. The turbulence model used for the study is RNG k-$\boldsymbol{\varepsilon}$ because it has minimum deviation with the experimental relative pressure drop values for iron ore slurry flow. Equations used by model

Numerical simulation of iron ore slurry flow is done using Eulerian-Eulerian multiphase model and RNG k-$\boldsymbol{\varepsilon}$ turbulent model using standard wall function and mixture multiphase properties. Carrier fluid i.e. primary phase used is water and dispersed phase is Iron ore (specific gravity 4.320). Boundary condition at inlet and outlet are velocity inlet with both the phases with equal and constant velocity and pressure outlet of 0 gauge pressure with No-slip wall condition. Simulation was carried at velocity varying from 2-5 m/s i.e. 2, 3, 4 and 5 m/s. and solid concentration ranging from 20-60% concentration i.e. 20, 30, 40, 50, and 60% (by weight). Pressure velocity coupling was obtained using PC-SIMPLE algorithm (**Patankar 1980)** and first order upwind scheme was used for discretization of momentum, volume fraction, turbulent kinetic energy (k), and turbulent dissipation rate ($\boldsymbol{\varepsilon}$). Convergence criteria were taken to be 10^{-4}.

Numerical model developed is used to study the effect of different parameters on pressure drop, volume fraction distribution and other flow characteristics for 90^0 pipe bend is discussed in this chapter.

5.1 FLOW DOMAIN

Pipeline geometry was modelled by using ANSYS R15.0 software package. The length of elbow was taken greater than 1 m which is sufficient enough to maintain fully developed flow. **Figure 5.1** schematic diagram of elbow geometry. The radius-to-diameters ratio (r/D) for elbow was taken as 1, 1.5, 2, 2.5, 3, and 4. Material of pipelines was considered as mild steel.

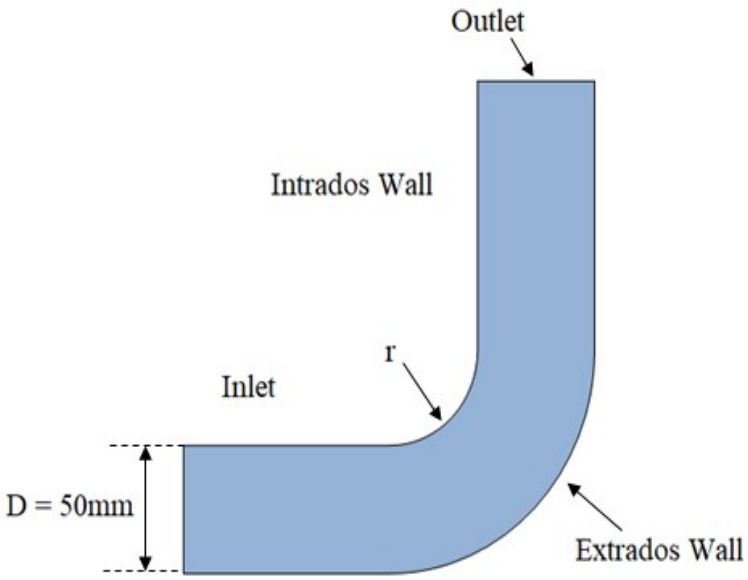

Figure 5.1 Schematic diagram of elbow geometry

5.2 Discretization of the domain

In order to evaluate the flow behaviour accurately at every section of pipe, the pipe was discretized into smaller number of elements. The systematic meshed domain of 90° elbow is shown in **Figure5.2.** In present work, the domain was divided into 221275, 226785, 232002, 224941, 243359, and 255308 tetrahedral elements for r/D ratios of 1, 1.5, 2, 2.5, 3, and 4.

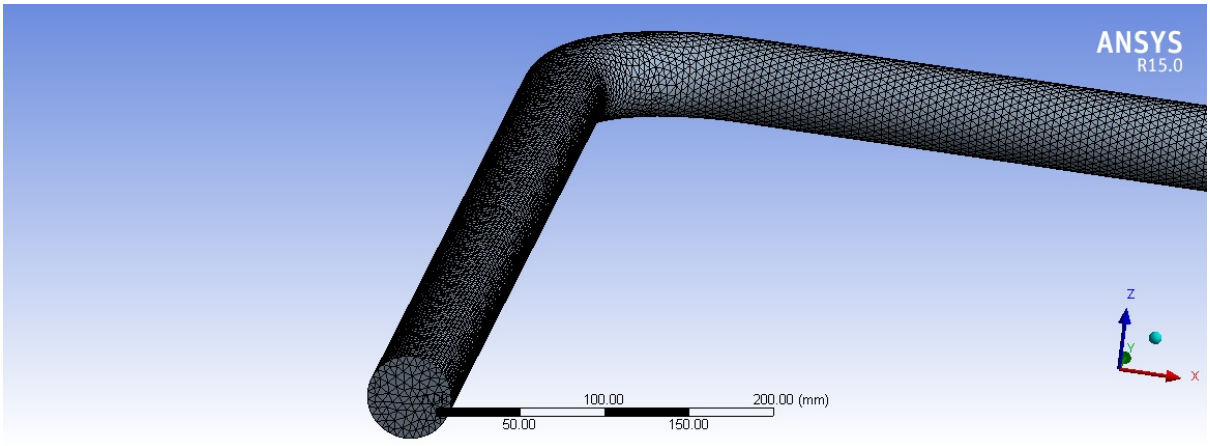

Figure 5.2 Meshed Domain of Bend

5.3 PRESSURE DROP IN PIPE ELBOW

5.3.1 Effect of radius-to-diameter ratio (r/D) in elbow

The pressure drop was investigated on pipe bends of different radius-to-diameter (r/D) ratios namely 1, 1.5, 2, 2.5, 3, and 4 respectively for bend angle of 90º. The solid concentration was taken as 60% (by weight) with particle size of 59µm at velocity of 5 m/s. **Figure 5.3**represents the pressure drop for different radius-to-diameter (r/D) ratios.

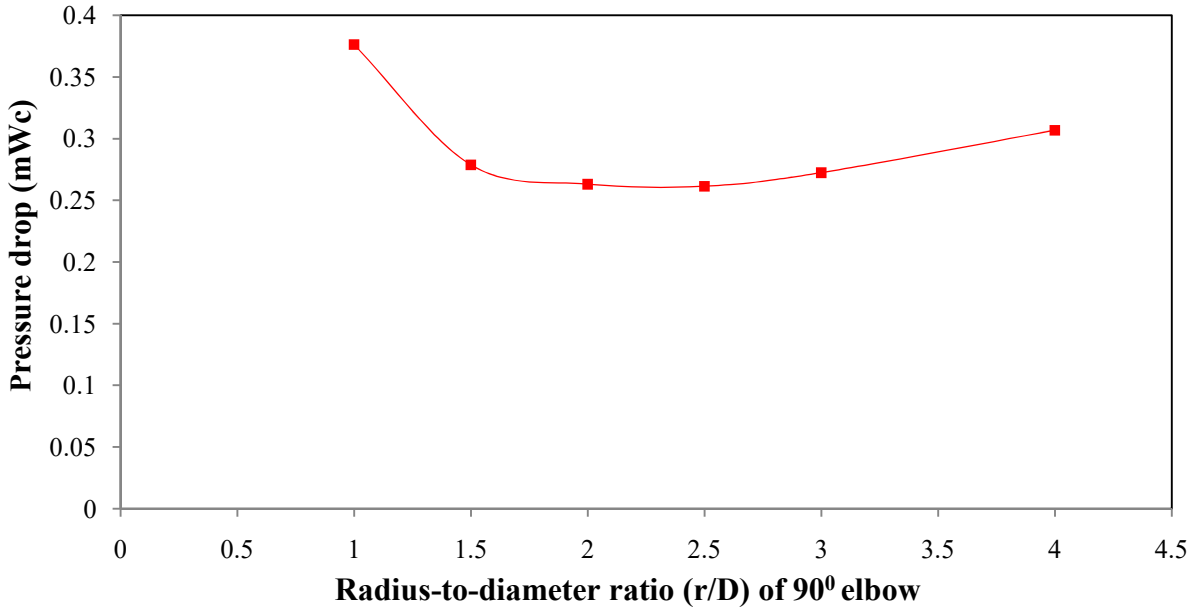

Figure 5.3 Effect of radius to diameter ratio (r/D) on pressure drop

It was found the pressure drop increases with increase in r/D ratio above and below 2.5. The pressure drop for r/D 2 and 2.5 was nearly equal. The pressure curve is having merely horizontal for r/D and 2.5. For smaller r/d ratio of 1 and 1.5 there is sudden change of flow path which results in greater turbulence and more flow separation and hence grater pressure drop. For larger r/D ratio the fluid has to travel large distance which results in increased frictional losses and pressure drop increased. So, there existed optimum r/D ratios which have minimum combined pressure losses. For r/D ratio 2 and 2.5 the pressure drop was 0.263mWc and 0.261 mWc. Hence, there was very marginal difference between the pressure drop for r/D ratio of 2 and 2.5. The r/D 2.0 was used for further simulation to study the effect of other parameters on head loss characteristics because as iron being highly abrasive material lower r/D ratio have more suitability as it as less erosion rate as compared to r/D 2.5 and more

practically viable. The increase in r/D ratio may cause in high particle-particle interactions which results in flow recirculation. Higher flow recirculation causes an action of force on particles and directs them towards the pipe wall results in higher erosion wear. Therefore r/D 2 was used for further study of effect of particle size, velocity and solid concentration of 90^0 pipe bend.

5.3.2 Effect of concentration and velocity

Figure 5.4shows the pressure drop characteristics for pipe bend of r/D 2 at different efflux velocities. The solid concentration was varied from 20-60 % (by weight) with particle size of 59 µm.

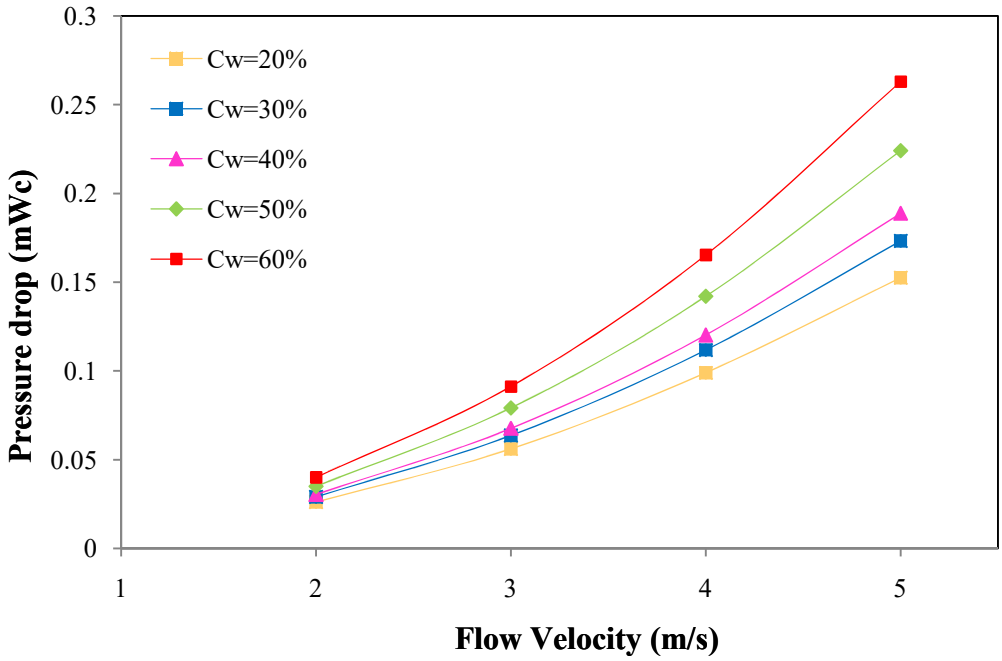

Figure 5.4 Effect of concentration and velocity on pressure drop for r/D=2

An increase in head loss was observed as the solids concentration increased along the pipe bend. The main reason for this is increase in viscosity and density with solid concentration. For solid concentration of 20%, the head loss was observed to increase 53.28%, 43.33%, and 35.03% with increase in flow velocity from 2-3, 3-4, and 4-5 m/s, respectively. It was also observed that with an increase in flow velocity, an increase in head loss was noticed along the pipe bend. At 5 m/s flow velocity, head loss increases by 11.98%, 8.24%, 15.75 and 14.8%

with increase in solid concentration from20-30%, 30-40%, 40-50%, and 50-60%, respectively. Hence, head loss was found to be non-linear function of solid concentration and flow rate.

5.3.3 Effect of particle size on pressure drop

Figure 5.5 shows the effect of particle size on head loss for 50 mm diameter pipe bend. The solid concentration was taken as 60% (by weight) with velocity varying from2-5 m/s. It was found that the head loss increases with increase in particle diameter and became maxima at 90µm particle size. The coarser particles slurry (90µm) showed the higher pressure drop at all velocities with nearly a linear trend as compared to finer particulate slurry. The reasons are same as explained for the straight pipe.

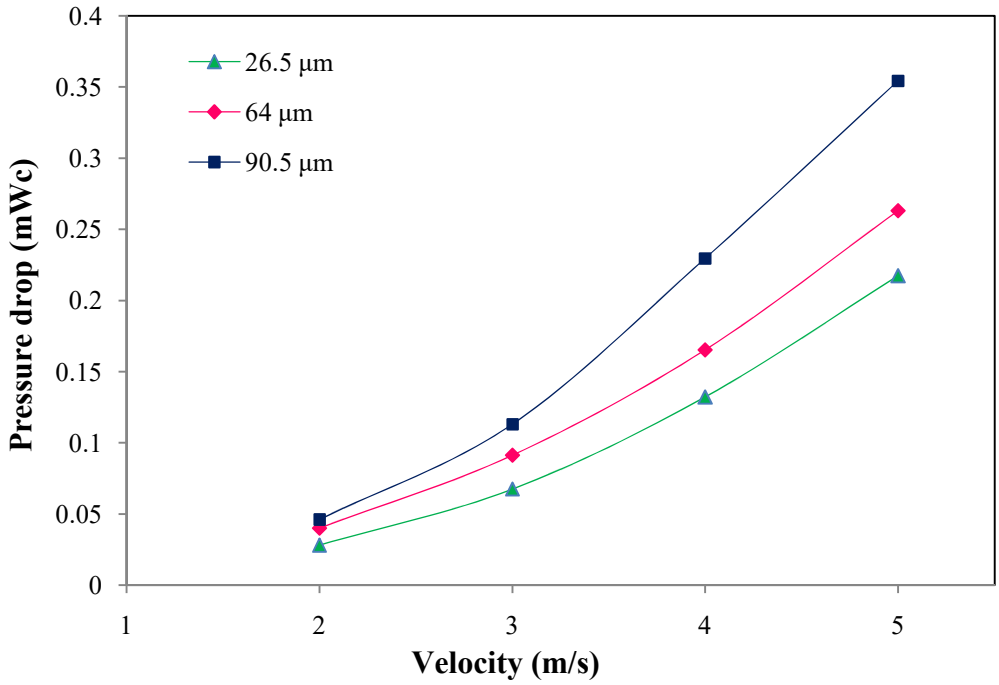

Figure 5.5 Effect of particle size on pressure drop

5.4 VOLUME FRACTION PROFILES FORPIPE ELBOW

5.4.1 Effect of radius-to-diameter ratio (r/D) in elbow

The effect of variation of radius-to-diameter (r/D) ratio on the volume fraction contours at the bend outlet is explained in **Figure 5.6**. The solid concentration was taken as 60% with velocity of flow to be 5 m/s for 50 mm diameter pipe. The r/d value was varied ranging from 1-4. From figure it was depicted that with increase in r/D ratio the distribution of solid concentration tends to gain stability. The deposition on the extrados of the pipe was due to the action of centrifugal force due to change in direction of flow.

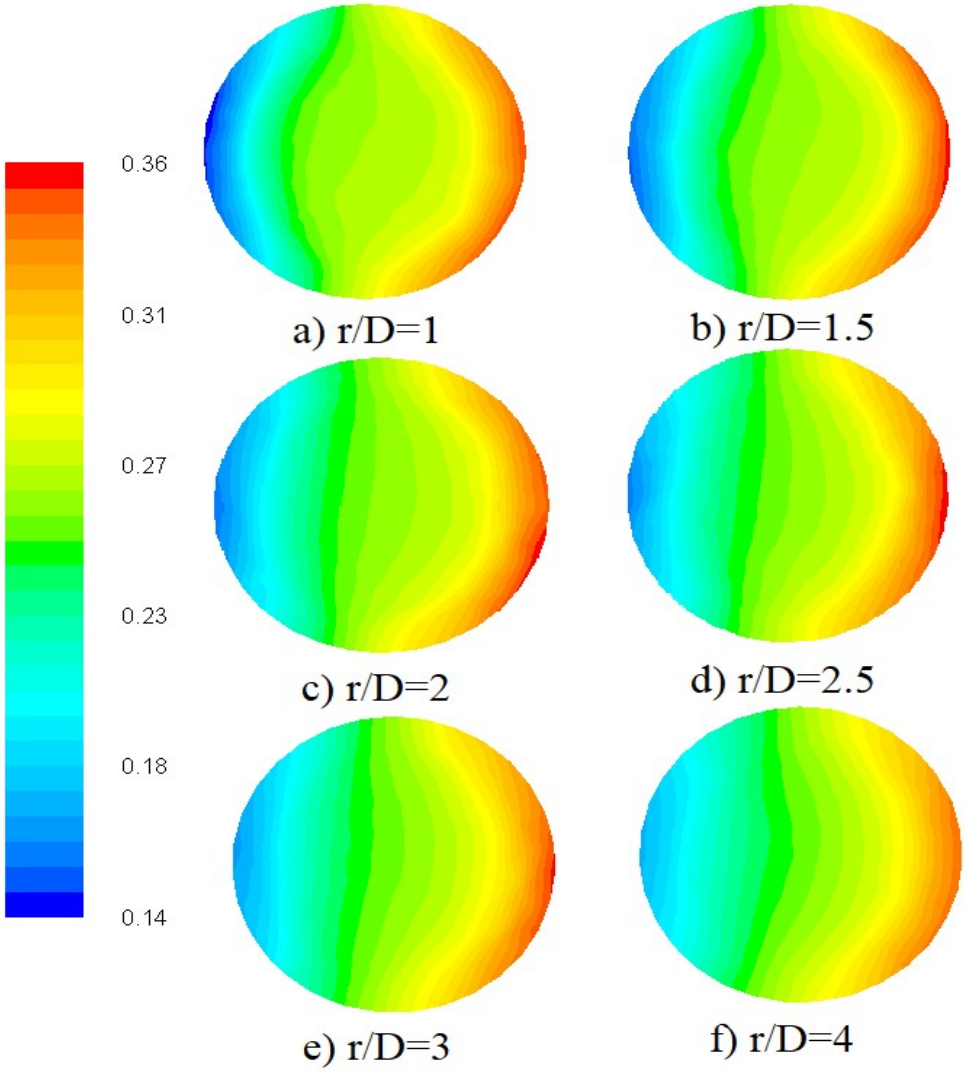

Figure 5.6 Effect of r/D on volume fraction contours

For r/D 1 there is large variation of solid volume distribution throughout the cross section. This uneven distribution was due to sudden change of direction of flow. The increase in r/D resulted in smooth transition in direction of flow and reduced turbulence. The decrease in turbulence resulted in more even distribution of solid volume fraction. The area of lean concentration and high concentration is maximum for r/D of 1 and keep on decreasing with r/D ratio. The volume fraction contours least blue or lean concentration for r/D of 4.

5.4.2 Effect of particle size

Effect of particle size on the volume fraction distribution of iron ore particles in iron-ore slurry flow through pipe bend with r/D 2 is as shown in **Figure 5.7**. The solid concentration was taken as 60% (by weight) with flow velocity as 5 m/s and pipe diameter of 50 mm. Higher volume fraction was observed at the outer periphery of the pipe due to the action of centrifugal force on solid particles. The higher concentration is denoted by red color while blue color represents the low concentration. From results it was depicted that with increase in particle size the volume fraction deposition increases. The maximum values of volume fraction deposited increased by 21.23 and 15.96% as size of particle was increased from 26-64 μm and 64-90 μm. The slurry containing the coarser particles develops heterogeneous flow while smaller sized particles developed homogeneous flow maintaining the homogeneous volume fraction distribution. The large difference in volume fraction with increase in particle size explains the reason due to which the fine sized particles are used for transportation of iron ore slurry.

Figure 5.8 depicts the region for flow separation or region of lean concentration towards the inner periphery of elbow. This flow separation is due to the change of flow angle and action of centrifugal force pushing the solid particles towards extrados of the pipe. This region is highly affected by the size of particle. From results it was found that regions of high concentration and low concentration are larger for coarser sized particle slurry. This can be explained due to the fact of inefficiency of larger sized particles to change in direction of flow.

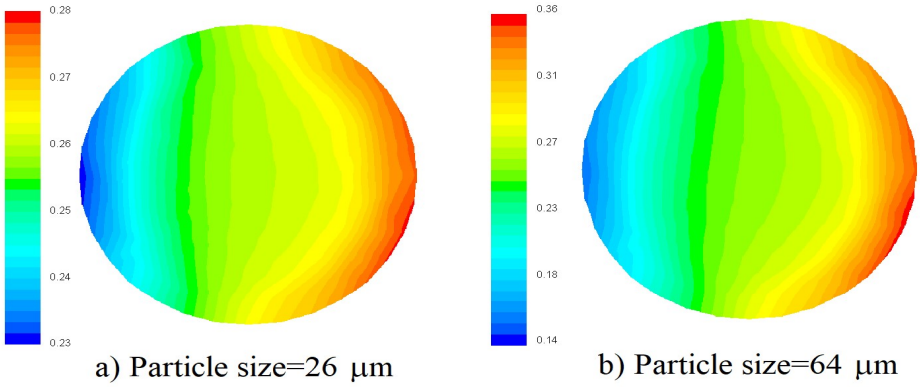

a) Particle size=26 μm

b) Particle size=64 μm

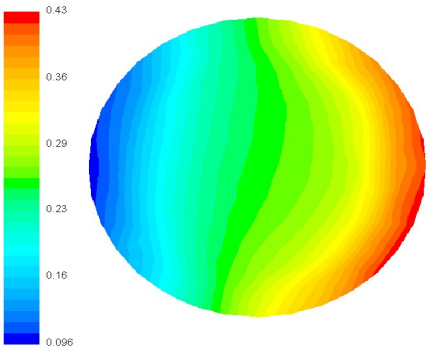

c) Particle size=90 μm

Figure 5.7 Volume fraction contours with varying particle size

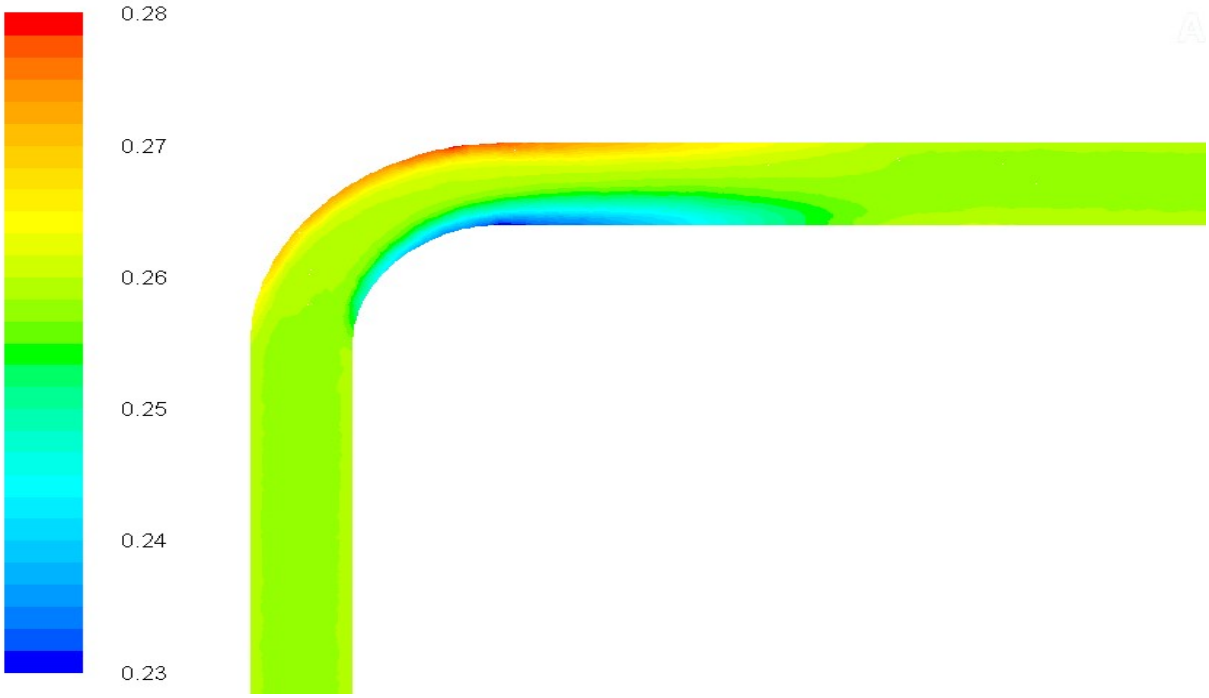

a) Particle Size=26 μm

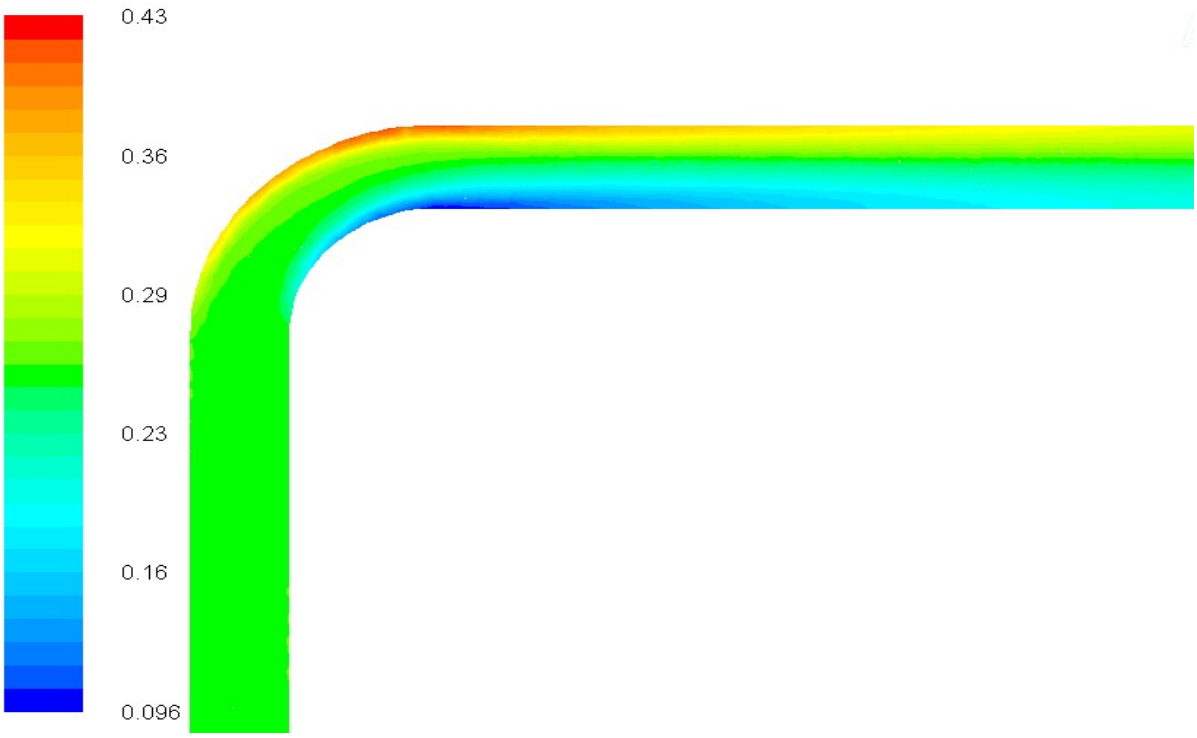

b) Particle Size=90 μm

Figure 5.8 Flow separation region with varying particle size

5.4.3 Effect of concentration and velocity

The volume fraction contours at varying solid concentration ranging from 20-60% with flow velocity of 5 m/sis shown in **Figure 5.9.**The increase in concentration results increase of volume fraction at the extrados of the pipe. The increase in concentration results in larger number of solid particles per unit volume. The higher concentration zone observed an increase due to increase in concentration.**Figure 5.10** represents the variation of flow velocity ranging from2-5 m/s at 60% solid concentration for iron ore slurry flow in 50 mm pipe diameter. The change in velocity decreases the titled profile of higher concentration on the extrados of the pipe. The lower velocity is not able to hold up particles more efficiently than higher velocities which results tilted profile of the concentrated profile downwards due to action of gravity. With increase in velocity theses tends to stabilize and remains only at the extrados of the pipe due to higher centrifugal effect

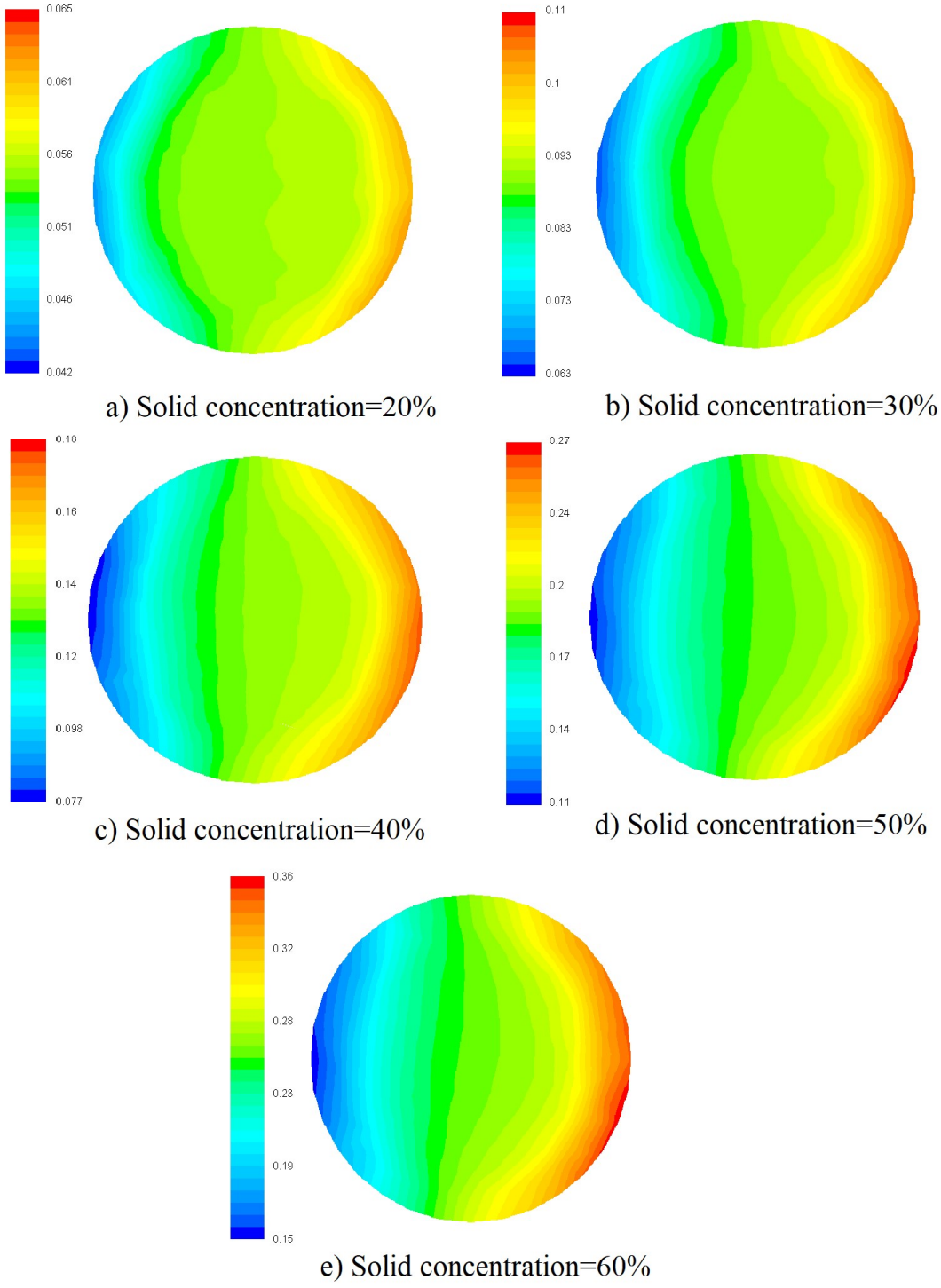

Figure 5.9 Volume fraction contours at varying solid concentration at 5 m/s flow velocity

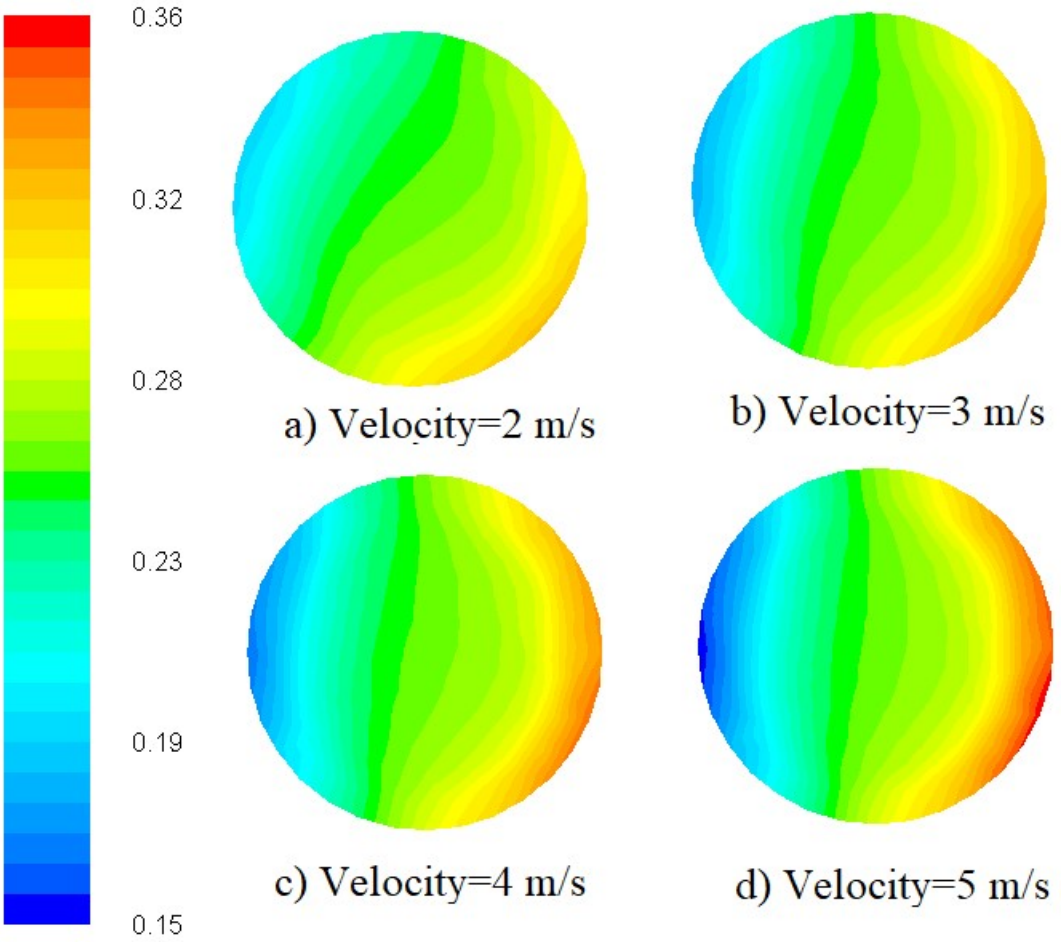

Figure 5.10 Volume fraction contours at varying velocity at 60% solid concentration

5.5 TURBULENCE INTENSITIES FOR ELBOW

5.5.1 Effect of radius-to-diameter ratio (r/D) in elbow

Radius to diameter ratio plays a very important role on the parametric variation of slurry flow in pipeline**. Figure 5.11** represents the effect of variation of r/D ratio on the turbulent intensity contours for the iron ore slurry flow with solid concentration 60% and flow velocity of 5 m/s through a 50 mm pipe diameter. Turbulent intensity counters are taken at the bend outlet. From results it was found that the turbulent intensity contours had a decreasing trend with r/D ratio. Further increase in r/D ratio the turbulent intensity contours are not much affected. The pattern tended to stabilize and have an even profile when the r/D is increased from 2 to 4. The decrease in turbulent intensity can be attributed to the fact that with increase in r/D ratio flow gets more time to adjust the change in direction of flow. As the change in direction of flow is smoother

for high r/D ratio hence the turbulence generated is reduced. Therefore, with increase in r/D ratio the contours have a stabilized and evenly distributed pattern at the bend outlet.

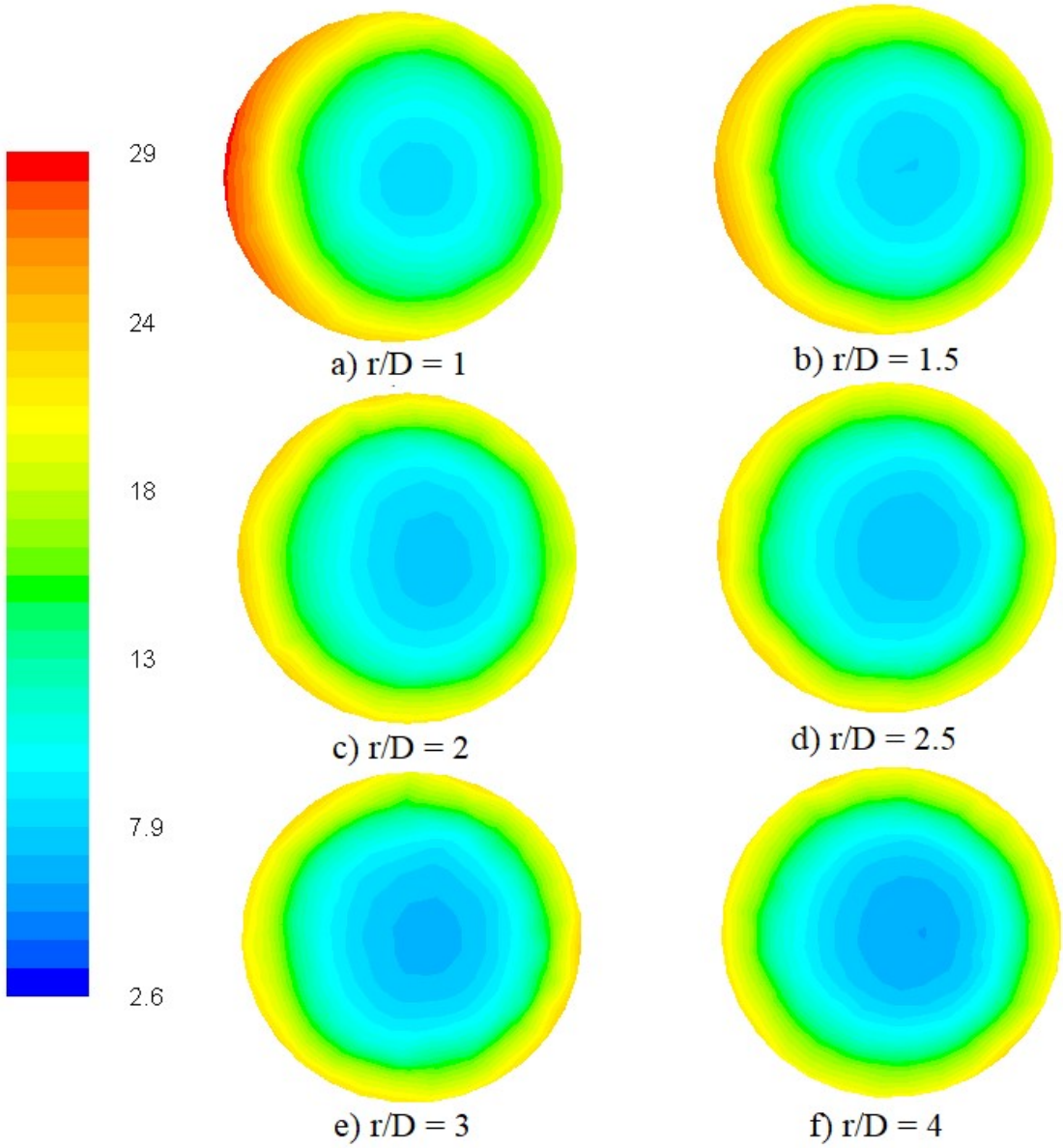

Figure 5.11 Effect of r/D on Turbulent intensity contours

5.5.2 Effect of particle size

Figure 5.12 shows the effect of increase in particle size on turbulent intensity contours for iron ore slurry flow through 90^0 pipe bend. The solid concentration of iron ore slurry flow was taken as 60% with flow velocity of 5 m/s through elbow of r/D 2. From results it was depicted that the increase in particle size of solid particles resulted in increase of turbulent intensity. This increase is very small when particle size is increased from 26-64 µm but when particle size was increased from 64-90µm an increase of 50.1% was observed. This large increase in turbulent intensity can be attributed due to the fact that the large sized particles posses more moment of inertia and hence exhibits more reluctance to the change in direction of flow. The sudden change is direction of flow results in large increase of inter-particle striking and hence the turbulence increases. This increase in turbulence results in large increase of turbulent intensity when particle size of the iron ore was increased from 64-90µm.

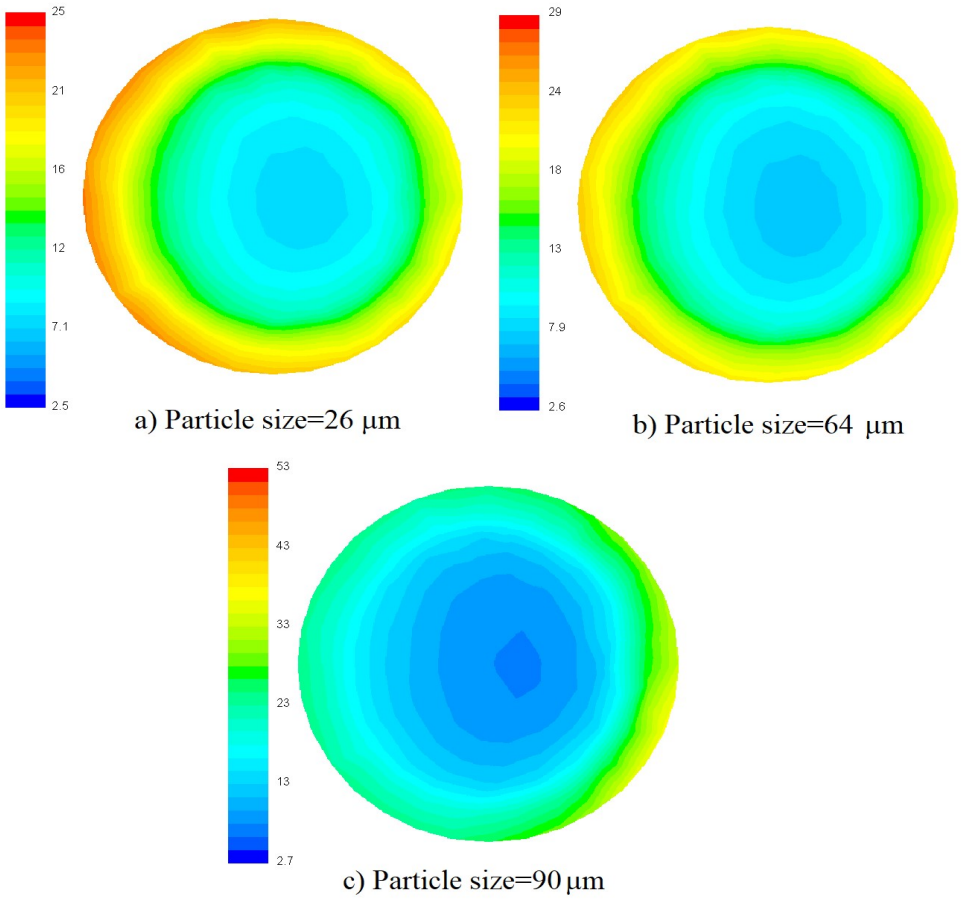

Figure 5.12 Turbulent intensity contours with varying particle size

5.5.3 Effect of concentration and velocity

The variation of turbulent intensities distribution at bend outlet under the action of variation produced due to change in velocity and solid concentration is shown in **Figure 5.13** and **Figure 5.14**. The effect of velocity on turbulent intensity at the outlet of 90^0 pipe bend for iron ore slurry flow of 60% solid concentration through 50 mm pipe diameter is shown in **Figure 5.13**. The increase in flow velocity resulted for increase in turbulent intensity. This increase can be attributed due to the fact that increase in velocity resulted in increase in turbulence. The maximum value for turbulent intensity increased 31.25%, 23.8%, and 19.23% with increase in flow velocity 2-3 m/s, 3-4 m/s and 4-5 m/s respectively. **Figure 5.14** represents the effect of variation in solid concentration for 5 m/s flow velocity slurry flow through pipe bend of r/D 2. From results it was found that increase in turbulent intensity was very marginal with increase in solid concentration. With increase in solid concentration from 20-60% the maximum value of turbulent intensities differed a little. The effect of variations in velocity on turbulent intensity was much more as compared to variation in solid concentration.

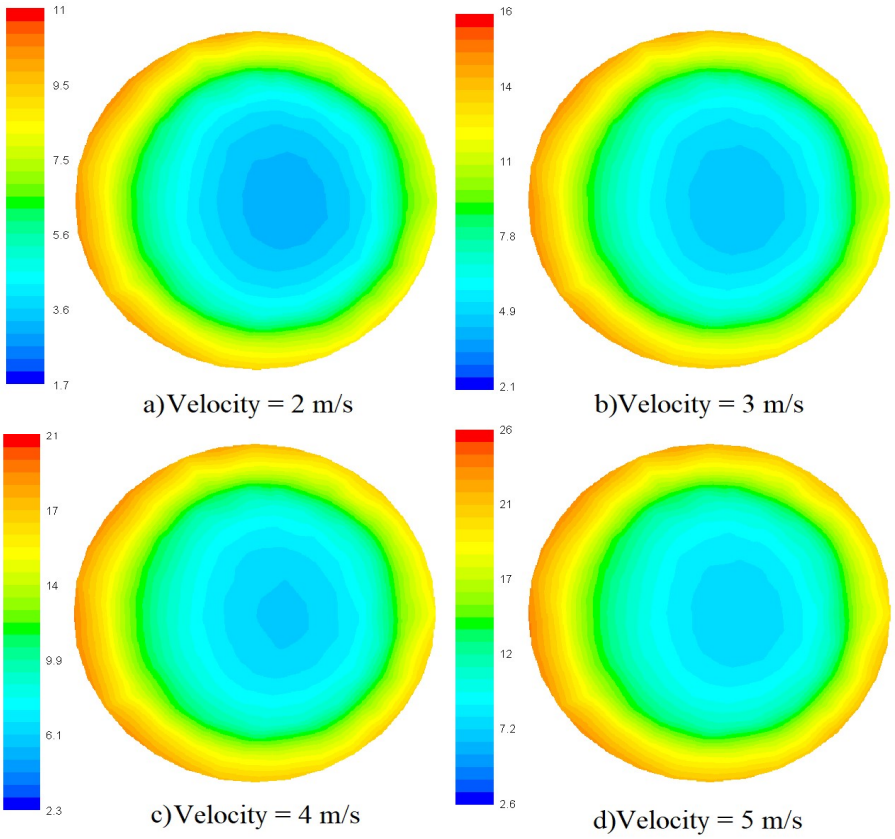

Figure 5.13 Turbulent intensity contours at varying velocity at 60% solid concentration

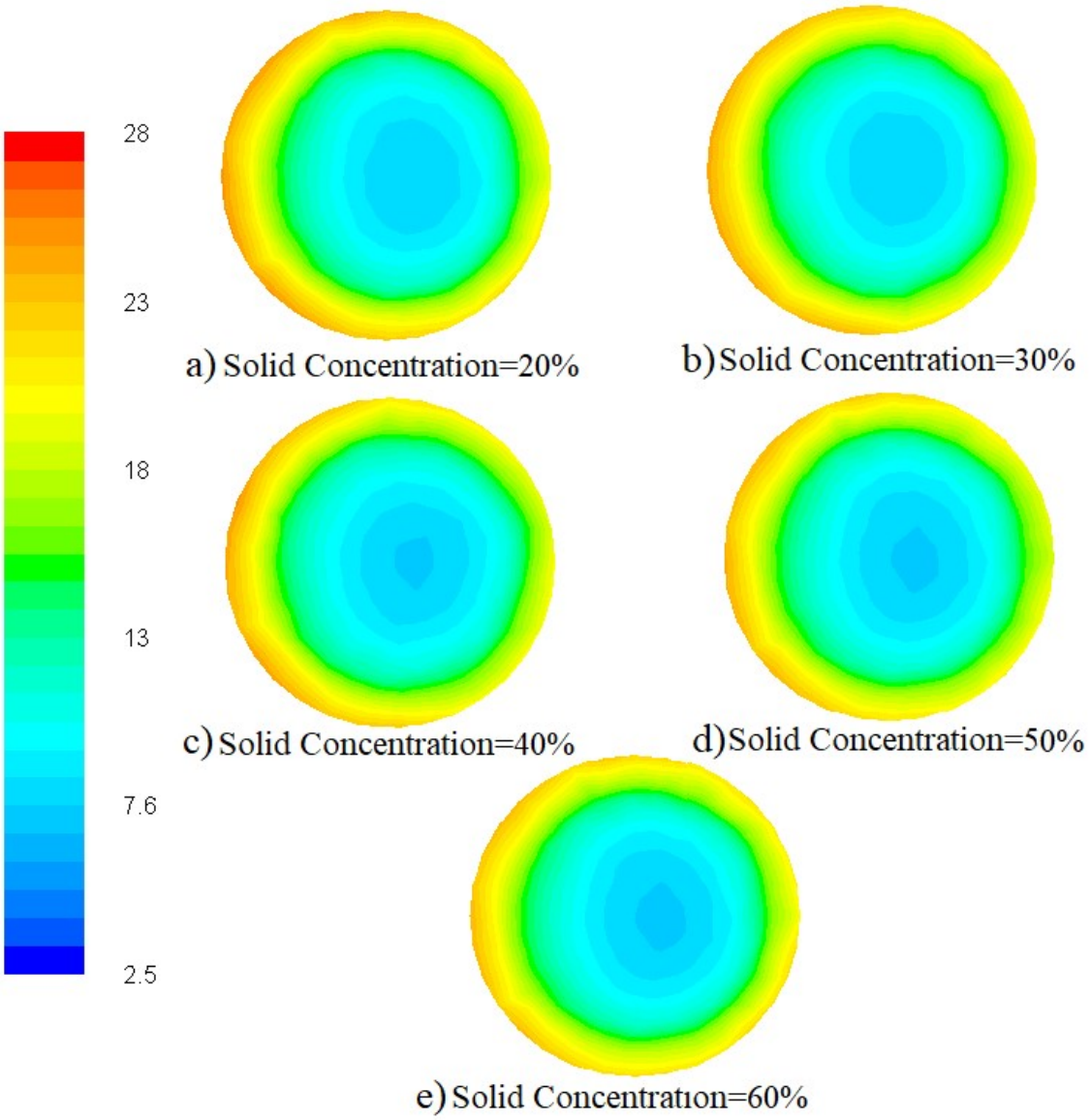

Figure 5.14 Turbulent intensity contours at varying solid concentration at 5 m/s flow velocity

5.6 SOLID PHASE VELOCITY PROFILES FOR ELBOW

5.6.1 Effect of radius-to-diameter ratio (r/D) in elbow

Effect of radius-to-diameter ratio (r/D) on velocity profile is shown in **Figure 5.15** for 60% solid concentration with flow velocity of 5m/s. Velocity profile are taken at the bend outlet. With increase in r/D ratio the velocity distribution tends to stabilize. For r/D ratio 1 the profile is having large number of particles having velocity less than 5 m/s. For r/D 1.5 the disturbances are highest. There are large numbers of particles which are having velocity of 4.5 m/s. These

disturbances are due to sudden change in angle of flow. For r/D ratio 2 the profile is very compact i.e. maximum number of particles are having velocity equal to flow velocity. Further increase in r/D ratio resulted in further increase in disturbances but rate of change is very minimal. Hence, increasing the r/D ratio beyond the value of 2 had very less effect on variation in velocity profiles. For lower r/D ratio the disturbances are highest due to sudden change in angle of flow.

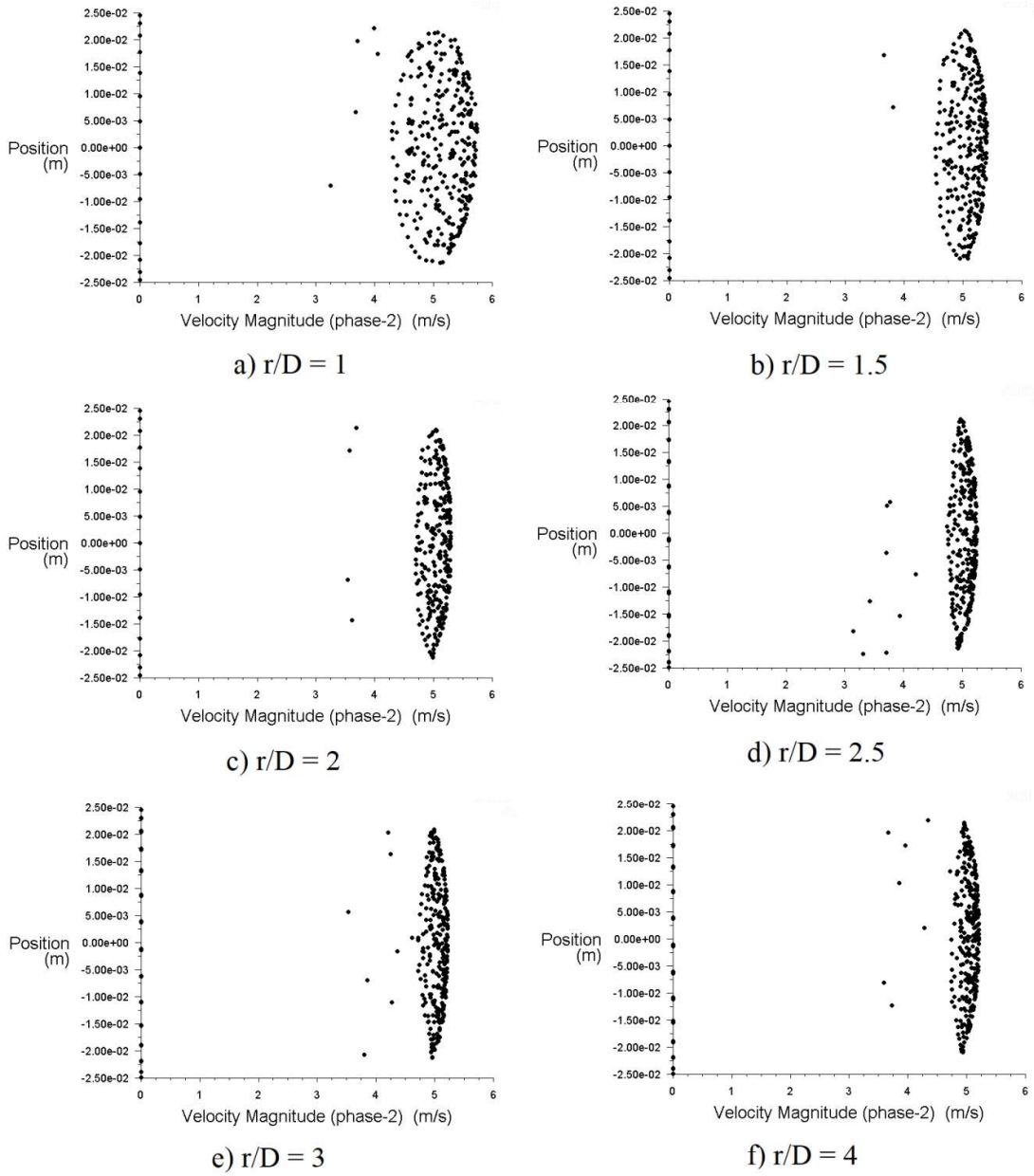

Figure 5.15 Effect of r/D on velocity profile at bend outlet

5.6.2 Effect of particle size

Effect of particle size on velocity profile with the variation in particle size for iron ore slurry flow with efflux concentration 60% and flow velocity of 5 m/s is as shown in **Figure 5.16**. From results it was depicted that the velocity profile is stable for fined sized particles i.e. less than 53µm. Mostly all particles are having the velocity equal to flow velocity 5 m/s. But with increase in particle size to 64 µm the disturbances are increased which results in variation of flow velocity. For coarser particles the velocity disturbances was having maximum disturbance. There were large number of particles having velocity less than 5 m/s. The profiles are asymmetric but the disturbances increases largely with increase in particle size.

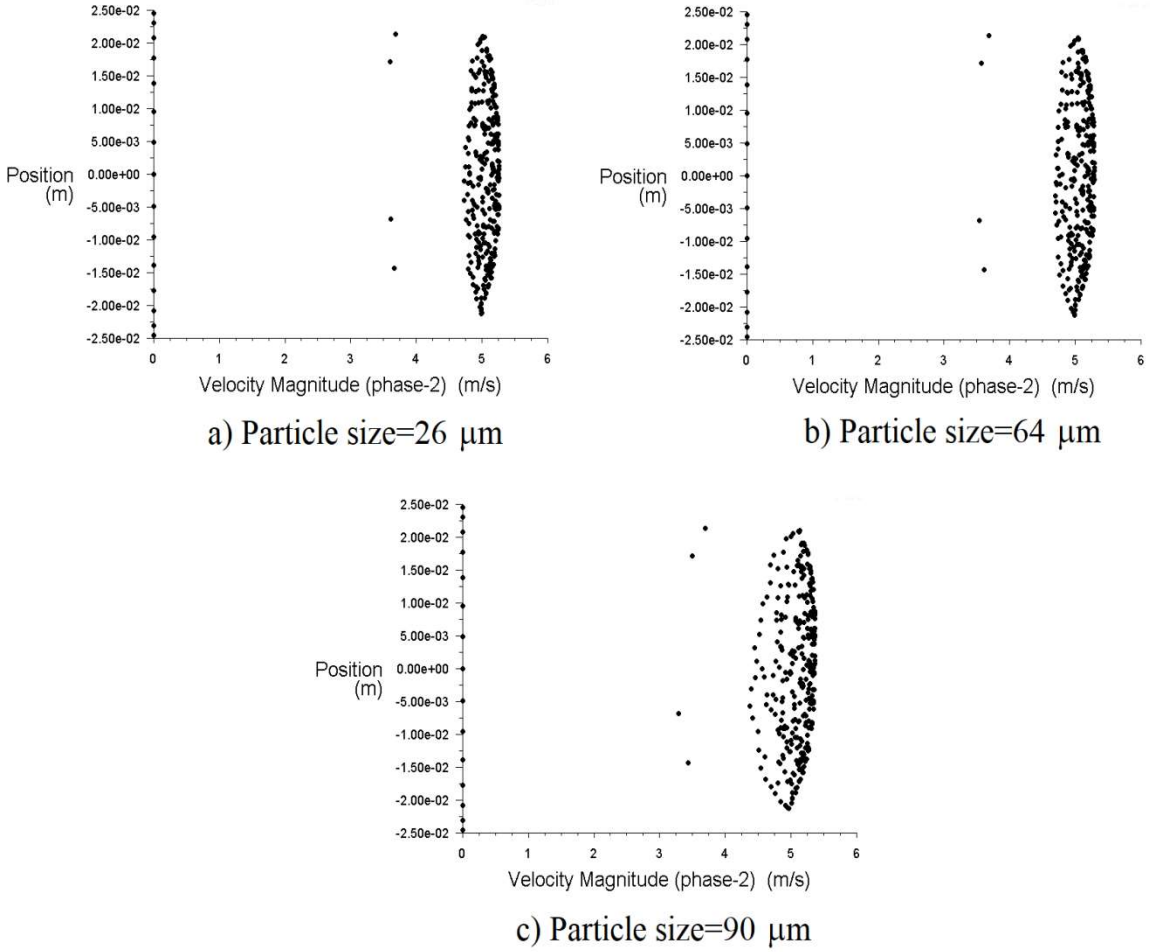

Figure 5.16 Velocity profiles with varying particle size

5.6.3 Effect of concentration and velocity

Effect of velocity on velocity distribution is shown in **Figure 5.17** for iron ore slurry flow with solid concentration of 60%. Flow velocity was varied from 2-5 m/s for pipe of 50 mm pipe diameter. Velocity distribution profiles are asymmetric with each other. The increase in velocity resulted in shifting of mean velocity curve to the given flow velocity.

The increase in concentration had a minimal effect on the velocity distribution curves. With increase in concentration of slurry flow there are generation of disturbances which generates the changes in the velocity profiles. These minimal changes can be seen from **Figure 5.18**when concentration is increased from 20-60% for flow velocity of 5 m/s. The main reason of change in velocity pattern was due to increase in viscosity and density of iron ore slurry with increase in concentration.

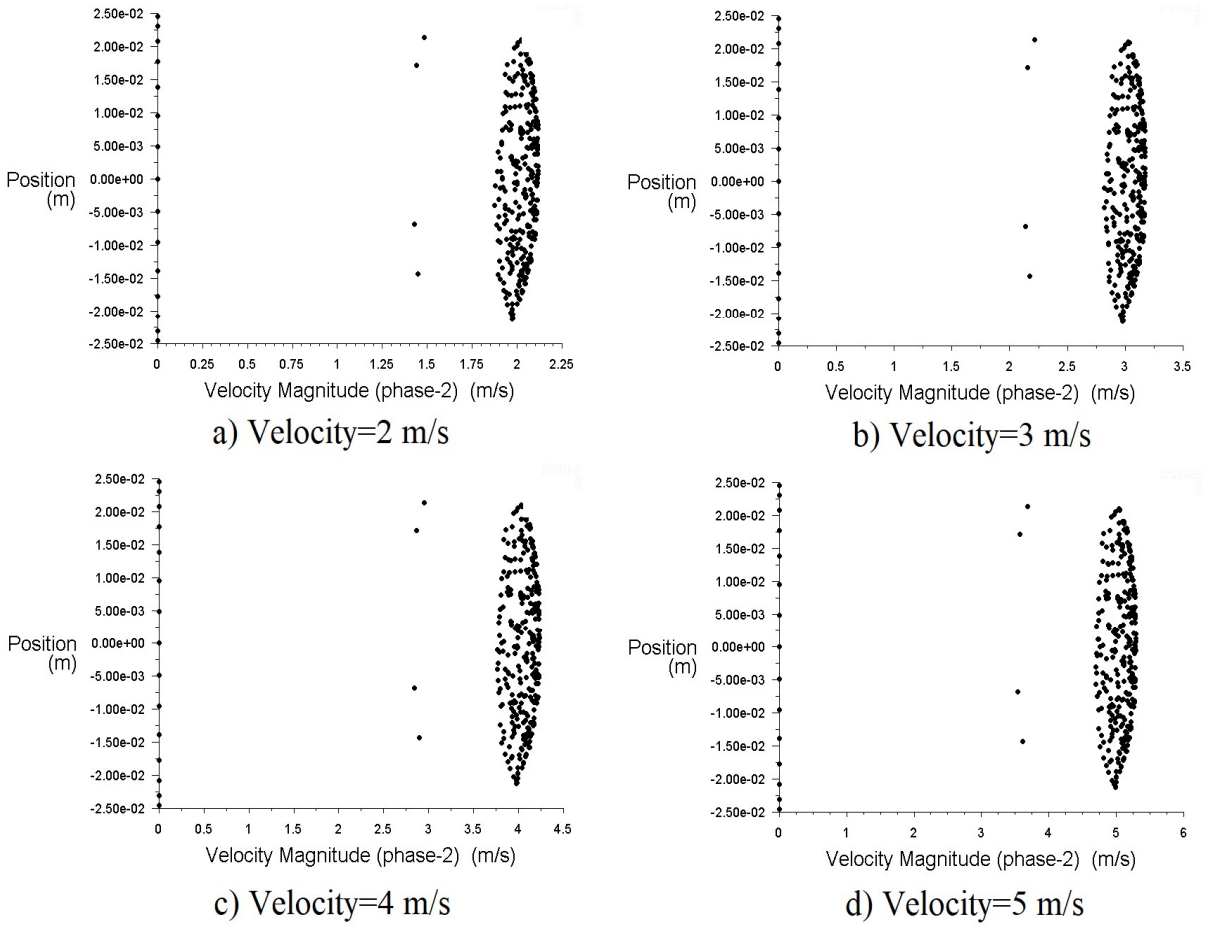

Figure 5.17 Velocity profile at varying velocity at 60% solid concentration

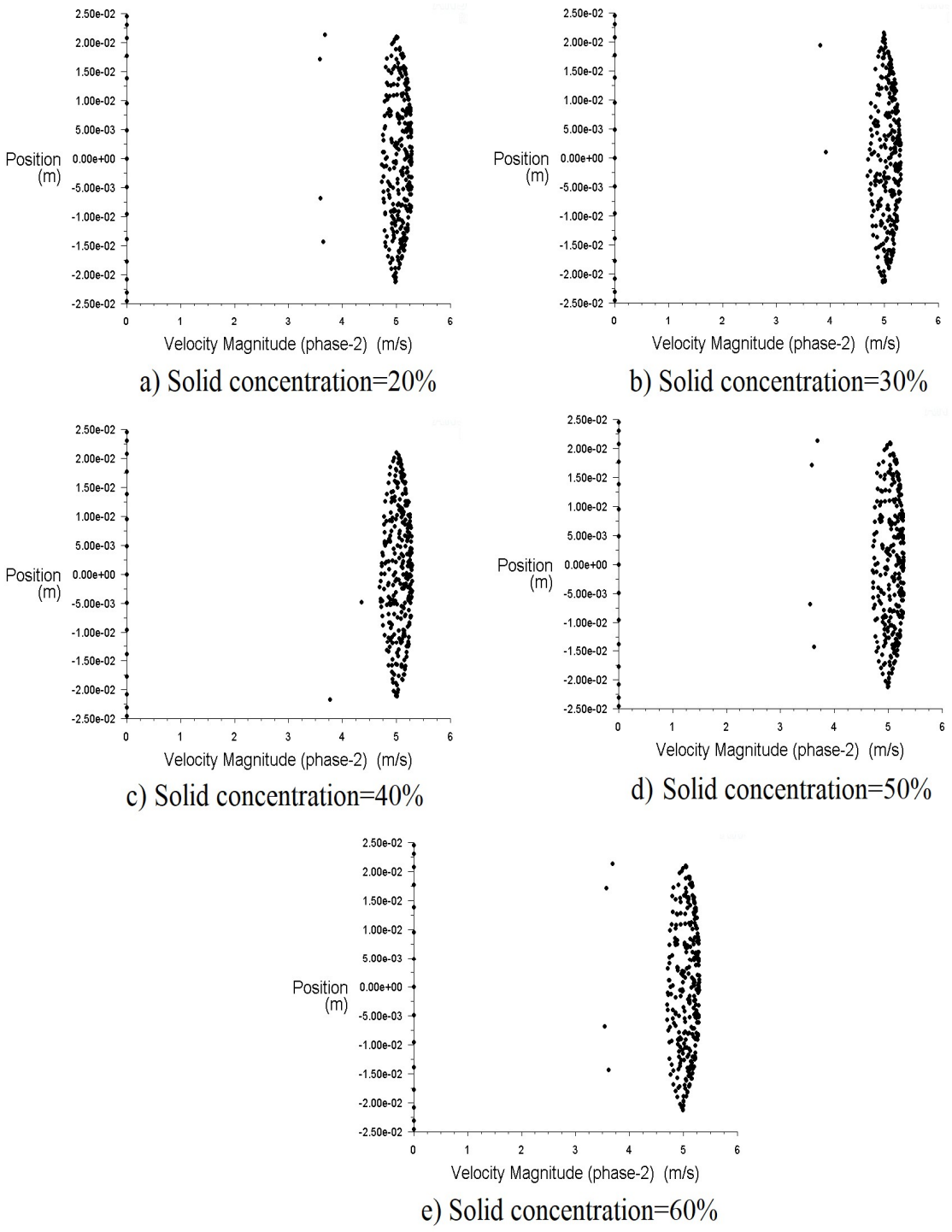

Figure 5.18 Velocity profile with varying solid concentration for flow velocity 5 m/s.

Chapter 6

CONCLUSION

The capability of CFD, in this study, is explored to model complex solid liquid slurry flow in pipeline. Present study employed RNG k-$\boldsymbol{\varepsilon}$ turbulent model with Eulerian multiphase approach for analysing the flow characteristics of iron-ore slurry with solid concentration ranging from 20-60% (by weight) in 50 mm diameter pipeline. The computational simulations are used for the prediction of head loss characteristics, velocity profile and concentration profile in straight pipe and elbow with variation in solid content, particle size and velocity.

6.1 CONCLUSIONS

- RNG k-ε turbulent model was found to have least deviation with the experimental data of Mukhtar et al. (1995) as compared to other models namely Standard k-ω, SST k-ω, Standard k-ε, and Realizable k-ε. Hence, RNG k-ε turbulent model was used for simulations.
- Numerical simulation results show that the pressure drop in straight pipe and 90^0 elbow increases nonlinearly with increase in flow velocity, solid concentration and particle size. This increase in pressure drop due to increases in velocity due to increase in kinetic energy and hence the turbulent and frictional losses increases. Increase in concentration and particle size results for increases in viscosity and density and hence the pressure drop increases.
- Pressure drop increases with increase in r/D ratio more or less than 2.5. This due to fact that below r/D 2.5 the flow bears sudden angle change and greater than r/D 2.5 results in increases in frictional losses.
- Volume fraction contours of straight pipe shows increase in lean and more concentrated region with increase in concentration and particle size but decreases with increase in velocity. The decrease in settling due increase in kinetic energy of fluid enabling increase in solid carrying capacity.
- Volume fraction contours for 90^0 elbows have higher solid concentration towards extrados of pipe due to the effect of centrifugal force and this region has an increasing trend with increase in velocity and concentration.

- The increase in particle size results in increase in more volume fraction of solid towards the extrados and the length of lean concentration along the inner periphery increases.
- Turbulent intensity contours for straight pipe and elbow observed a increase with increase in particle size, velocity. The increase was marginal for increase in concentration.
- Turbulent intensity contours tended to stabilize with increase in radius ratio.
- Velocity profiles of solid phase for straight pipe and bend observed marginal effects of increase in concentration and velocity.
- Velocity profile for elbow observed instability with increase in radius ratio and particle size. This instability was highest for lower r/D ratio due to sudden change in direction of flow.

6.2 FUTURE SCOPE

The present study was focused for prediction of pressure drop, volume fraction, turbulent intensity and velocity profile of iron ore slurry flow in straight pipe and elbow. Further study can extend for other geometric configurations namely different pipe bends (40^0, 60^0, 120^0) converging and diverging section that are encountered during a slurry pipeline system so this work can be augmented by doing numerical simulation on these bends and sections.

List of Publications

Mandeep Singh, Satish Kumar, Sagar Kumar, Gopal Nandan. Characterization of Iron-ore suspension at In-situ conditions. ***Materials Today's: proceedings***

REFERENCES

Abulnaga, B., 2002, Slurry System Handbook, Mcgraw-Hill

Anderson, J.D. and Wendt, J., 1995. *Computational fluid dynamics* (Vol. 206). New York: McGraw-Hill.

ANSYS FLUENT (2011) ANSYS FLUENT User's Guide, ANSYS Inc., Pennsylvania, USA

Brennen, C.E. and Brennen, C.E., 2005. *Fundamentals of multiphase flow*.Cambridge university press.

Eesa, M. and Barigou, M., 2009.CFD investigation of the pipe transport of coarse solids in laminar power law fluids.*Chemical Engineering Science*, *64*(2), pp.322-333.

El-Nahhas, K., El-Hak, N.G., Rayan, M.A. and El-Sawaf, I., 2009.Effect of particle size distribution on the hydraulic transport of settling slurries.In *Thirteenth International Water Technology Conference.Hurghada, Egypt,* pp. 198-210.

Gopaliya, M.K. and Kaushal, D.R., 2015. Analysis of effect of grain size on various parameters of slurry flow through pipeline using CFD.*Particulate Science and Technology*, *33*(4), pp.369-384.

Hashemi, S.A., Sadighian, A., Shah, S.I.A. and Sanders, R.S., 2014. Solid velocity and concentration fluctuations in highly concentrated liquid–solid (slurry) pipe flows. *International Journal of Multiphase Flow*, *66*, pp.46-61.

Hossain, A., Naser, J. and Imteaz, M.A., 2011. CFD investigation of particle deposition in a horizontal looped turbulent pipe flow.*Environmental Modeling & Assessment*, *16*(4), pp.359-367.

Kaushal, D.R., Sato, K., Toyota, T., Funatsu, K., Tomita, Y., 2005.Effect of Particle Size Distribution on Pressure Drop and Concentration Profile in Pipeline Flow of Highly Concentrated Slurry.*International Journal of Multiphase Flow*, 31, pp.809-823.

Kaushal, D.R., Thinglas, T., Tomita, Y., Kuchii, S. and Tsukamoto, H., 2012. CFD modeling for pipeline flow of fine particles at high concentration.*International Journal of Multiphase Flow*, *43*, pp.85-100.

Kaushal, D.R., Kumar, A., Tomita, Y., Kuchii, S., Tsukamoto, H., 2013. Flow of Mono-Disperesed Particles Through Horizontal Bend. *International Journal of Multiphase Flow*, 52, pp.71-91.

Kim, C., Han, C., 2013, Numerical simulation of hydraulic transport of sand- water mixtures in pipelines, Open Journal of Fluid Dynamics, 3, 266-270.

Kumar, N., Kaushal, D.R., Kumar, A., 2012. Computational Study of the Two Phase Flow in Horizontal Slurry Pipeline.*International Journal of Mechanical and Production Engineering,* 1(1), pp.2315-4489.

Lahiri, S.K., Ghanta, K.C. 2010, Slurry Flow Modeling by CFD, *Chemical Industry & Chemical Engineering Quarterly*, 16(4), pp.295-308.

Launder, B. E., and D. B. Spalding. 1974. The numerical computation of turbulent flows. *Computer Methods Applied Mechanics and Engineering,* 3 (2), pp.269–89.

Lei, L., Usui, H., Suzuki, H. 2010, Study of Pipeline Transportation of Dense Fly Ash-water Slurry, *Coal Preparation*, 22(2), pp.65-80.

Liu, M. and Duan, Y.F., 2009.Resistance properties of coal–water slurry flowing through local piping fittings.*Experimental Thermal and Fluid Science*, *33*(5), pp.828-837.

Lu, H., Yin, J., Yuan, Y., Wang, J. 2010. Effect of Particle Size Distribution on Flow Pattern and Pressure Drop in Pipeline Flow of Slurries, *2nd Conference on Environmental Science and Information Application Technology.*

Lun, C. K. K., S. B. Savage, D. J. Jeffrey, and N. Chepurniy. 1984. Kinetic theories for granular flow: inelastic particles in couette flow and slightly inelastic particles in a general flow field. *Journal of Fluid Mechanics,* 140, pp.223–56.

Mazumder, Q.H., 2012. CFD analysis of the effect of elbow radius on pressure drop in multiphase flow. *Modelling and Simulation in Engineering*, p.37.

Messa, G.V., Malavasi, S., 2013, Numerical investigation of solid-liquid slurry flow through an upward facing step, *Journal of Hydrology Hydromech*., 2, pp.126-133.

Miller, A. and Gidaspow, D., 1992. Dense vertical gas-solid flow in a pipe.*AIChE journal*, 38(11), pp.1801-1815.

Mishra, R., Ghanta, K.C., Mullick, A.N. and Sinha, S.L., 2017. Numerical prediction of flow behavior and erosion prediction of coal water and copper ore water slurries.*Journal of Advanced Research in Dynamical and Control System,* 4, pp. 2368-2388.

Mukhtar, A., Singh, S.N. and Seshadri, V., 1995. Pressure drop in a long radius 90° horizontal bend for the flow of multisized heterogeneous slurries. *International journal of multiphase flow*, *21*(2), pp.329-334.

Nabil, T., El-Sawaf, I. and El-Nahhas, K., 2013, November.Computational fluid dynamics simulation of the solid-liquid slurry flow in a pipeline.In *Proc. 17th International Water Technologies Conference IWTC17* (Vol. 57).

Nayak, B.B., Chatterjee, D. and Mullick, A.N., 2017. Numerical prediction of flow and heat transfer characteristics of water-fly ash slurry in a 180° return pipe bend. *International Journal of Thermal Sciences*, *113*, pp.100-115.

Ofei, T.N. and Ismail, A.Y., 2016. Eulerian-Eulerian Simulation of Particle-Liquid Slurry Flow in Horizontal Pipe.*Journal of Petroleum Engineering*, *2016*.

Panda, D. and Pradhan, B., 2014.Hydraulic transport of fly ash and fly ash-bottom ash mixtures at high concentrations. *International Journal of Chemical Engineering and Applied Sciences*, *4*(1), pp.1-4.

Patankar, S., 1980.*Numerical heat transfer and fluid flow*. CRC press.

Rawat, A., Singh, S.N. and Seshadri, V., 2016.Computational methodology for determination of head loss in both laminar and turbulent regimes for the flow of high concentration coal ash slurries through pipeline.*Particulate Science and Technology*, *34*(3), pp.289-300.

Ravelet, F., Bakir, F., Khelladi, S., Rey, R., 2013, Experimental study of hydraulic transport of large particles in horizontal pipes, *Experimental Thermal and Fluid Science*, 45, pp.187-197.

Seitshiro, I., Fujii, S., Yokoyama, N., Sato, I. and Sato, H., 2012. The Multi-Sized Slurry Flows in Horizontal Pipes: Innovated Models and Verification. *International Journal of the Society of Materials Engineering for Resources*, *19*(1_2), pp.24-31.

Tebowei, R., Hossain, M., Islam, S.Z., Droubi, M.G. and Oluyemi, G., 2017.Investigation of sand transport in an undulated pipe using computational fluid dynamics. *Journal of Petroleum Science and Engineering*.

Verma, A.K., Singh, S.N. and Seshadri, V., 2006. Pressure drop for the flow of high concentration solid-liquid mixture across 90º horizontal conventional circular pipe bend. *Indian Journal of engineering and Material Science,* 13, pp. 477-483.

Wilson, K.C., Addie, G.R., Sellgren, A., Clift, R., 2005, Slurry Transport Using Centrifugal Pumps, Springer.

Wu, D., Yang, B. and Liu, Y., 2015. Pressure drop in loop pipe flow of fresh cemented coal gangue–fly ash slurry: Experiment and simulation. *Advanced Powder Technology*, *26*(3), pp. 920-927.